

ornl

OAK
RIDGE
NATIONAL
LABORATORY

UNION
CARBIDE

OPERATED BY
UNION CARBIDE CORPORATION
FOR THE UNITED STATES
DEPARTMENT OF ENERGY



3 4456 0059927 0

ORNL/TM-7695

Computer Model for Determining Fracture Porosity and Permeability in the Conasauga Group, Oak Ridge National Laboratory, Tennessee

James J. Sledz
Dale D. Huff

ENVIRONMENTAL SCIENCES DIVISION
Publication No. 1677

OAK RIDGE NATIONAL LABORATORY
CENTRAL RESEARCH LIBRARY
CIRCULATION SECTION
4500N ROOM 175

LIBRARY LOAN COPY

DO NOT TRANSFER TO ANOTHER PERSON

If you wish someone else to see this
report, send in name with report and
the library will arrange a loan.



Printed in the United States of America. Available from
National Technical Information Service
U.S. Department of Commerce
5285 Port Royal Road, Springfield, Virginia 22161
NTIS price codes—Printed Copy: A08 Microfiche A01

This report was prepared as an account of work sponsored by an agency of the United States Government. Neither the United States Government nor any agency thereof, nor any of their employees, makes any warranty, express or implied, or assumes any legal liability or responsibility for the accuracy, completeness, or usefulness of any information, apparatus, product, or process disclosed, or represents that its use would not infringe privately owned rights. Reference herein to any specific commercial product, process, or service by trade name, trademark, manufacturer, or otherwise, does not necessarily constitute or imply its endorsement, recommendation, or favoring by the United States Government or any agency thereof. The views and opinions of authors expressed herein do not necessarily state or reflect those of the United States Government or any agency thereof.

Contract No. W-7405-eng-26

COMPUTER MODEL FOR DETERMINING FRACTURE POROSITY AND
PERMEABILITY IN THE CONASAUGA GROUP,
OAK RIDGE NATIONAL LABORATORY, TENNESSEE¹

James J. Sledz² and Dale D. Huff

ENVIRONMENTAL SCIENCE DIVISION
Publication No. 1677

NUCLEAR WASTE PROGRAMS
(Activity No. AR 05 15 15 0; ONL-WL14)

¹Submitted as a thesis by James J. Sledz to the Graduate Council of the University of Tennessee in partial fulfillment of the requirements for the degree of Master of Science.

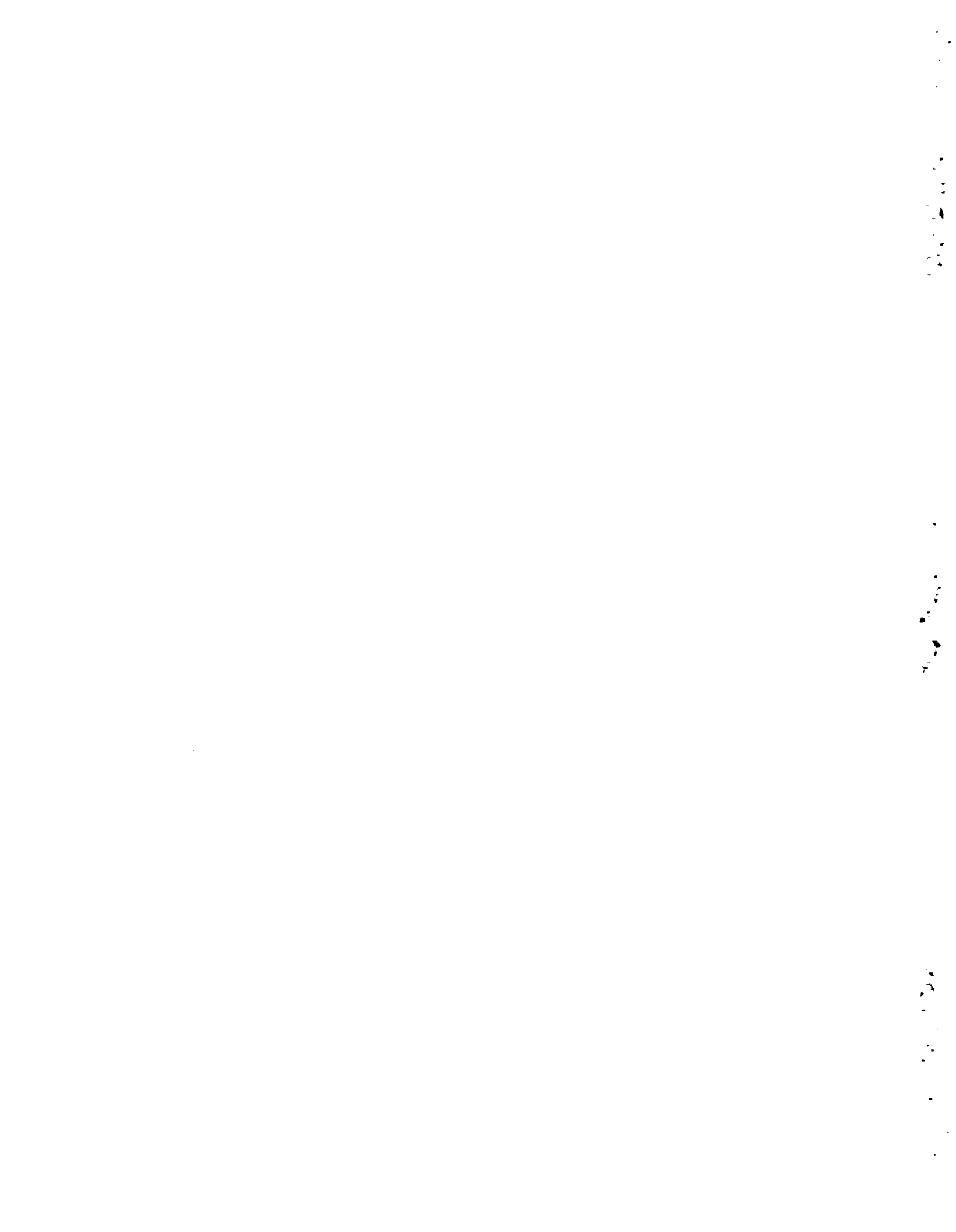
²Present address: Conoco Inc., R&D West, P.O. Box 1267, Ponca City, OK 74601

Date Published: April 1981



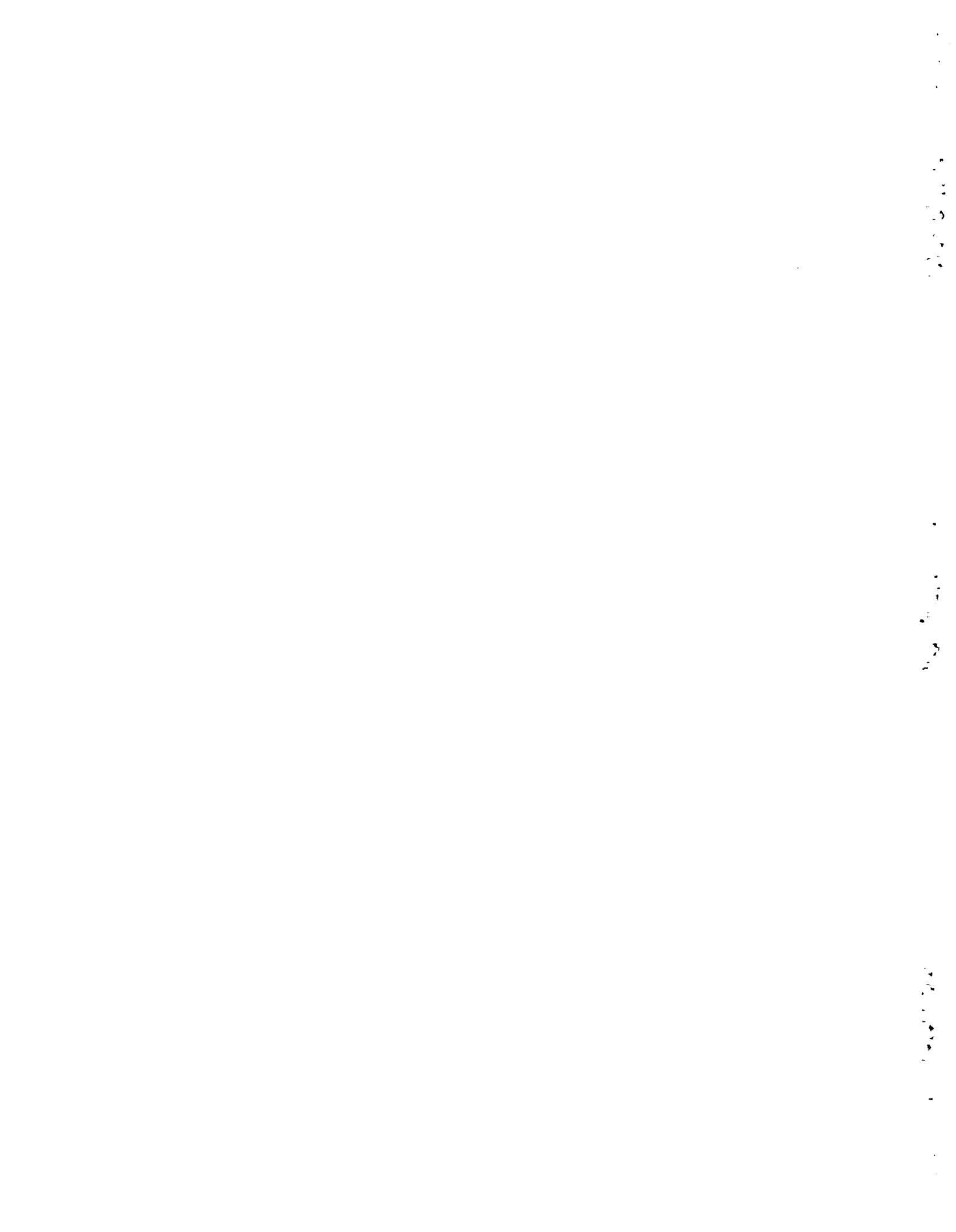
3 4456 0059927 0

OAK RIDGE NATIONAL LABORATORY
Oak Ridge, Tennessee 37830
operated by
UNION CARBIDE CORPORATION
for the
DEPARTMENT OF ENERGY



ACKNOWLEDGMENTS

The senior author wishes to express his thanks to his graduate committee at The University of Tennessee, Knoxville: Dr. D. Roeder his major professor for his help and suggestions; Dr. J. Higgins for innumerable discussions and assistance; and Dr. F. Keller for suggestions in the early developmental stages of the study. A special thanks is also given to Dr. S. Haase for his critical review of the manuscript and his assistance in the latter portion of the study. Other members of the Oak Ridge National Laboratory staff who offered useful suggestions include Dr. T. Tamura, Dr. G. Brunton, J. Jones, and O. M. Sealand.



ABSTRACT

SLEDZ, J. J., and D. D. HUFF. 1981. Computer Model for Determining Fracture Porosity and Permeability in the Conasauga Group, Oak Ridge National Laboratory, Tennessee. ORNL/TM-7695. Oak Ridge National Laboratory, Oak Ridge, Tennessee. 142 pp.

Joint orientations for the shale and siltstone beds of the Conasauga Group were measured from outcrop exposures on the Oak Ridge National Laboratory Reservation. The data collected from two strike belts (structural trends) were analyzed with the use of the computer and subdivided into individual joint sets. The joint set patterns in the Northern outcrop belt were too complex for orientation prediction; joint formation is believed to be influenced by polyphase deformation. The Southern Conasauga Belt contains an orthogonal joint set consisting of strike and a-c joints in all outcrops measured. These are believed to be tension joints formed during thrust sheet emplacement.

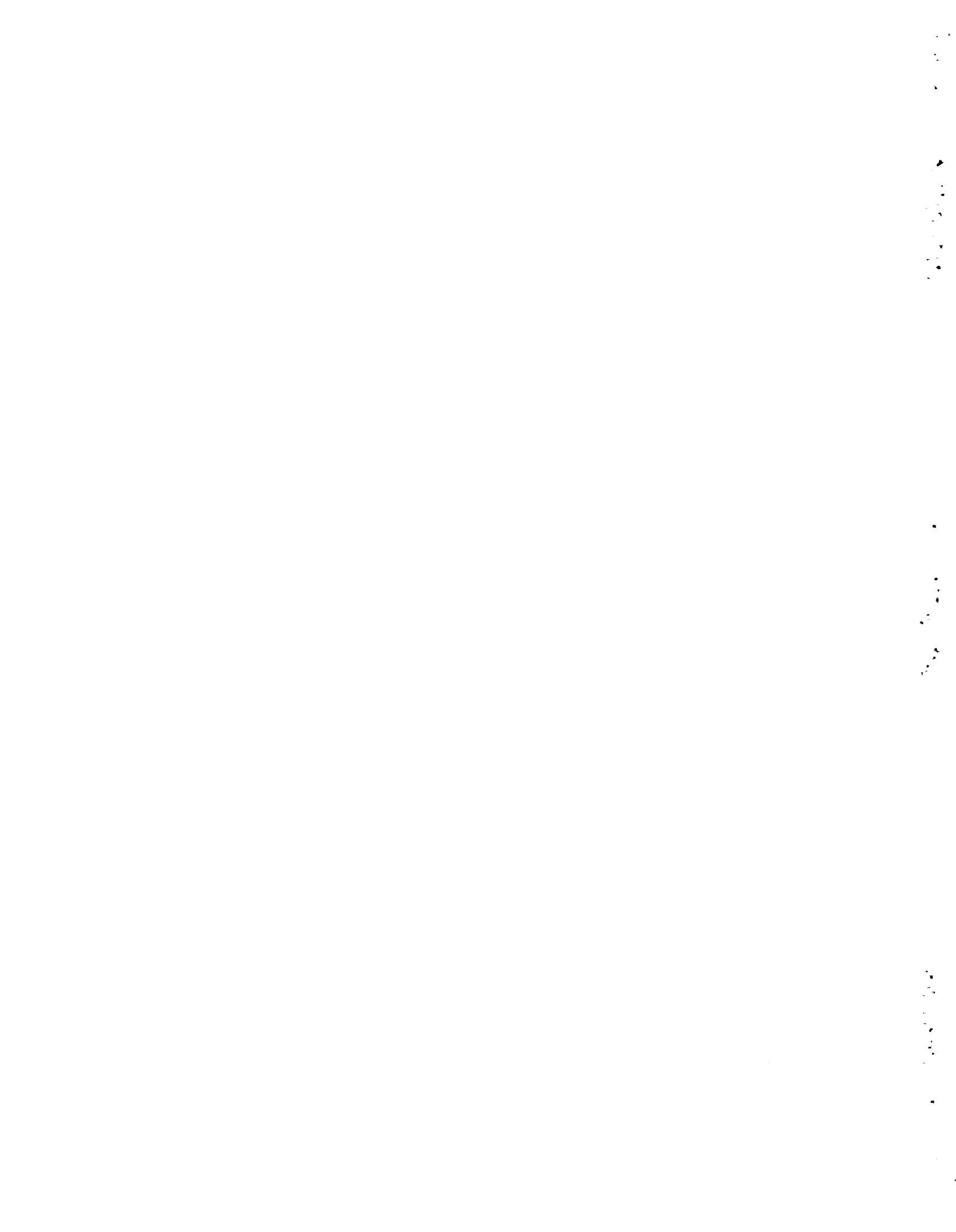
Joint length and spacing, measured in the field, were found to be extremely variable within each exposure and highly dependent upon surficial weathering. The measurements from all locations were combined for detailed analysis and trend prediction. In the siltstone beds, mean joint length varied from 2 cm to 76 cm with a mean range of 6 to 45 joints per meter. The shale beds contained a nearly constant mean joint length of 12 cm with 12 to 28 joints in a one-meter traverse. Results showed that the joint length and spacing increased with increasing bed thickness in the siltstone, while the bed thickness variations in the shale had little effect on the joints.

A computer model was developed by combining the joint orientation, joint spacing, and joint length data collected in the field with subsurface drill core information for the purpose of calculating the fracture porosity and permeability of the rocks. The joint gap width was measured from both outcrop and subsurface samples with ranges from 0.1 mm to 0.7 mm in the siltstones and less than 0.2 mm in the shales. The value for the joint gap width was found to be the major factor in the fracture porosity and permeability calculation. A gap width of 0.19 mm in a pure shale bed had a fracture porosity of 0.09 percent and fracture permeability of 0.09 darcy. In a pure siltstone bed, the porosity and permeability were 0.03 percent and 0.001 darcy. It was determined that increasing the gap width by a factor increases the fracture porosity by the same factor and causes the permeability to increase by the cube of the factor.

The results of the model suggest that the migration of fluids through highly jointed clastic rocks should be considered when defining groundwater flow patterns.

TABLE OF CONTENTS

	<u>Page</u>
ABSTRACT	v
LIST OF TABLES	ix
LIST OF FIGURES	xi
CHAPTER	
I. INTRODUCTION	1
Purpose and Methods	1
Location	3
Regional Geology	3
II. JOINT MEASUREMENT AND ANALYSIS	11
Introduction	11
Data Collection	13
Orientation Analysis	19
Joint Density and Length Analysis	43
Summary	54
III. COMPUTER MODEL AND RESULTS	56
Introduction	56
Overview	58
Spatial and Lithologic Calculations	60
Porosity and Permeability Calculation	72
Results	83
Summary	96
IV. CONCLUSION	98
LIST OF REFERENCES	101
APPENDIX A. FORTRAN PROGRAM	107
APPENDIX B. USER'S GUIDE	127
APPENDIX C. TABLES	133



LIST OF TABLES

TABLE	PAGE
1. Results of cluster analysis of joint orientations for all sub-locations in the Northern Conasauga Belt.....	26
2. Combined results of cluster analysis of joint orientations for all locations in the Northern Conasauga Belt.....	28
3. Results of cluster analysis of joint orientations for all sub-locations in the Southern Conasauga Belt.....	36
4. Combined results of cluster analysis of joint orientations for all locations in the Southern Conasauga Belt.....	38
5. Listing of the calculated fracture porosity and permeability for each subcell location.....	85
C-1. Listing of commonly used variable names in the FRAFLO program.....	134
C-2. Descriptions of files used in the FRAFLO program.....	135



LIST OF FIGURES

FIGURE	PAGE
1. Map of East Tennessee displaying study area location and the major thrust faults within the area.....	4
2. Study area location map displaying geology, outcrop locations, and drill hole locations.....	5
3. Generalized facies map of the Conasauga Group in a west (W) to east (E) traverse of Eastern Tennessee.....	7
4. Structural cross sections and stratigraphic column of study area.....	10
5. Photograph of drill core in the Southern Conasauga Belt taken at a depth of 23 m.....	15
6. Block diagram of a joint projection on a three-dimensional surface.....	16
7. Block diagram displaying joint length and spacing measurements.....	18
8. Example of a joint frequency diagram.....	21
9. Rose diagrams of the Northern Conasauga Belt joint orientations for sampling locations N1 through N4.....	24
10. Equal-area projection of poles to joint planes for outcrop locations N1 through N4 in the Northern Conasauga Belt.....	30
11. Base map projection of joint orientations representing joint sets J-1 through J-4.....	31
12. Summary diagram of clustered joint orientations in the Northern Conasauga Belt.....	32
13. Rose diagrams of the Southern Conasauga Belt joint orientations for sampling locations S1 through S7.....	35
14. Equal-area projection of poles to joint planes for outcrop locations S1 through S7 in the Southern Conasauga Belt.....	39

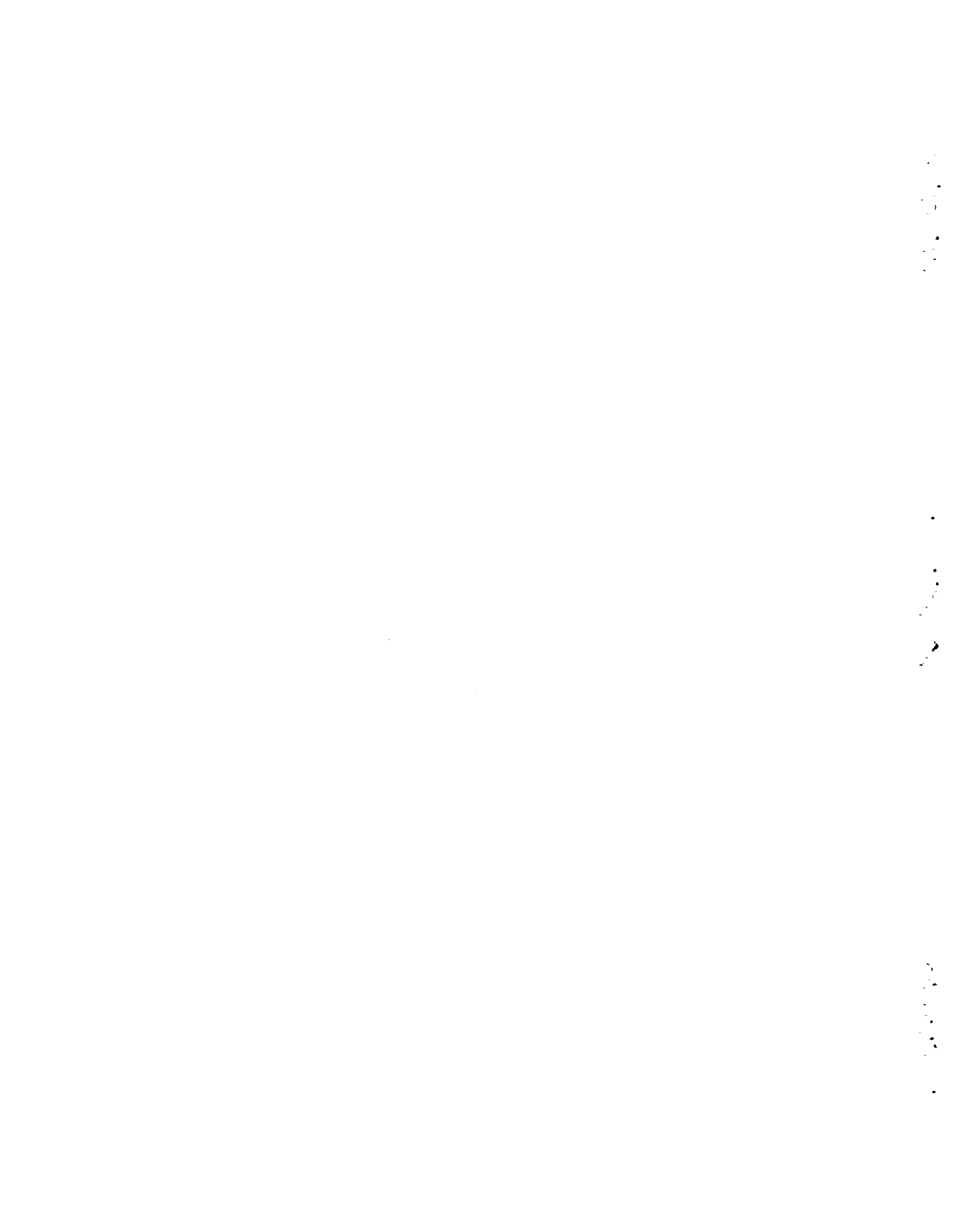
FIGURE	PAGE
15. Summary diagram of clustered joint orientations in the Southern Conasauga Belt.....	41
16. Photograph of drill core from the Southern Conasauga Belt taken at a depth of 9 m.....	42
17. Joint length versus bed thickness in shale beds of the Conasauga Group.....	45
18. Number of joints per meter versus bed thickness in shale beds of the Conasauga Group.....	46
19. Joint length versus number of joints per meter in shale beds of the Conasauga Group.....	47
20. Joint length versus bed thickness in siltstone beds of the Conasauga Group.....	49
21. Number of joints per meter versus bed thickness in siltstone beds of the Conasauga Group.....	50
22. Joint length versus number of joints per meter in siltstone beds of the Conasauga Group.....	51
23. Generalized flow chart of the FRAFLO model.....	59
24. Surface elevation of Southern Conasauga Belt.....	64
25. Cell plot of surface elevations at 100 subcell locations.....	67
26. Cell plot of surface elevations at 676 subcell locations.....	68
27. Simplified flow chart of the fracture porosity and permeability calculation.....	73
28. Frequency distribution of bed thickness values in shale beds measured within the study area.....	75
29. Fracture porosity surface calculated for each subcell location.....	84
30. Calculated fracture porosity at various percentages of siltstone for joint gap widths of 0.1921 mm and 0.3842 mm.....	88
31. Variations in joint density and joint length with changes in bed thickness for shale and siltstone beds.....	89

FIGURE	PAGE
32. Variations in the calculated fracture porosity and permeability with changes in the percentage of siltstone.....	92
33. Effects of increasing the total bed thickness (TT) on the porosity and permeability calculation.....	93



LIST OF SYMBOLS

T	bed thickness
NEL	calculated elevation
D	distance
EL	elevation
θ	fracture porosity
C	hydraulic conductivity
I	integer factor
K	intrinsic permeability
JSET	joint set number
LA	latitude at ORA grid system
LC	length of the cell
LJ	length of the joint
LO	longitude at ORA grid system
GJ	mean gap width of the joint
γ	measured dip of the joint
α	measured strike of the joint
NJ	number of joints
LITH	rock type
ν	specific weight of the fluid
TT	total bed thickness
TBEDS	total number of beds
TJ	total number of joints
μ	viscosity of the fluid
WC	width of the cell



CHAPTER I

INTRODUCTION

Purpose and Methods

Surface exposures of shale and siltstone often contain abundant fractures and joints. Joints are defined as fractures where the component of displacement parallel to the fracture is zero or microscopic (Hobbs et al., 1976). The joints may be formed by tectonic deformation (Price, 1966), or they may be a response to compaction and dewatering processes (Nickelsen and Hough, 1967). The determination of a systematic relationship between joints is extremely valuable for trend and predictive purposes. Measured joint orientations in different outcrops can be divided into individual groups of joint sets exhibiting similar orientations (Babcock, 1973). The joint sets can be compared and related to the orientation of the existing structural features (Murray, 1968); and if a relationship exists between adjacent exposures in a single area, the systematic orientation of the joints in the entire area can be predicted.

Joint length and joint spacing (density) are two important parameters that can be measured in outcrops (Hodgson, 1961). The length and density of the joints are primarily a function of the rock type and bed thickness. Data of this type can be analyzed and an empirical relationship derived for calculating joint length and density as a function of these interrelated parameters.

By determining the gap width (opening distance) of individual joints and combining the joint orientation, length, and density for a given area, the void volume of the rock related to joints can be calculated. The volume or porosity formed by the fractures is typically very small compared to the porosity between the grains in a coarse-to-medium-grained clastic rock (Stearns and Friedman, 1972). Shale beds, however, consist of very fine grained minerals, and a large portion of their overall porosity is provided by the joints. The value for the fracture porosity of shale is relatively low (less than 0.05 percent), but with the presence of joints a means is created for fluid to flow through the strata (Snow, 1968). Permeability, which is directly proportional to the rate of this flow, may be high if the joints are systematic and form continuous conduits through the rock. The determination of the fracture permeability is important when considering the amount of hydrocarbon (Regan and Hughes, 1949) or groundwater-related radionuclide migration in an otherwise impermeable rock (Webster, 1976).

The purpose of this study is to determine the systematic relationship between joints in shales and siltstones of the Conasauga Group on the Oak Ridge National Laboratory Reservation and to calculate the fracture porosity and permeability of these rocks. Making use of the computer, the importance of each joint parameter may be individually evaluated and combined in an analytical model to generate a quantitative picture of the fracture porosity and permeability within the Conasauga Group. These estimates can then be used with a general groundwater model to predict flow in a physical system.

Location

The study area is located in the Oak Ridge National Laboratory Reservation in Roane and Anderson counties approximately one kilometer southwest of Oak Ridge, Tennessee (Figure 1). The reservation is physiographically located in the Valley and Ridge province of the Appalachian Mountains. Two major thrust faults, which play an integral role in the development of the fractures studied, transect the area and extend for distances of over 160 kilometers (100 miles) along strike.

Regional Geology

Stratigraphy

The geology on the reservation consists of a repetition of Cambrian and Ordovician rocks within two major strike belts that lie parallel to the thrust faults. A geologic map of the area (with the Oak Ridge Administration Grid System superimposed) is shown in Figure 2. The oldest rocks found in the area are the Lower Cambrian Rome Formation, which forms the two major ridges in the reservation. These ridges, Pine Ridge to the north and Haw Ridge to the south, have an average topographic elevation of 300 meters (1000 feet). The Rome Formation is composed of shale interbedded with sandstone and siltstone, with a total stratigraphic thickness between 240 and 300 meters (800-1000 feet). Overlying the Rome Formation in gradational contact is the Middle Cambrian Conasauga Group, which is composed predominantly of shales with a few thin beds of siltstone and limestone. The Conasauga Group is of prime interest for this study

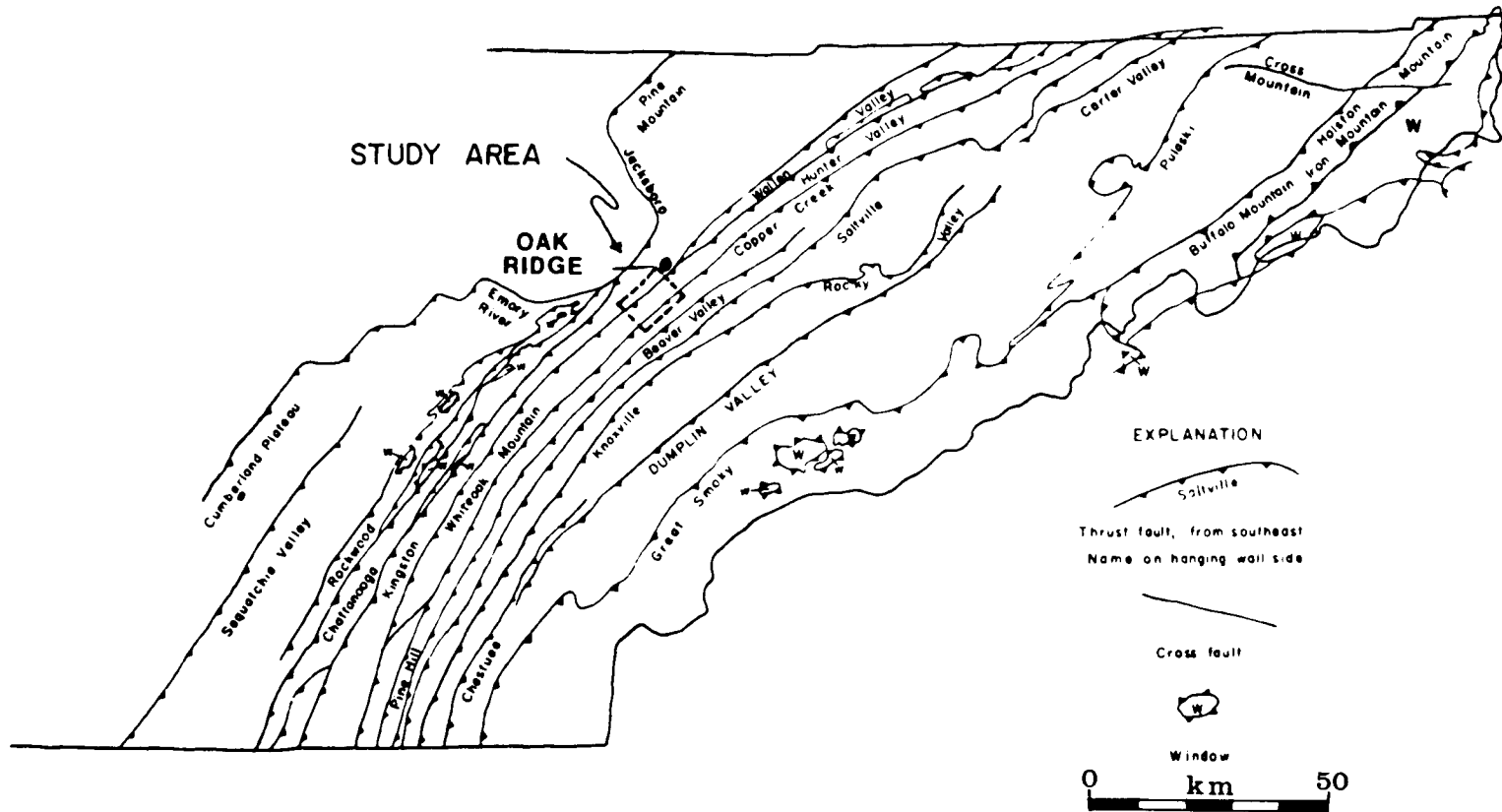


Figure 1. Map of East Tennessee displaying study area location and the major thrust faults within the area (after Hatcher, 1965).

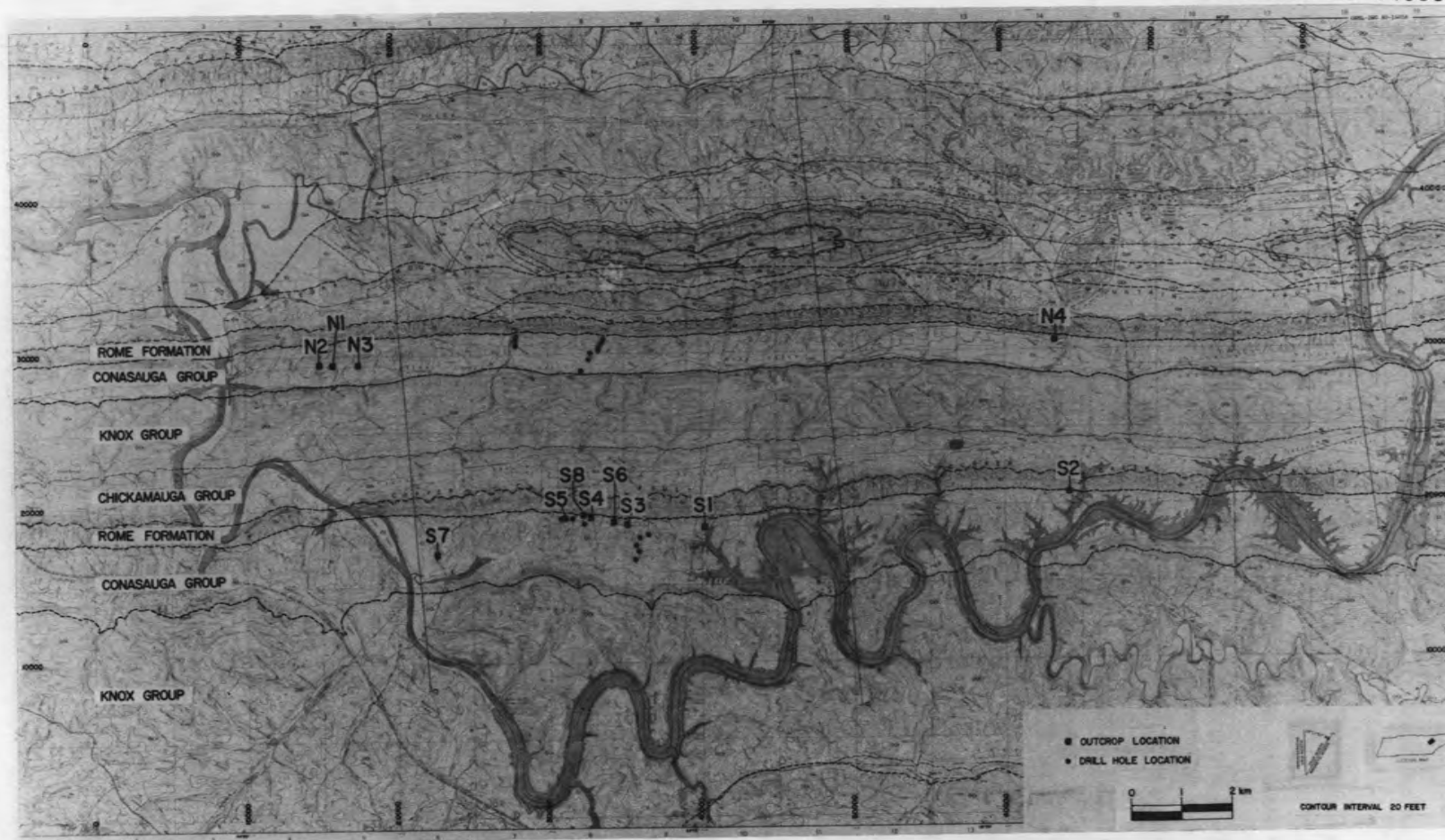


Figure 2. Study area location map displaying geology, outcrop locations, and drill hole locations (after McMaster, 1962). Map coordinates represent Oak Ridge Administrative Grid system. Legend and cross sections A, B, C, are given in Figure 4.

and is the rock unit for which the computer model was developed. The Conasauga Group is composed of three limestone formations and three shale formations (Figure 3). The lowermost formation, Pumpkin Valley Shale, is a highly calcareous glauconitic siltstone interbedded with shale. This is exposed in road cuts along the slopes of the ridges and is the formation from which all data were collected. Near the top of the Pumpkin Valley Shale there is a decrease in the amount of siltstone present and an increase in the abundance of shale. The thick unit of shale (Rogersville and Nolichucky Shale Formations) contains numerous interfingering beds of limestone believed to be equivalent to the Rutledge and Maryville Limestone Formations. Near the top of the Conasauga Group, the shale beds are less prominent, with limestone becoming more abundant until at the top, only limestone is present (Maynardville Limestone Formation).

The surface exposures of the Conasauga Group consist of shale and siltstone of the Pumpkin Valley Shale Formation. Numerous drill cores taken in the Melton Valley region revealed an extensive amount of calcium carbonate present within the shales. These cores also revealed the total depth of weathering to be greater than 30 meters (100 feet), which was the depth of the deepest core inspected.

Overlying the Conasauga is the Lower Ordovician Knox Group, which consists of massive siliceous dolomite. This is the thickest unit in the area with an estimated overall stratigraphic thickness of 900 meters (3000 feet). The Knox contains abundant solution channeling throughout the reservation. The top of the Knox is unconformably overlain by the Middle Ordovician Chickamauga Group, a

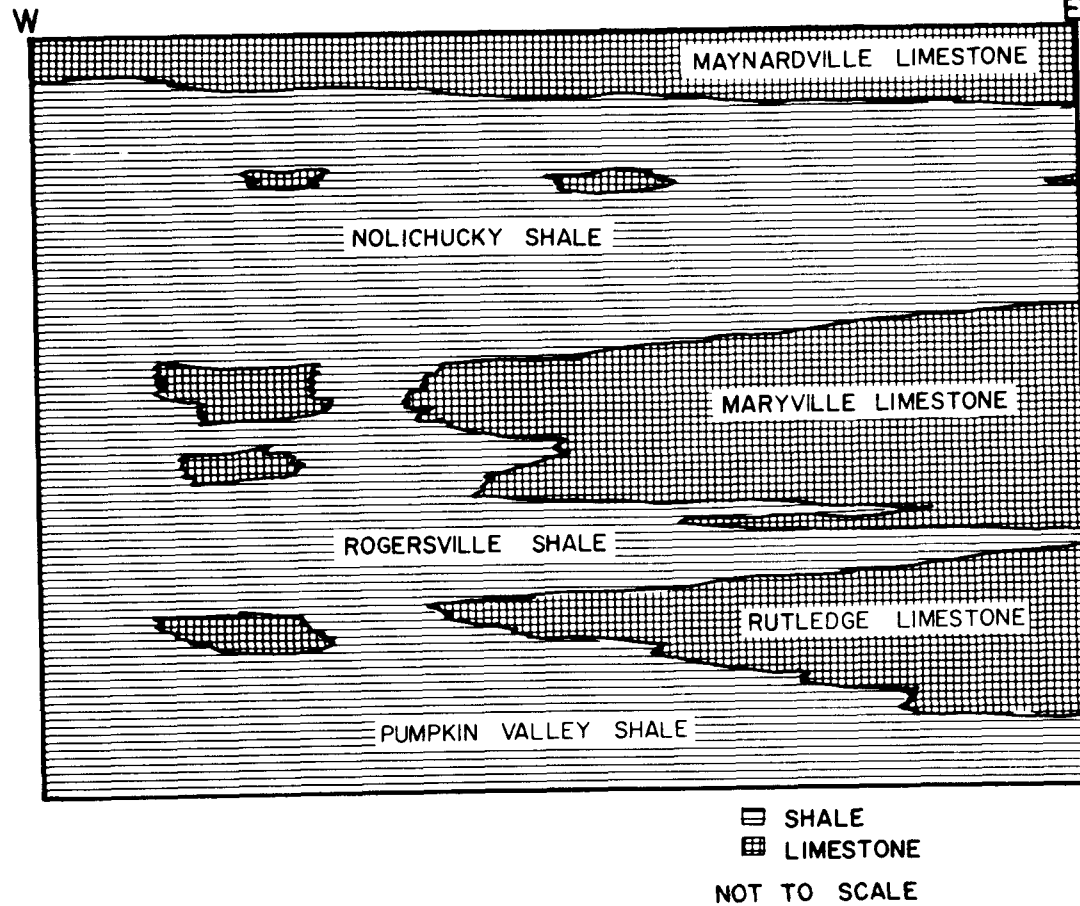


Figure 3. Generalized facies map of the Conasauga Group in west (W) to east (E) traverse of Eastern Tennessee (after Rodgers, 1953). The study area is believed to be located near the central portion of the diagram.

thick-bedded limestone with lenses of shale and siltstone.

North of Pine Ridge are exposures of younger rocks of ages to the Early Mississippian, but they are not of interest in this study.

Depositional History

The depositional environment from Cambrian through Early Ordovician time was that of a gradually subsiding basin with westward transgression of a carbonate shelf (Harris and Milici, 1977). The Rome Formation was deposited on a shallow carbonate bank of the Lower Cambrian Shady Dolomite. The influx of clastic material from the west supplied the peritidal environment of the Rome (Samman, 1975). The basin then gradually began to subside forming a deeper water coastal lagoon sequence on its western edge. With the shoreline to the west and the carbonate banks migrating from the east, the deeper water shales, siltstones, and thin-bedded limestones of the Conasauga Group were deposited (Milici et al., 1973). By the end of the Cambrian Period, this deeper water carbonate-shelf sequence transgressed westward, covering the entire area and depositing great thickness of the Knox Dolomite. After a short period of quiescence, the carbonate shelf was uplifted and exposed, resulting in surficial weathering and the widespread development of karst topography.

During Middle Ordovician time, a second transgression of the seas occurred and a deep basin developed. The influx of carbonate and clastic material deposited the Chickamauga Limestone over the submerged Knox Group. The basin continued to fill and by the Late Paleozoic time, a great thickness of deltaic and alluvial deposits was formed.

Structure

The two major thrust faults that transect the study area are the Whiteoak Mountain fault to the north and the Copper Creek fault to the south (Figure 2, p. 5). The thrust faults cut up-section northwestward, bringing the Lower Cambrian Rome Formation over Middle Ordovician Chickamauga Limestone (Figure 4). The thrust faults are not exposed, but their orientations are inferred from the strata at the surface. The dip of the rocks at the surface along the Copper Creek fault is to the southeast at 45-55 degrees (Ossi, 1979), and at depth is nearly horizontal, forming a bedding-parallel fault. This is part of the major decollement of the Southern Appalachian thin-skinned orogenic thrust belt (Roeder et al., 1978a). The horizontal displacement of the thrust fault is believed to be between 15 and 20 kilometers (9-13 miles).

The Conasauga Group is exposed in two strike belts that lie parallel to the thrust faults. The northern exposure, in Bear Creek Valley near the Whiteoak Mountain fault, will be referred to as the Northern Conasauga Belt. This consists of approximately 460 meters (1500 feet) of shale striking at N59E and dipping from 45-60 degrees to the southeast. The Southern Conasauga Belt, which is exposed south of the Copper Creek Fault in Melton Valley, has a total stratigraphic thickness of 550 meters (1800 feet). These strata have a mean strike of N58E and dip from 30-40 degrees to the southeast.

The late Paleozoic tectonism of the Alleghenian Orogeny that produced the thrust faults also produced numerous low amplitude folds which are abundant in the area. These were noted in shallow trenches dug in the area and are not apparent on the outcrop.

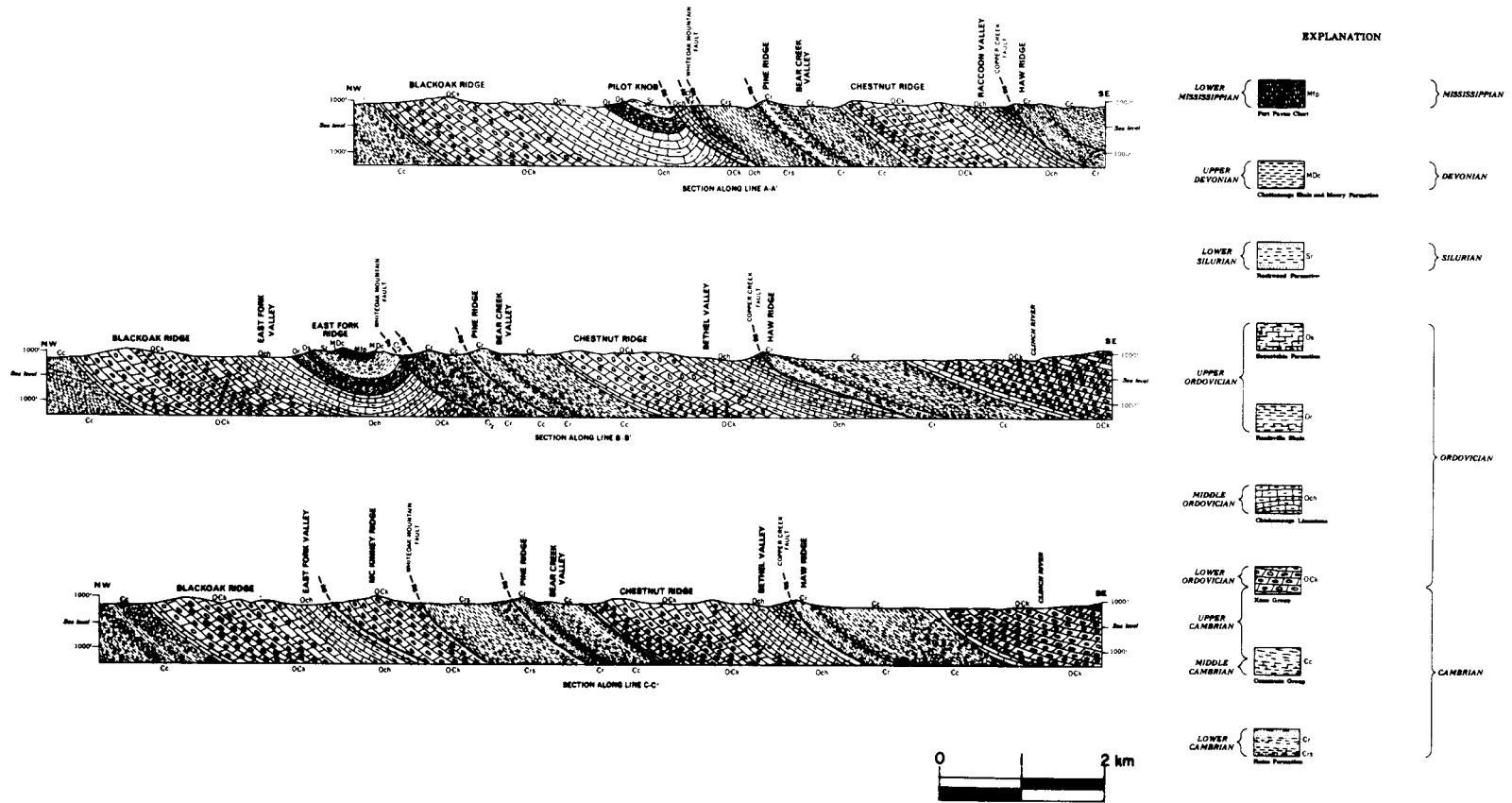


Figure 4. Structural cross sections and stratigraphic column of study area (after McMaster, 1962)

CHAPTER II

JOINT MEASUREMENT AND ANALYSIS

Introduction

A computer model for fracture porosity and permeability determination must consider many different variables, including joint density, length, orientation, and joint gap width. Each of these parameters is interrelated, and field measurement of them is essential. The primary goal of the calculation is to predict joint orientations in a given area, which may be viewed over a wide region on the basis of the tectonic forces involved in their formation.

Studies of jointing in clastic rocks have been primarily done on a regional scale. Work by Nickelsen and Hough (1967) and by Parker (1942) in the Northern Appalachian mountains region of New York and Pennsylvania demonstrated that three to five different joint sets can be determined by field measurement on a regional scale. In the Western United States, Hodgson (1961) found a regional joint pattern in the Cab Ridge-Navajo Mountain area of Arizona and Utah which displayed many similarities to those in the Northern Appalachians. The sequence of joint formation, including their relationship with tectonic structures, has been studied in detail by several authors (Harris et al., 1960; Babcock, 1973, 1974; Currie and Reik, 1977). Spencer (1959) discussed the geologic evolution of the Beartooth Mountains by the use of fracture patterns. Stress systems, as displayed by joint sets, were determined for the Cardium Sandstone in

Alberta by Muecke and Charlesworth (1966), while Price (1966) described a similar study in the Southern Rocky Mountains.

The density of joints in shales can vary locally within a single outcrop as well as on a regional scale (Nickelsen and Hough, 1967). This variation is dependent on bed thickness as well as the rock type (Hodgson, 1961). Hobbs (1972) determined the relationship empirically and suggested that joint density varies inversely with bed thickness for a given lithology. The density of joints is also influenced by the degree of tectonic deformation (Price, 1967). An increase in deformation results in an increase in the abundance and density of the joints.

The length of joints has not been studied in great detail, but it is believed that joint length is directly proportional to the bed thickness (Price, 1966).

One major factor that is difficult to model is the degree of weathering that has taken place on the outcrop. This is an important factor when considering both joint density and length. Thin section studies of the Conasauga Group suggest that joint spacing is on a microscopic scale (Krumhansl, 1979), while surface exposures contain a much larger spacing. The number of joints exposed in an outcrop is directly related to the amount of weathering. A quantitative value of weathering is difficult to estimate, and the lack of this information places a qualitative limit to joint predictions.

Data Collection

A reconnaissance of the entire reservation was undertaken to provide the necessary information on the location and quality of outcrops. The majority of the outcrops studied required extensive excavation to expose enough surface area for data collection. These exposures were predominately road cuts that are parallel to the strike of the strata, allowing for measurements on single or multiple bedding-plane surfaces.

Eleven outcrops were selected for orientation analysis, four in the Northern Conasauga Belt and seven in the Southern Conasauga Belt (Figure 2, p. 5). For each outcrop, a minimum of two separate sub-locations was selected for excavation and measurements. Enough weathered material at each sub-location was removed to facilitate measurements. The number of joint measurements needed for a valid representation of the joints is difficult to quantify. Pincus (1951) suggested that at least 80 joints should be measured for statistically valid results. Muecke (Babcock, 1973) measured 250-300 joints, while Spencer (1959) recorded 100-120; Babcock (1973) measured a maximum of 150 joints at each outcrop. Based on a preliminary study, the author measured 200 and 240 joints from two different outcrops and after analyzing the data, it was decided that 120 measurements at each outcrop would be recorded.

The orientation of all joints (strike and dip) were recorded at each of two sub-locations until 50-60 joints were measured. The data from both sub-locations were combined, resulting in a single sample of joint orientations for each outcrop location.

The joint gap, the perpendicular opening distance of the joints, proved difficult to measure quantitatively. The gap width on the weathered bedding plane surface differed greatly from the gap of the unexposed bed. Because of this, it was decided that the gap width should not be measured on the outcrop, but a range of values should be recorded from unweathered material contained in drill cores. Figure 5 is a photograph of a siltstone core taken from a depth of 23 m (75.5 feet) with abundant calcite-filled joints. There is a very wide variation in the gap width of the many joints within this sample, making it difficult to determine a mean width. Some of the differences in gap width, as seen in the figure, are due to the oblique angle of sectioning; the actual width, therefore, was measured from either end of the core. The core also displays weathering of the gap with calcite removed by dissolution. In this case the effective gap width is actually the dissolved portion, but this complication cannot be predicted. Results of the gap width measurements will be discussed in the next chapter.

Orientation and gap width data can be combined for fracture porosity determination as follows. Figure 6 is a joint projection diagram (cavalier perspective) depicting a joint surface. The orientation along a bedding plane has the components of strike (α) and dip (β) oriented with respect to true north. By combining the gap width (GJ) information with the thickness of the bed (T) and the length (L) and width (W) forming a unit volume, the porosity provided by the single joint can be calculated.

The length and density of the joints were measured at locations

ORNL-PHOTO 2636-80



Figure 5. Photograph of drill core in the Southern Conasauga Belt taken at a depth of 23 m. This core (approximately 3.5 cm across) displays abundant jointing in a siltstone bed.

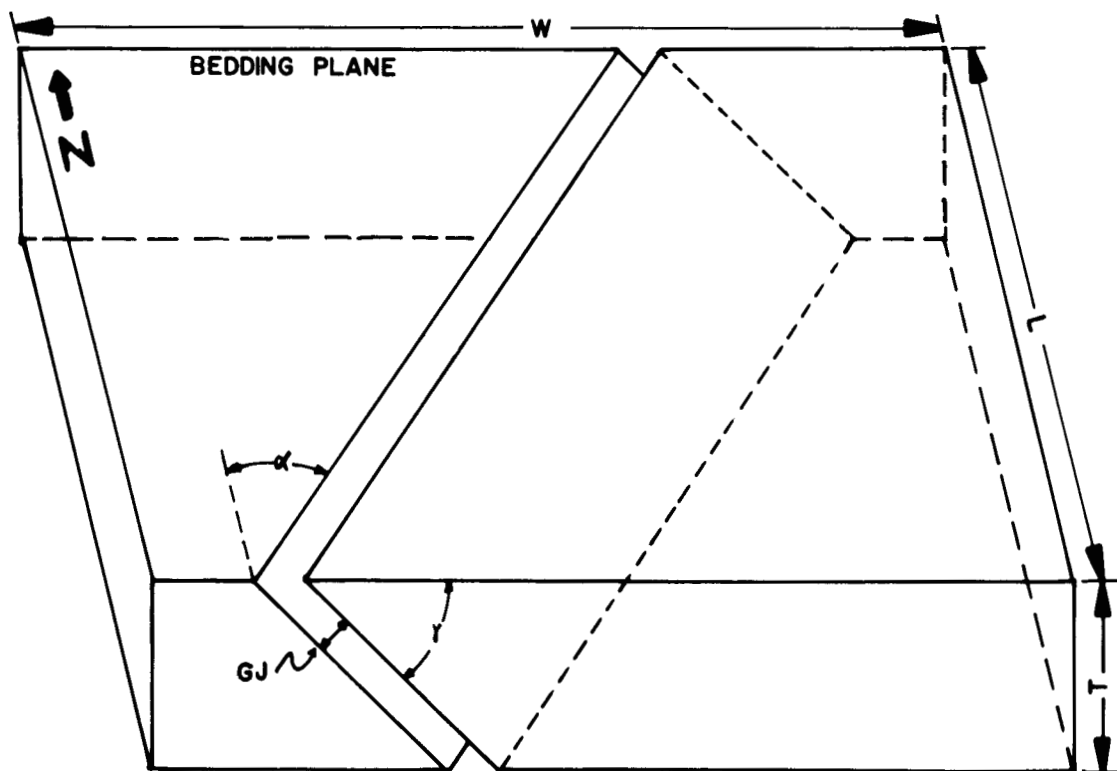


Figure 6. Block diagram of a joint projection on a three-dimensional surface. The block (cavalier perspective) contains a unit volume of width (W), length (L), and bed thickness (T) with the joint strike (α), dip (γ), and gap width (GJ) illustrated.

N4, S1, S4, S5, S7, and S10 (Figure 2, p. 5). Each outcrop was cleared along a single bedding plane surface in the same manner as for the orientation data collection.

There are principally two methods for determining the density of joints in a given area. One method is to determine a lithology factor (Harris et al., 1960) by counting the number of joints within a unit area. The results are normalized to a datum bed of a certain rock type and thickness. This method was found to be inappropriate for the study area because of the thin bedding of the shales and the difficulty of exposing a large enough surface area for measurements to be taken. The method found to be most useful in dealing with very thin beds is to determine the fracture number for each rock type and bed thickness (Stearns and Friedman, 1972). Using a block diagram (Figure 7), this method of field collection of data can be easily explained. For each rock type along a bedding-plane surface, a traverse (S) of a unit length was measured normal to each joint set. The number of joints crossing the traverse was counted, yielding a fracture frequency for various bed thicknesses. From the fracture frequency, the density of fractures within each unit length measured can be easily calculated.

The length (JL) of each of the joints was measured with an accuracy to the nearest 1.3 cm (0.5 inch). The rock type, bed thickness (T), and joint lengths were recorded at numerous sites within each outcrop location. With this information, the density and joint length, based on joint set, lithology, and bed thickness can be determined.

ORNL-DWG. 80-13352R

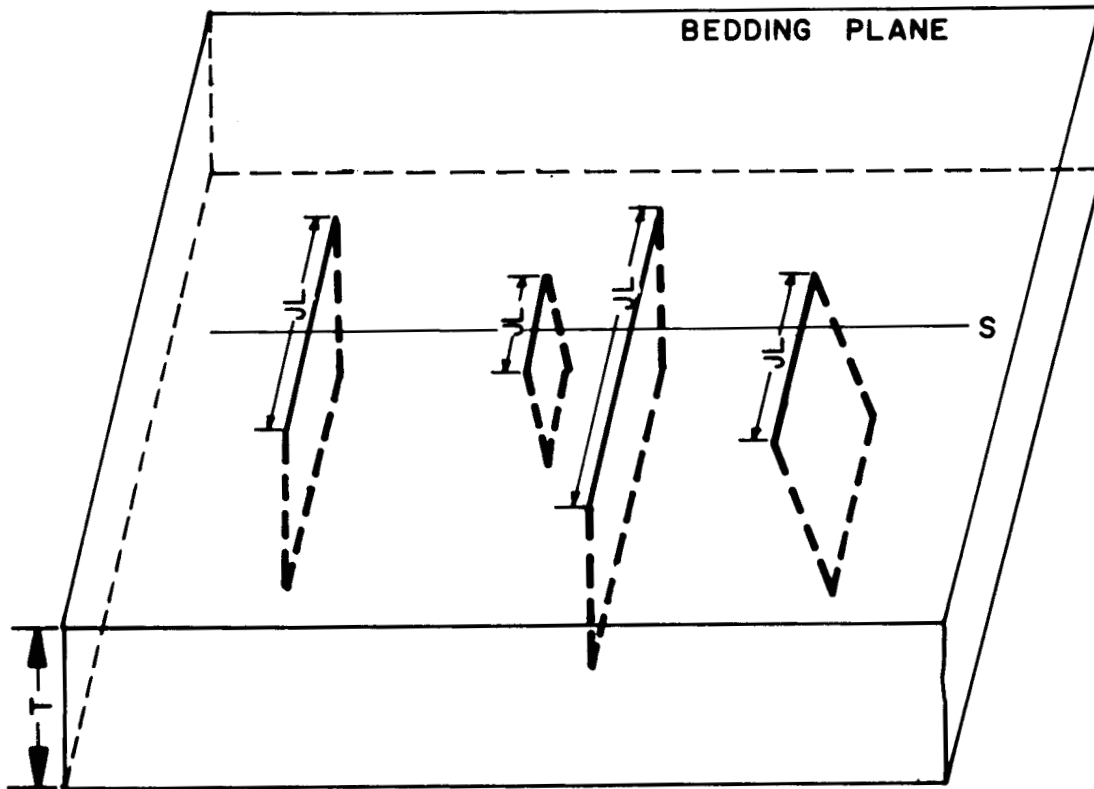


Figure 7. Block diagram displaying joint length and spacing measurements. Joint length (JL) and spacing are recorded along traverse (S) of a bed thickness (T).

Because shale is the predominant rock type in the area and limestone was rarely found in outcrops, the majority of the data was collected from shales; few data were collected from siltstones, and none from limestones. The only surface exposures of limestone within the study area existed in a single outcrop in the Southern Conasauga Belt. The total extent of the exposure was insufficient for any detailed orientation analysis to be performed. In general, the joints were spaced on the order of one per meter with joint lengths greater than the height of the exposure (1.5 m).

Orientation Analysis

The detailed determination of joint strike and dip over a specified region is essential to the prediction of joint trends. Measuring joint orientations and determining the number of different joint sets present will provide needed parameters for input into the computer model. In this section, an attempt is made to determine if joint orientation can be related to tectonic structures and to develop a systematic relationship between joint orientation and their geographic location within the study area.

Frequency Analysis

Orientation data collected at each location were processed by computer to produce joint-frequency (rose) diagrams. A FORTRAN program (ROSETT), was developed to plot the frequency of joints in the direction of their strike (azimuth) and the joint surface dip direction. The magnitude of dip was not considered in these diagrams. The upper (northern) half circle implies northern dip

direction, and the lower (southern) half circle represents a southern dip direction. Figure 8 is an example of this type of plot with the primary group of data striking N75E and dipping north and the secondary group is dipping to the south with a N30W mean orientation. The predominant group contains over 60 observations (OBS) displaying its high frequency of orientation. This type of diagram displays the amount of dispersion of the joints at each location, in conjunction with the azimuth frequency of the joints measured.

Cluster Analysis

All orientation data collected were entered into the computer for the purpose of analysing and determining clusters of individual joint set patterns. The computer program used (PATCH) was a modification of two existing programs written by Mahtab et al. (1972) and Jeran and Mashey (1970), which were originally designed for use on coal cleats. The statistical techniques and calculations performed by the cluster analysis program will be briefly discussed below.

The program divides a uniform hemispherical surface into 100 equal area patches or cells which encompass a total of nine circular bands from the equator to the pole. The joint normals, as calculated by the program, are plotted onto the lower hemisphere, by projecting their intersection with the sphere as a point. The number of intersections within each patch is calculated and used to determine the existence of a cluster. The points may cluster about a single point, suggesting a single preferred direction (or unimodal distribution; Watson, 1966) or they may be widely dispersed. The

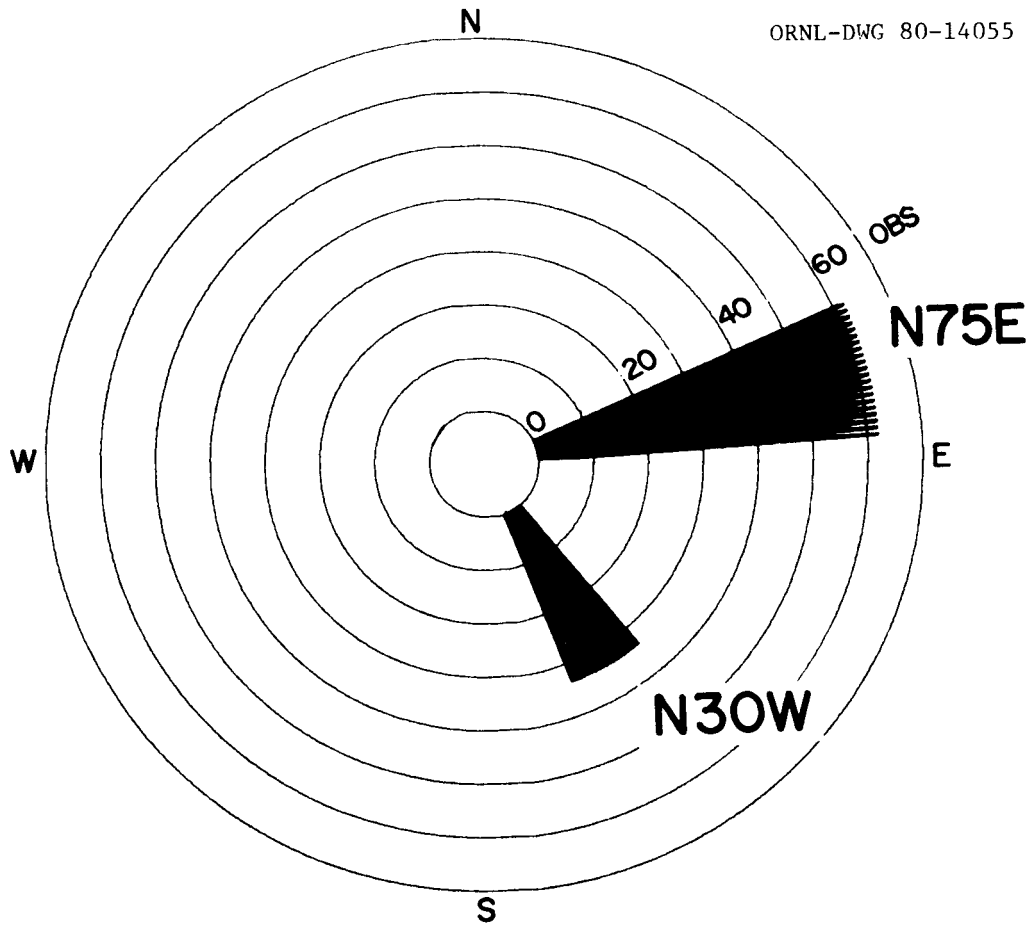


Figure 8. Example of a joint frequency diagram. Diagram displays 62 observations (OBS) striking N75E and dipping north and 35 observations striking N30W and dipping to the south.

program uses the Poisson distribution model, a test of the level of the significant number of points piercing the spherical surface, to determine if clustering has occurred in any adjacent patches. The Poisson model has been demonstrated as an effective method of determining the anisotropy of a point diagram (Stauffer, 1966). When a clustering of points that satisfies the model is found, the unit vectors and their directional cosines are calculated. The angular coordinates of the vector can be determined to define a single mean unit vector for each cluster. The Fisher distribution test (Fisher, 1953) is used for determining a normal distribution of points on a sphere about the central axis.

To determine if the data within each cluster contains a Fisher distribution, the chi-square goodness-of-fit test is applied. This test measures the divergence between the observed frequencies and the Poisson frequency. The results will approximate the frequencies expected if the diagram were drawn, at random, from a uniform population (Flinn, 1958). This chi-square test has been used or recommended for fabric diagrams with various cell patterns by many authors (Winchell, 1937; Stauffer, 1966; Vistelius, 1966; Knoring, 1970; Mahtab et al., 1973) with satisfactory results. The calculated chi-square must be less than the theoretical chi-square determined from tables for a possible existence of a normal Fisher distribution (Knoring, 1970).

Dispersion (scatter) of data about the mean can be calculated by rotating the mean to the center of the sphere before determining the dispersion. When the value for the dispersion of data about the mean

is found to be significant, the data points tend to be tightly grouped around the mean. A high value of dispersion suggests a wide variation in the clustering of data. A confidence interval for the mean orientation can be calculated, but its validity assumes the existence of a normal distribution.

Use of the program PATCH allows joint clustering to be considered at all geographic locations and provides a statistically valid means of subdividing the data into individual joint sets.

Discussion

The analysis and results of the orientation data will be discussed in two sections with respect to the Northern and Southern Conasauga Belt.

Northern Conasauga Belt. The rose diagrams for the data collected in the Northern Conasauga Belt are reproduced in Figure 9. Location N1 through N4 represent the four sites of joint measurements noted on the sample location map (Figure 2, p. 5). Joint data plotted from location N1 appear to have a high degree of variation between joint measurements, with only weak evidence for a dominant orientation of joints. The other locations have less variation and exhibit multiple prominent joint orientations. In general, there are multiple joint orientations or sets with azimuths ranging from N-S to nearly E-W. The majority of the dip directions are to the north. The lesser number of joints with southerly dip directions have approximately the same orientation as the northerly dipping joints found in other locations. An example of this is N2, which has one

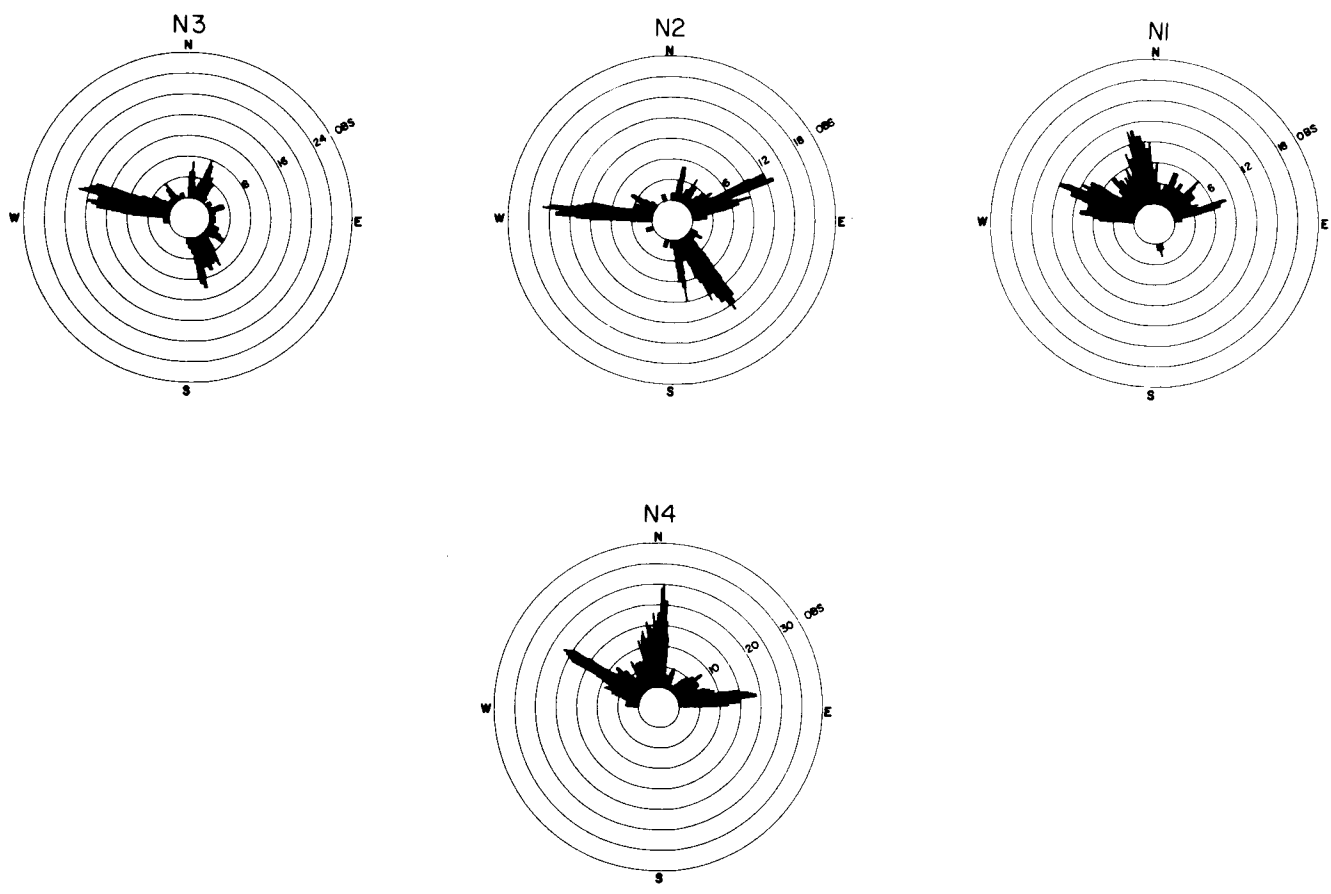


Figure 9. Rose diagrams of the Northern Conasauga Belt joint orientations for sampling locations N1 through N4.

set striking N30W and dipping south, while N1 has approximately the same high frequency of orientation (N39W), but the joints dip in the northern direction. The data collected at N1 were recorded from siltstones, while those in N2 came from shales. This dip direction change may be due to a change in the competency of the rocks (Nickelsen and Hough, 1967) and will be discussed later.

The results of the cluster analysis have been reproduced in Table 1, which lists results for each sub-location of the four northern locations. The different sub-locations of a single location display relatively wide variations in mean strike. This problem is related to the fewer than adequate number of measurements used to define a single cluster, as discussed earlier. When this sub-location data is combined in single locations, N1 through N4, consisting of a minimum of 120 joints per location, comparable results are observed. Table 2 is the summary of mean clusters when each sub-location is combined into its unit location. This data clearly suggests the existence of the two primary joint sets at each location with a third set evident at locations N3 and N4. The percentage of data within each cluster is not strictly related to its frequency. A high frequency of clustering of a single set may be related to its ease of weathering along the joint plane. Such a differential weathering process would expose joints of certain orientations more readily than others, and the measured joint may not actually be part of the most predominant set formed in the rock.

The percentage of unclustered data for location N3, in the summary table, is much higher than at the other locations. This data

KEY	LOCATION	SEC	STRUCTURE	N	S	D	DISP	CLUS			
N1	BCR-EAST USNFFF	A	BEDDING		N49E	51SE					
			J1	31	N44W	73NE	13	52			
			J2	25	N39E	40NW	23	42			
			OTHER	4				6			
		B	BEDDING		N60E	42SE					
			J1	21	N14W	78NE	44	35			
			J3	23	N56W	52NE	28	38			
			OTHER	16				27			
			N2	BCR-USNFFF	A	BEDDING		N60E	53SE		
						J1	19	N26W	66SW	47	32
J2	33	N83E				30NW	39	55			
OTHER	8							13			
B	BEDDING				N58E	47SE					
	J1	14			N35W	73SW	129	23			
	J2	19			N65E	35NW	45	30			
	J3	12			N89W	47NE	14	16			
	OTHER	15						25			
	N3	BCR-ZION PATROL RD.			A	BEDDING		N42E	47SE		
J1			10	N49W		85SW	35	16			
J2			16	N15E		43NW	46	27			
J3			18	N70W		63NE	109	30			
OTHER			16					27			
B			BEDDING		N65E	46SE					
			J1	21	N68W	78SW	23	35			
			J2	4	N14E	21NW	169	7			
			J3	22	N80W	51NE	270	37			
			OTHER	13				21			
			N4	Y12	A	BEDDING		N67E	59SE		
						J1	4	N04W	64NE	448	9
						J2	8	N03E	66NW	1066	17
						J3	26	N68W	31NE	45	57
OTHER	8							17			
B	BEDDING				N65E	60SE					
	J2	29			N81E	31NW	19	73			
	OTHER	11						27			
C	BEDDING				N62E	66SE					
	J1	5			N16W	73NE	64	6			
	J3	8	N62W	26NE	51	57					
	OTHER	1				7					
D	BEDDING		N61E	67SE							
	J1	17	N23W	68NE	53	40					
	J2	18	N81E	23NW	18	43					
OTHER	7				17						
E	BEDDING		N64E	57SE							
	J1	3	N07W	57NE	141	13					
	J2	3	N06E	58NW	82	13					
	J3	15	N76W	37NE	29	65					
	OTHER	2				9					
F	BEDDING		N63E	62SE							
	J1	4	N07W	63NE	52	24					
	J2	8	N09E	56NW	27	47					
	J3	4	N80E	38NW	56	24					
	OTHER	1				5					
G	BEDDING		N68E	59SE							
	J1	8	N08W	73NE	56	44					
	J3	10	N88E	37NW	78	56					
	OTHER	0									

Table 1. (continued)

The following legend applies to all tables in this report,
but all of the terms do not occur in each table.

KEY	outcrop location
LOCATION	field location
SEC	sub-location
STRUCTURE	bedding, joint set, or non clustered joints
N	number of measurements
S	strike of structure
D	dip of structure
DISP	dispersion
CLUS	percent clustered
CONF	cone of confidence of the strike/dip

Table 2. Combined results of cluster analysis of joint orientations for all locations in the Northern Conasauga Belt

KEY LOCATION	STRUCTURE	N	S	D	DISP	CLUS	CONF
N1 BCR-WEST USNFFF	BEDDING		N54E	46SE			
	J1	37	N59E	40NW	18	31	
	J2	61	N39W	69NE	10	51	
	OTHER	22				18	
N2 BCR-USNFFF	BEDDING		N59E	50SE			
	J1	62	N76E	33NW	41	52	
	J2	34	N30W	67SW	47	28	
	OTHER	24				20	
N3 BCR-ZION PATROL RD	BEDDING		N54E	45SE			
	J1	12	N14E	41NW	62	10	
	J2	40	N76W	55NE	107	33	
	J3	15	N46W	85SW	37	13	7/7
	OTHER	53				44	
N4 Y12	BEDDING		N64E	61SE			
	J1	22	N04E	62NW	213	11	2/2
	J2	107	N84W	30NE	22	53	
	J3	42	N13W	67NE	44	21	4/3
	OTHER	30				15	

were collected from a 5-cm (2.0-inch) thick siltstone bed at one sub-location (N3-A) and a 1.3-cm (0.5-inch) bed of siltstone at the other (N3-B). This wide variation in bed thickness may be the result of the thicker bed being more competent and having a lower value of dispersion. The mean dispersion at N3 sub-location A is 63 while that at sub-location B is 154.

Data from each sample location were plotted as poles to joint surfaces on the lower hemisphere of an equal area projection and contoured using the computer (Figure 10). This graphical representation of data considers both the magnitude and the direction of the dip. The diagrams show broad and highly dispersed girdles with dips ranging from 35 degrees to near vertical. When the data are rotated to the position where the bedding becomes horizontal, 90 percent of the joints fall within the dip range of 80 to 90 degrees. This rotation flattens out the Whiteoak Mountain thrust. The mean strike of the joints does not appear to be analogous in all locations, suggesting that they may have a complex mode of formation.

Plotting the mean clustered joint orientations for each location onto the original base map displays the relationship between the joint sets in an east to west direction (Figure 11). For an increase in clarity, the joint orientations for the Northern belt have been plotted in Figure 12 and reoriented so that magnetic north is at the top of the drawing. This diagram clearly shows the relationship between each joint set and the Whiteoak Mountain thrust fault. The angle between joint sets is 90 degrees in locations N3 and N4, 74 degrees in N2 and 82 degrees in N1.

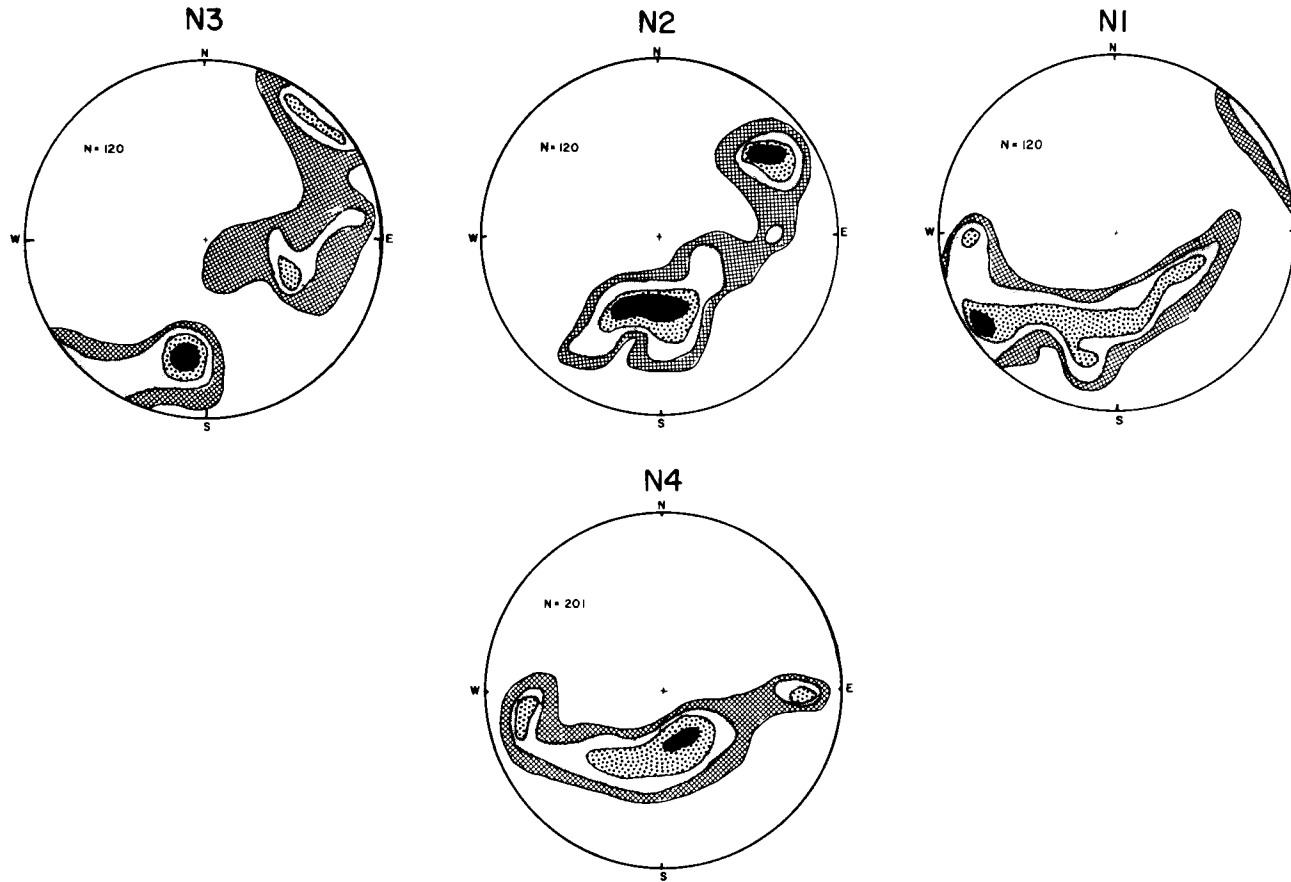


Figure 10. Equal-area projection of poles to joint planes for outcrop locations N1 through N4 in the Northern Conasauga Belt. N represents the total number of measurements contoured at 1%, 3%, 5%, and 10% intervals.



Figure 11. Base map projection of joint orientations representing joint sets J-1 through J-4.

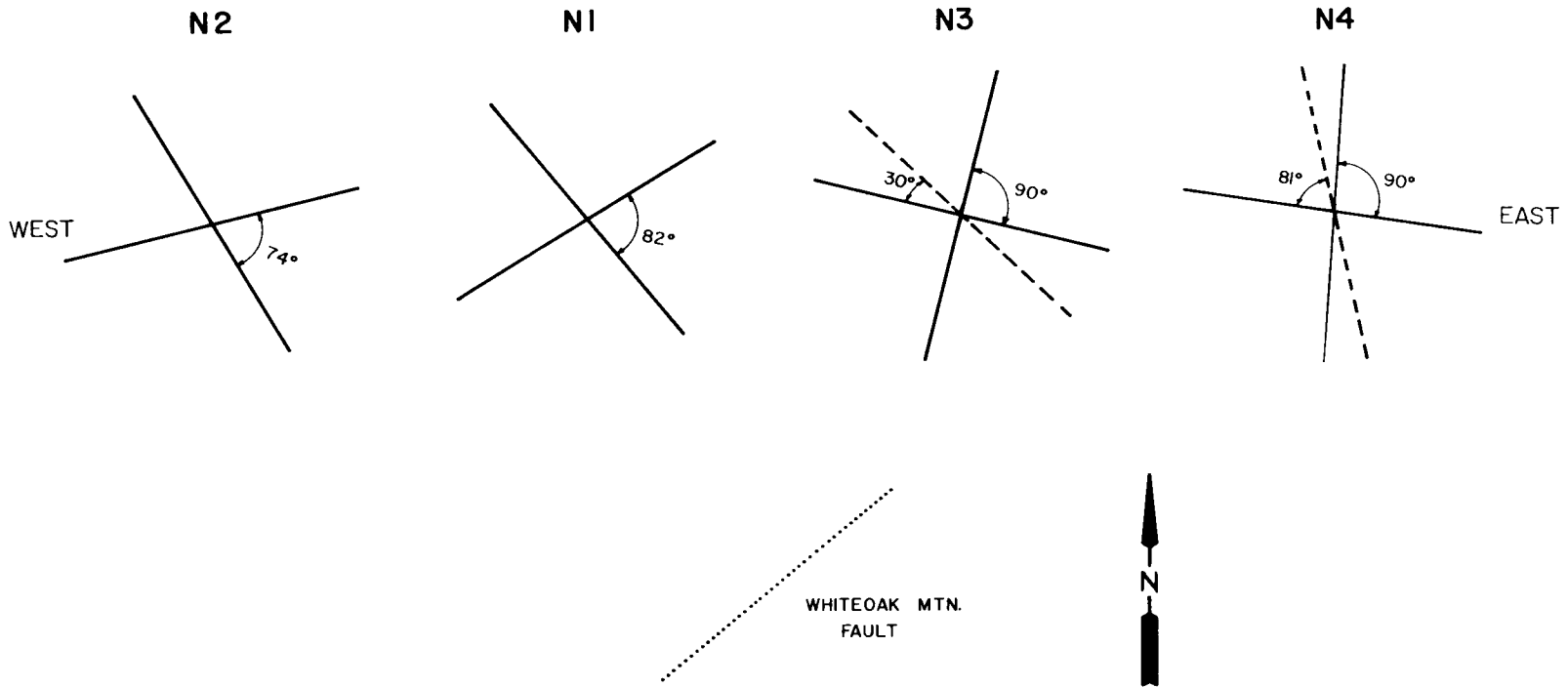


Figure 12. Summary diagram of clustered joint orientations in the Northern Conasauga Belt. The diagram depicts an east to west traverse of outcrop locations N1 through N4. The strike of the Whiteoak Mountain Fault is also displayed.

The assumption that jointing occurred during the thrusting is supported by the fact that upon restoring the thrust to its pre-ramp position, the mean joints clustered nearly vertical. This assumption allows the determination of the kinematic types of joints formed. The joints parallel to the thrust fault are called strike joints and the set normal to this is called an a-c set (Price, 1966). The combination of these two sets would be part of a single orthogonal set (Stearns and Friedman, 1972). The joints, as seen in locations N1 and N2, are tension fractures (Hodgson, 1961) where fracturing has occurred at right angles to the direction of the maximum stress. The formation of the joints can be explained by considering the forces occurring during thrust sheet transport. The a-c joints could have formed by a compressional force acting on the thrust plate and the strike joints may have formed by a warping of this sheet as it was being transported over the underlying sediments. This is only one of numerous possibilities for the formation of the joints and reflects the lack of current understanding of the subject.

The joints at locations N3 and N4 are more difficult to explain. The orthogonal set in this case appears to deviate from the orientation of the thrust and may suggest forces with a shear as well as a tension component. They could be related to the thrusting or may have formed during a later period of repositioning of the thrust system, which would overprint the original set. The Whiteoak Mountain thrust fault system is very complex and it is believed to be a polyphase deformation structure in this area (Ossi, 1979). If this is the case, it would explain the wide dispersion and unsystematic

relationship between the joints measured.

The lack of exposures in the Northern Conasauga Belt along with the complex nature of the thrusting results in a relatively unsystematic pattern of joint orientations. It is believed that the prediction of jointing, based on the few and complex results obtained, would lead to inaccurate results. Therefore, the Northern Conasauga Belt was not considered for the fracture porosity and permeability determination.

Southern Conasauga Belt. Data collected in the Southern Conasauga Belt is plotted on frequency diagrams (Figure 13) with locations S1 through S7 corresponding to the locations labeled on the base map (Figure 2, p. 5). The rose diagrams indicate that some sample locations contain a large scatter between measurements, as in location S1 and S7, while a few locations, S2 and S5, have very low scatter with well defined multiple prominent joint orientations. All locations contain two major joint sets with strikes of approximately N30E and N35W and dip directions varying from north to south.

Mean cluster analysis results for each sample sub-location are listed in Table 3 with a total of 930 joint orientations reported at the seven locations. The percentage of data not falling within one of the calculated clustered sets is low, with a mean value of 20 percent. At location S6-A, the data was recorded from a 13-mm (0.5-inch) bed of siltstone while S6-B was collected from a 6.3-mm (0.25-inch) bed of shale. The strike direction of each joint set is very similar at each of the sub-locations, but the joints are dipping in the opposite direction. This is related to the siltstone

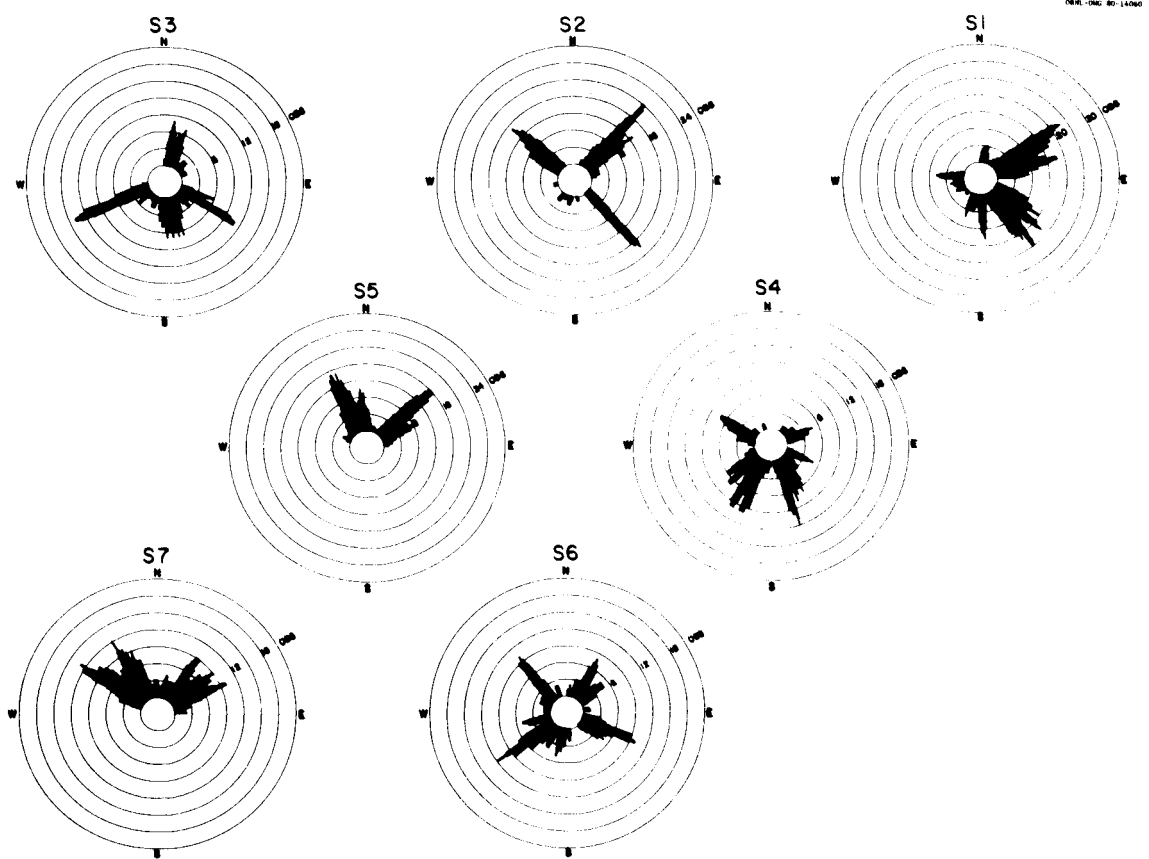


Figure 13. Rose diagrams of the Southern Conasauga Belt joint orientations for sampling locations S1 through S7.

Table 3. Results of cluster analysis of joint orientations for all sub-locations in the Southern Conasauga Belt

KEY	LOCATION	SEC	STRUCTURE	N	S	D	DISP	CLUS		
S1	BEARDEN LAKE	A	BEDDING		N68E	44SE				
			J1	31	N32W	81SE	17	52		
			J2	17	N59E	51NE	61	28		
			J3	4	N70E	31NW	440	7		
			OTHER	12				13		
		B	BEDDING		N66E	37SE				
			J1	20	N35W	86SW	141	33		
			J2	6	N17E	88SE	31	10		
			J3	19	N71E	44NW	37	32		
			OTHER	15				25		
		C	BEDDING		N50E	27SE				
			J1	8	N42W	45SW	15	14		
			J2	7	N02E	69NW	260	12		
			J3	29	N78E	29NW	45	49		
			J4	5	N59W	82SW	144	8		
			OTHER	10				17		
D	BEDDING		N50E	42SE						
	J1	33	N46W	80SW	15	55				
	J2	13	N58E	75NW	36	22				
	J3	9	N66E	50NW	83	15				
	OTHER	5				8				
S2	BULL BLUFF	A	BEDDING		N53E	40SE				
			J1	25	N44W	87NE	290	42		
			J2	20	N45E	47NW	297	33		
			OTHER	15				25		
		B	BEDDING		N52E	40SE				
			J1	29	N51W	76NE	93	48		
			J2	16	N44E	62NW	38	27		
			OTHER	15				25		
		S3	MVR-EAST	A	BEDDING		N76E	40SE		
					J1	9	N48W	73SW	17	15
J2	13				N06E	32NW	104	21		
J3	20				N69E	84SE	187	33		
OTHER	19							31		
B	BEDDING				N55E	29SE				
	J1			7	N64W	75SW	64	18		
	J1			4	N07E	50SE	157	10		
	J2			8	N31E	30NW	133	20		
	OTHER			25				52		
S4	MVR-HFIR	A	BEDDING		N56E	30SE				
			J1	17	N44W	77SW	17	28		
			J2	17	N25E	87SE	252	28		
			J4	10	N63W	76NE	82	17		
			OTHER	16				27		
		B	BEDDING		N60E	33SE				
			J1	23	N27W	83SW	38	38		
			J2	14	N42E	82SE	71	23		
			J3	10	N73E	43NW	21	17		
			OTHER	13				22		
S5	MVR-SWSA	A	BEDDING		N50E	42SE				
			J1	27	N18W	53NE	47	45		
			J2	25	N55E	74NW	18	42		
			OTHER	8				13		
		B	BEDDING		N80E	41SE				
			J1	22	N26W	65NE	125	44		
			J2	21	N47E	60NW	153	42		
			OTHER	7				14		
S6	MVR-WEST	A	BEDDING		N37E	40SE				
			J1	22	N63W	85SW	113	37		
			J2	24	N38E	49NW	56	40		
			OTHER	14				23		
		B	BEDDING		N69E	26SE				
			J1	12	N47W	78NE	79	20		
			J2	33	N51E	65SE	17	55		
			OTHER	15				25		
S7	WHITE WING ROAD	A	BEDDING		N75E	38SE				
			J1	30	N48W	73NE	23	50		
			J2	14	N66E	55NW	45	23		
			OTHER	16				27		
		B	BEDDING		N79E	30SE				
			J1	24	N46W	76NE	45	40		
			J2	19	N41E	62NW	44	32		
			OTHER	17				28		

having greater competence than the shale, as was noted in the Northern section, so that it would require a larger stress to be applied for jointing to occur and with an added shear component may be responsible for the difference of joint dip. The summary table (Table 4) of the clustered mean for each location results in two joint sets, J1 and J2, present at all locations. Locations S1, S3, S4, and S6 have multiple joint sets with varying levels of dispersion. In most instances, the two major sets have lower values of dispersion (most prominent) than other sets clustered at the same location. The confidence limits about the mean of the joints are relatively low (2 to 7 degrees) when a normal Fisher distribution is present.

The contoured equal area projection of the data (Figure 14) displays similiar features as discussed in the frequency diagrams. In locations S1, S5, and S6, relatively tightly clustered girdles are apparent, while in locations S3 and S7, the girdles formed are very broad and dispersed. The dip magnitude, in most cases, is greater than 75 degrees and is independent of the dip direction. The two major joint sets appear in all diagrams with only slight variations in the dip direction (S6). The mean clustered orientations calculated for these two sets are joint strikes of N45W and N54E and dip magnitudes of 83 and 52 degrees, respectively.

The mean azimuth for each clustered location was plotted on the base map (Figure 11, p. 31) and displays a more uniform sampling distribution in the Southern Belt than locations measured in the Northern Belt. The mean orientations were plotted on a diagram

Table 4. Combined results of cluster analysis of joint orientations for all locations in the Southern Conasauga Belt

KEY LOCATION	STRUCTURE	N	S	D	DISP	CLUS	CONF
S1 BEARDEN LAKE	BEDDING		N58E	38SE			
	J1	78	N40W	83SW	22	33	
	J2	46	N54E	49NW	16	19	
	J5	24	N73E	32NW	128	10	4/4
	OTHER	91				38	
S2 BULL BLUFF	BEDDING		N52E	40SE			
	J1	45	N48W	85NE	53	38	
	J2	30	N46E	49NW	165	24	3/2
	OTHER	45				38	
S3 MVR-EAST	BEDDING		N66E	34SE			
	J1	16	N54W	74SW	22	16	
	J2	18	N68E	85SE	374	18	2/2
	J4	22	N15E	31NW	70	22	7/4
	OTHER	45				44	
S4 MVR-HFIR	BEDDING		N57E	32SE			
	J1	32	N30W	82SW	29	27	
	J2	11	N64E	36NW	44	9	
	J3	6	N60W	77NE	631	5	3/3
	J4	30	N31E	85SE	76	25	
	OTHER	41				34	
S5 MVR-SWSA	BEDDING		N64E	41SE			
	J1	49	N21W	57NE	46	45	4/3
	J2	46	N51E	67NW	24	42	
	OTHER	15				13	
S6 MVR-EAST	BEDDING		N49E	32SE			
	J1	12	N47W	78NE	79	10	
	J2	27	N56E	68SE	29	23	
	J3	22	N63W	85SE	113	18	
	J4	27	N35E	47NW	34	23	
	OTHER	32				26	
S7 WHITE WING ROAD	BEDDING		N76E	34SE			
	J1	57	N41W	75NE	27	48	
	J2	45	N48E	60NW	20	38	6/5
	OTHER	18				14	

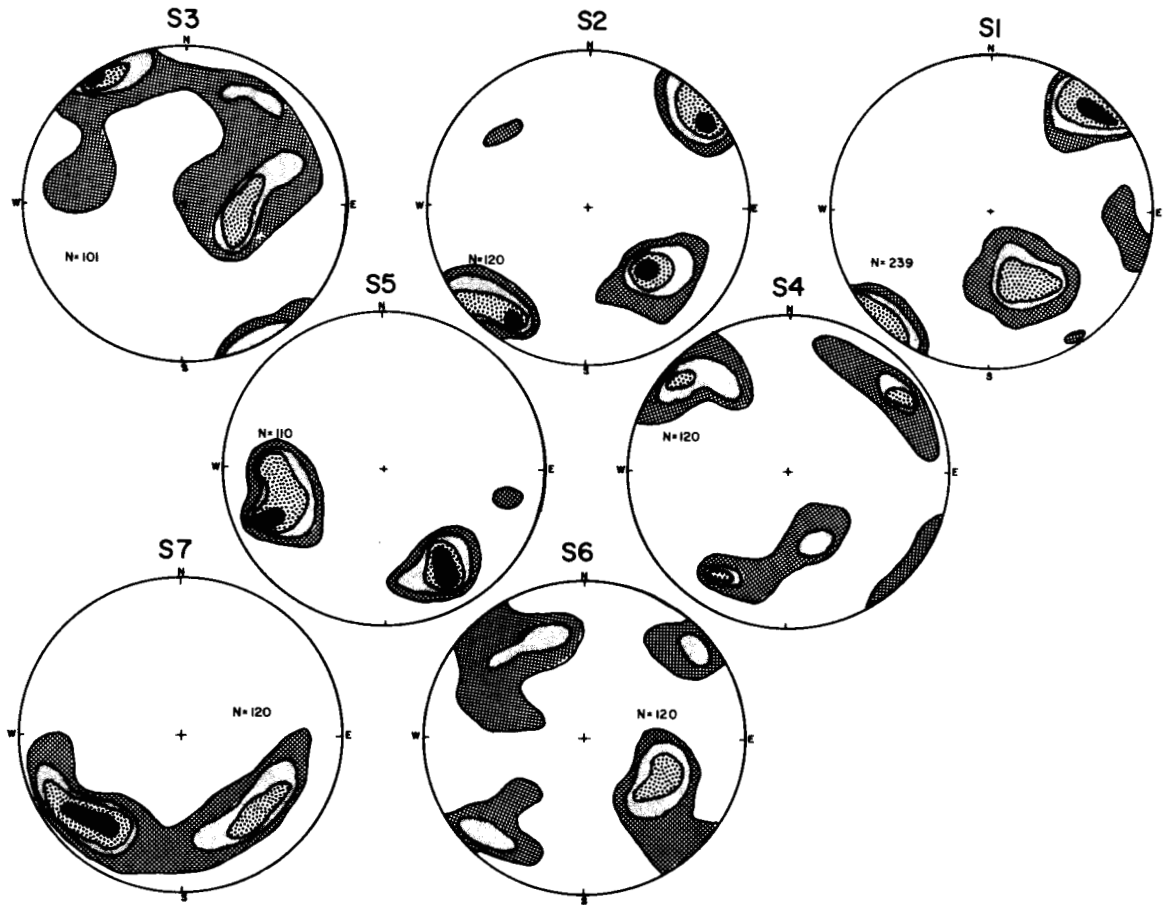


Figure 14. Equal-area projection of poles to joint planes for outcrop locations S1 through S7 in the Southern Conasauga Belt. N represents the total number of measurements contoured at 1%, 3%, 5%, and 10% intervals.

(Figure 15) representing a continuous traverse in an east to west direction of the base map. The two major joint sets, as plotted, have an acute angle of intersection between 69 and 89 degrees, suggesting that the joint sets are orthogonal. The diagrams also graphically display the approximate azimuths of three different fabric elements measured within the study area (Ossi, 1979). The fold (F1) and the fault (T2) represent two earlier periods of deformation occurring prior to thrust sheet emplacement.

The strike joints (parallel to the Copper Creek fault) and the a-c joints (normal to the strike joints) appear in all seven locations with little change in orientation along the entire traverse. The orthogonal set is believed to be created by tensile stresses (Hodgson, 1961) in a manner analagous to the tension joint formation discussed for the Northern Belt. Locations S3, S4, and S6 contain a secondary joint set very closely related to the azimuth of fault T1. These joints, along with the S4 and S6 sets that are parallel to fold F2, may be related to a pre-thrusting stage of deformation. Due to the difficulty in determining the age relationship of joints (Price, 1967), the multiple joint sets could also be related to a later stage of loading of the thrust sheet after its emplacement.

Data collected from the drill cores support the existence of the orthogonal set. A drill core sample (Figure 16) taken at a depth of 9 m (29.5 feet) displays normal joint sets in a shale bed. The orientation of the joints within this core is not known, as no studied drill cores were oriented. Oriented drill cores would have

ORNL-DWG 81-5904 ESD

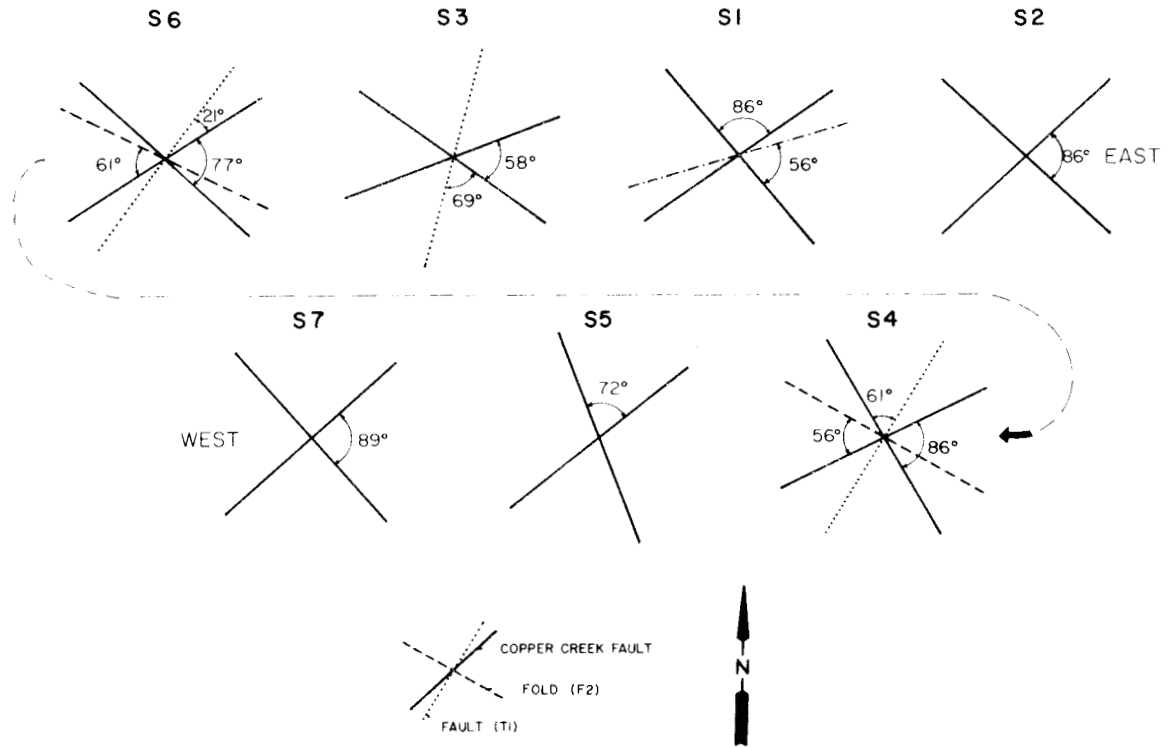


Figure 15. Summary diagram of clustered joint orientations in the Southern Conasauga Belt. The diagram depicts an east to west traverse of outcrop locations S1 through S7. The strike of the Copper Creek Fault and two earlier episodes of deformation are also displayed.

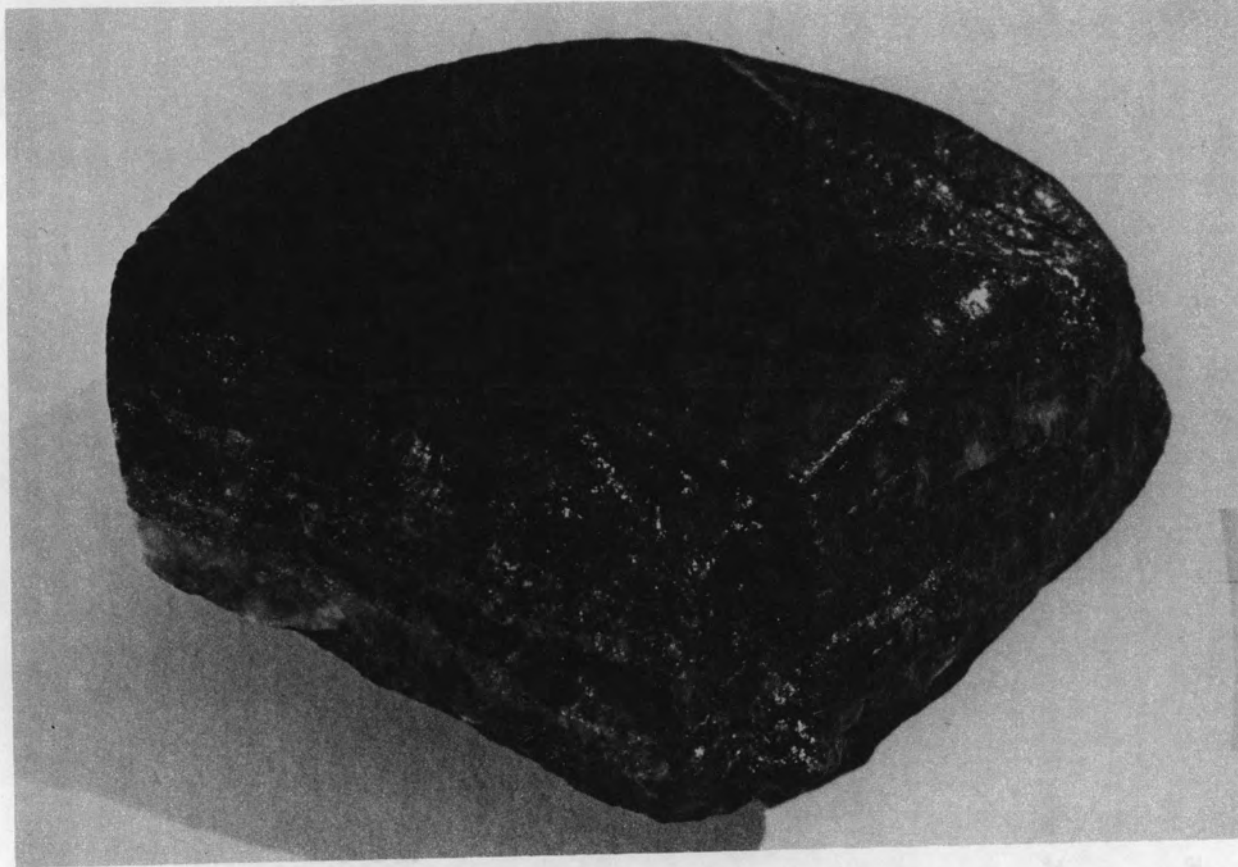


Figure 16. Photograph of drill core from the Southern Conasauga Belt taken at a depth of 9 m. This core (approximately 3.5 cm across) displays two joints intersecting at 90 degrees within shale beds.

been useful in the study to evaluate other parameters of joints and also relate the surface measurements to depth. Slight weathering has occurred along both joint planes and is displayed by the growth of calcite in filling the joint.

Joint Density and Length Analysis

The data collected for the density and length analysis of the shales and siltstones were very difficult to quantify. The joint density was measured at 47 different sites; a total of 518 joint lengths were recorded. This data was analyzed using the Statistical Analysis System (SAS) programming package (Barr et al., 1979). Linear regression analysis was used to develop mathematical relationships existing between the parameters (joint length, density, and bed thickness). Numerous models were applied in order to get the best possible fit to the data. The residuals were examined in detail (Draper and Smith, 1966) for outlier elimination as well as to aid in producing the best fitting models.

The results of all of the applied methods indicate very little correlation between the different parameters. The r-square value, in many cases, was less than 5 percent for the best fitting model. The major reason for this lack of correlation is probably due to differential weathering between outcrops as well as irregular bed thicknesses on a localized scale. These two factors can not be quantified, and their estimated numerical impact on the results is difficult to determine.

It was finally decided that the only way to handle this data was

to combine all joint sets and locations together into a single group. The factors affecting the length and density that would be considered were the bed thickness and the lithology. The mean values for all of the data were calculated along with their standard deviations. This result was then graphically displayed, and appropriate relationships were developed.

Discussion

Bed thickness is the most critical parameter in relating length and density of joints. The graph of joint length versus bed thickness in shale (Figure 17) is plotted with each point representing 50-150 measurements. The mean plus and minus one standard deviation unit is plotted to display the range of data measured. The length of the joints in the shale appear to be independent of bed thickness with a mean joint length value of approximately 12 cm (5 inches) for bed thicknesses ranging from 2 to 11 mm (0.08 to 0.4 inches). The density of joints in shale (Figure 18) displays a decrease in the number of joints with increasing thickness. For a 2-mm bed thickness, there are approximately 27 joints per meter, while at an 11-mm thickness, density decreases to 10 joints within a one meter length.

By plotting the joint length versus joint density for each of the thicknesses measured (T), the results show a poorly defined relationship (Figure 19). The thicker beds have slightly shorter joint lengths than the thin beds. The important factor to be considered when describing this plot is the actual mean range of data. For joint lengths ranging from 10 to 12 cm (2.5 to 5 inches),

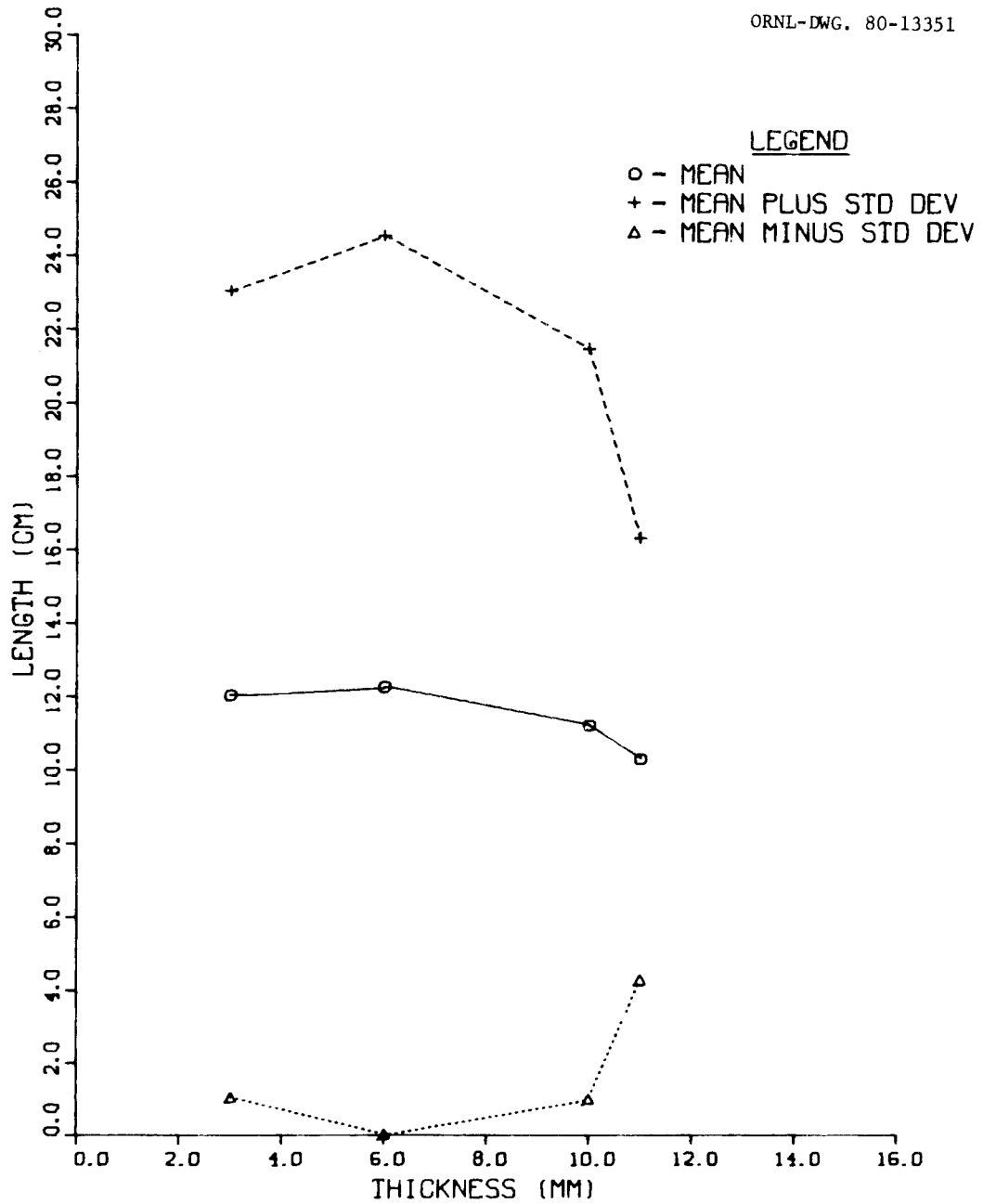


Figure 17. Joint length versus bed thickness in shale beds of the Conasauga Group. The data plotted represents 400 measurements.

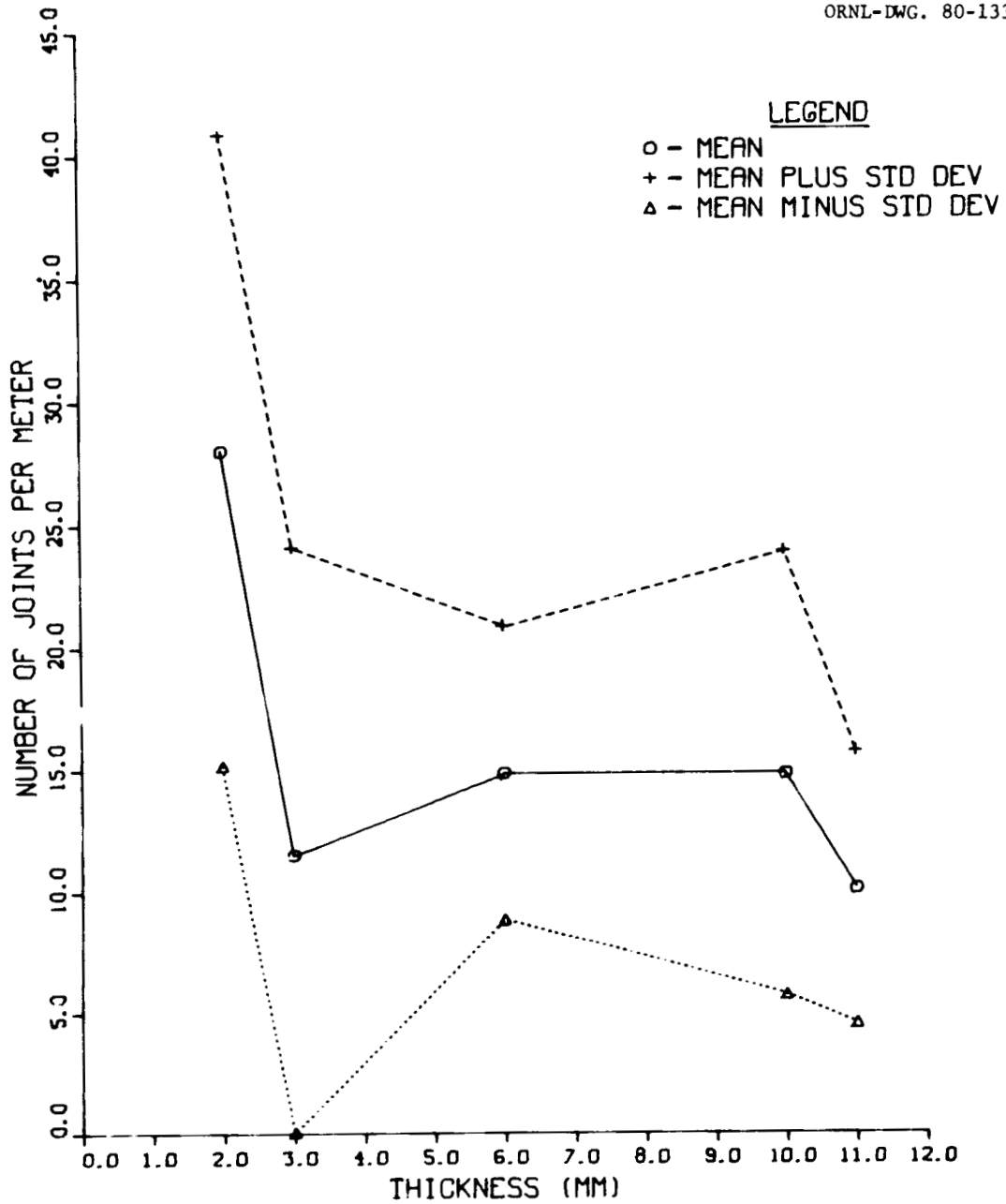


Figure 18. Number of joints per meter versus bed thickness in shale beds of the Conasauga Group. The data plotted represents 31 measurements.

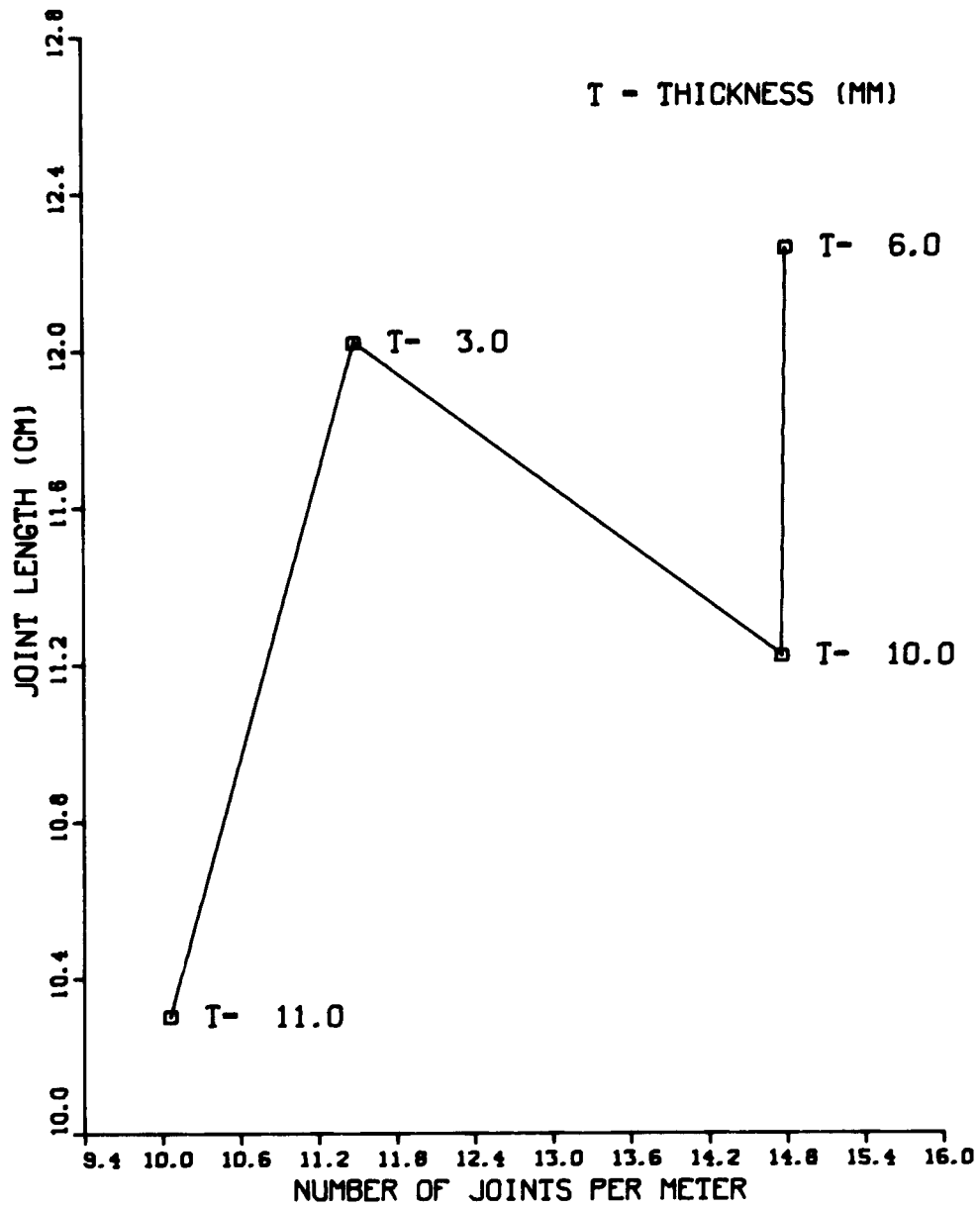


Figure 19. Joint length versus number of joints per meter in shale beds of the Conasauga Group.

joint density ranges between 10 and 15 joints per meter. This is a relatively narrow band of results which is significant and can be considered in the model.

The siltstone data graphically displays definite trends with changing bed thickness. Joint length in the siltstone (Figure 20) increases with an increase in bed thickness. The 76-mm (3 inches) bed thickness represents 23 percent of the siltstone data, so the trend is very significant. Joint density has an inverse relationship with bed thickness (Figure 21). An increase in bed thickness results in a decrease in the density of joints present.

Plotting the joint density against the length of joints for each thickness value (T) yields a systematic relationship (Figure 22). The thick beds of siltstone have very few long joints, while the thinner beds have abundant short joints. This is a very significant relationship and is analagous to that discussed by many authors when measuring data in thick clastic units (Price, 1966; Nickelsen and Hough, 1967).

Interpretation

Comparison of the results of the data collected in the shale and siltstone beds reveals a very interesting relationship. For example, by selecting a mean bed thickness of 10 mm (0.4 inches), the influence of lithology on joint length and density can be examined. This representative bed is relatively thin for a siltstone, as seen in the field, but it provides a means of comparison between the two lithologies.

The mean joint length in a 10-mm bed of shale is 12 cm (4.7

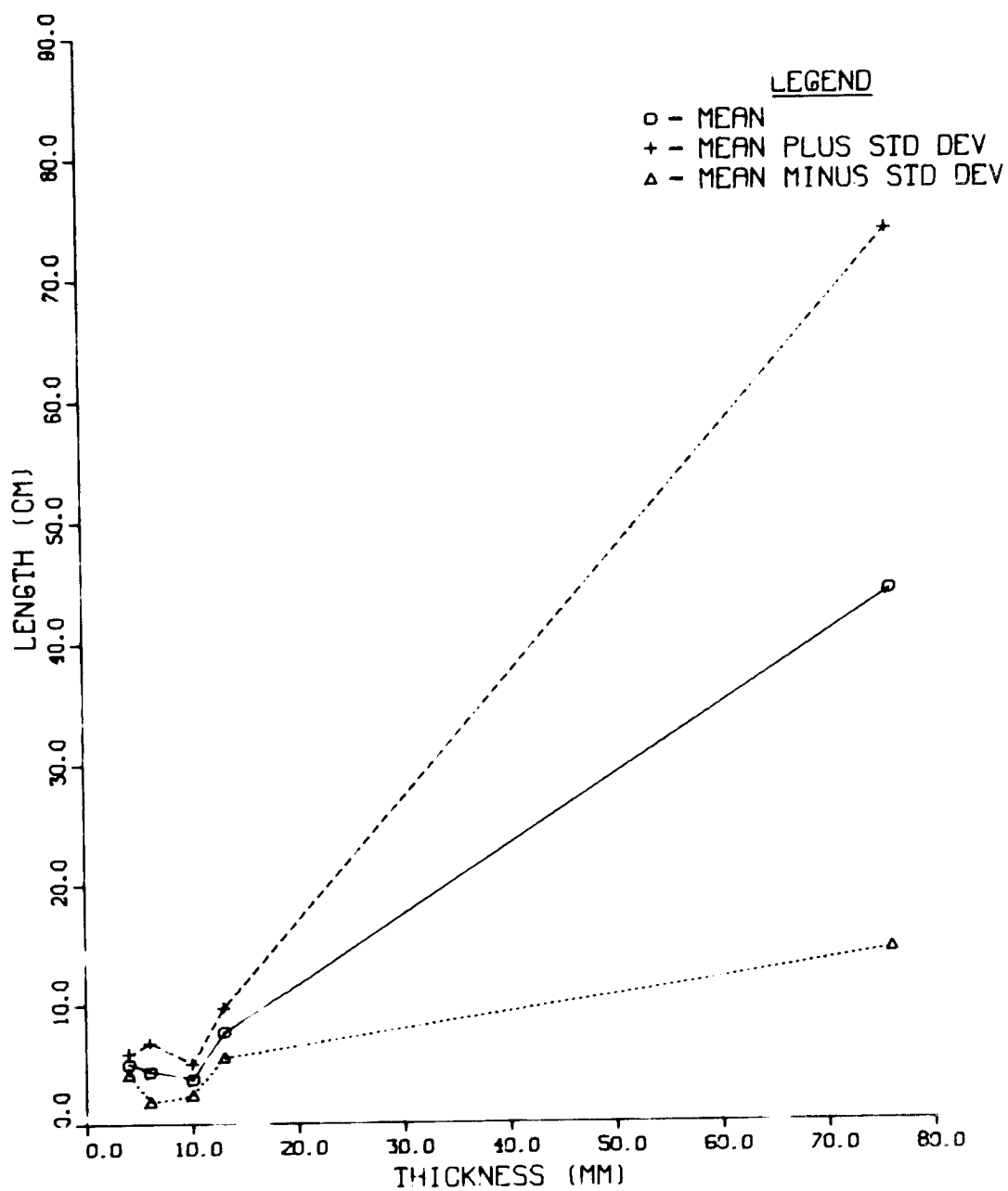


Figure 20. Joint length versus bed thickness in siltstone beds of the Conasauga Group. The data plotted represents 105 measurements.

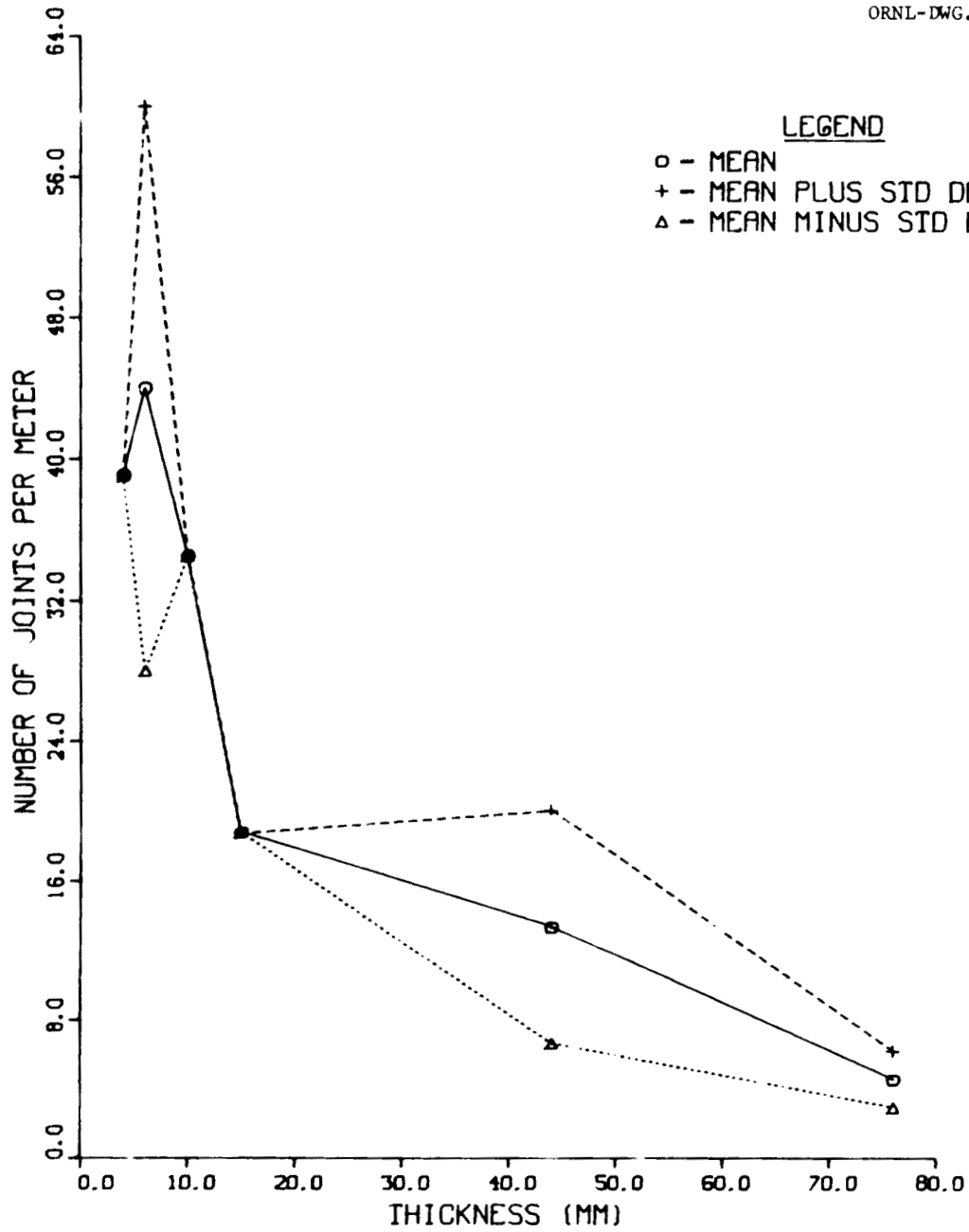


Figure 21. Number of joints per meter versus bed thickness in siltstone beds of the Conasauga Group. The joint data plotted represents 11 measurements.

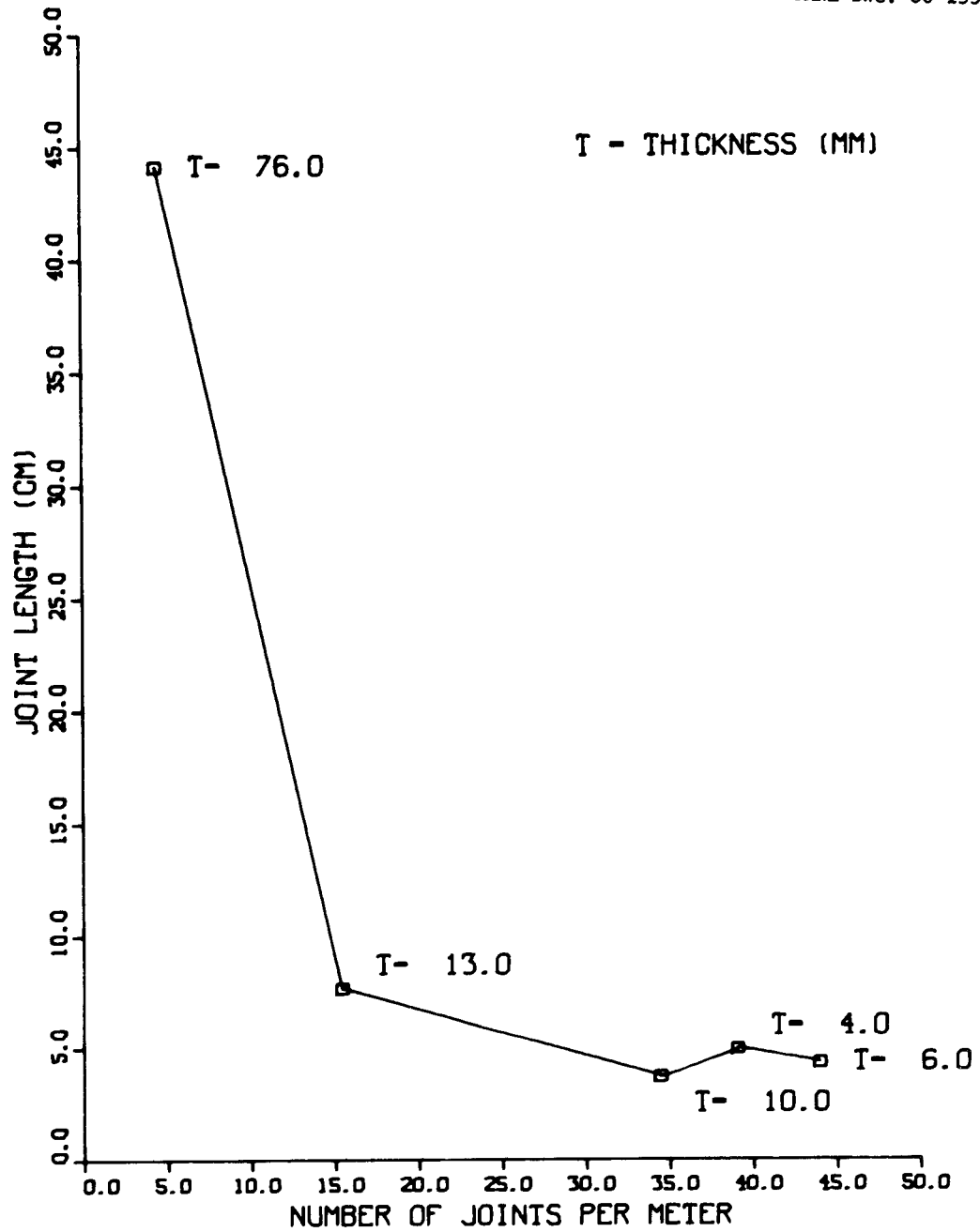


Figure 22. Joint length versus number of joints per meter in siltstone beds of the Conasauga Group.

inches) and in the same bed thickness of siltstone, the joint would have a mean length of only 6 cm (2.4 inches). The shale bed would contain 15 of these 12-cm joints for each meter traversed while the siltstone joint density is 30 joints per meter. In the shale bed, the joint density and length is lower than measured in the siltstone. Such observations may be related to the variations in the brittleness of beds in differing lithologies. Shale beds are normally ductile and tend to flow under stress (Harris et al., 1960). The same amount of stress applied to the siltstones may result in brittle fracturing. Price (1966) suggests the brittleness of a rock may be a function of the amount of strain energy originally stored within the rock; the strain energy stored in the siltstone is greater under equal stress conditions than that contained in the shale.

An increase in bed thickness results in a decrease in joint density and, in the siltstones, an increase in joint length. This can be explained by the frictional forces acting along a bedding plane (Price, 1966). The thicker beds, being more competent, will have less intense frictional forces acting on them, and the developed joints will increase in length rapidly. The thin beds contain large frictional forces acting on them and result in the formation of many short joints. This relationship is noted in thick clastic rocks of differing lithologies (Harris et al., 1960).

Results

Joint length and density analysis show that the values of these properties in the siltstones are quite dependent upon changes in bed thickness, while in the shales, joint length and density respond

somewhat more independently to the bed thickness change. The problems that may affect this independent reaction of shale parameters to changes in bed thickness are numerous; the primary parameters are discussed below.

One of the most obvious factors affecting the results is the precision of bed thickness measurements. The shale beds are discontinuous and very thinly bedded, so that only an average thickness could be recorded. The influence of weathering is important; and although it cannot be quantified, when the data from different sites is combined, it may explain the wide ranges in results.

The question of what constitutes a bed in a stress field is another important problem. The shales may have reacted to tectonic pressures as a unit and not as individual beds (Hodgson, 1961). The data was measured from a single bedding plane with the total extent of the joints' penetration into the strata not determined. This effect is important when considering the brittleness of individual beds. The shale beds in some sites may have been more brittle than in others; i.e., their responses to the same tectonic stresses differed. The more brittle beds would have a higher density of joints than the less brittle ones (Harris et al., 1960). Combining all of the data would result in a wide range of density values.

The above problems may have all played an important role in modifying the data measured in the field. In an analytical model, though, quantifying the results is essential. It is believed that the trends produced from the collected data are the same as what

might be seen in the field at any one location, so that the results of this data relating length and density of joints to bed thickness in both shales and siltstones will be used in the model.

Summary

Joint orientations were measured from surface exposures of the Conasauga Group along the two major strike belts. The data were analyzed with the aid of the computer, and the joints were subdivided into individual sets.

The Southern Conasauga Belt displayed a single orthogonal joint set with one group of joints parallel to the strike of the rocks (strike joints) and the other group normal to these (a-c joints). The joint set was apparent at all locations and was found to dip in a near perpendicular direction to the strata. The mode of formation of the joints is believed to be related to tension developed in the rocks during the thrusting event.

Joints in the Northern Conasauga Belt were measured and multiple joint sets were determined to reflect a complex mode of origin. These joints were believed to be a result of the polyphase deformation of the thrust sheet.

The results of the orientation analysis in the Southern Conasauga Belt were found to be applicable to prediction and will be used in the computer model.

Joint length and density measurements proved to be very sensitive to surficial weathering effects along with bed thickness measurements. The results for the individual joint sets proved

ineffective for prediction, and the data was combined into a single unit for trend determination. The shale beds were found to respond independently to changes in bed thickness. This is believed to be related to the competency of the beds along with the weathering factor. In the siltstone beds, the joint length increases and joint density decreases with increases in the bed thickness values.

CHAPTER III

COMPUTER MODEL AND RESULTS

Introduction

The determination of the fracture porosity and the parameters contributing to its calculation are a primary consideration of the model. Fracture porosity is defined as the ratio of the volume created by the joints to the total volume of the rock. This calculation has been used by many authors with data collected primarily from subsurface drill cores (Babcock, 1978; Parsons, 1966; Snow, 1968). Many assumptions are normally required to obtain values for the various parameters involved in the calculation because drill core analysis alone cannot provide sufficient data. The model developed here, however, will combine the data from drill cores with that collected at the surface to approximate the fracture porosity in the Conasauga Group at the Oak Ridge National Laboratory Reservation.

The fracture porosity is not the only porosity present in the rocks. Pirson (1953) described two other types of porosity that may be developed. Primary porosity is intergranular porosity which is caused by void spaces between constituent mineral grains. A secondary type of porosity is vesicular porosity caused by leaching and weathering of the rock near the ground surface. The fracture porosity is also considered a secondary porosity because it is created after the rock was deposited and lithified. The combined effects of the three types of porosity is the property that is

normally measured in the laboratory or field and called total porosity. The model developed in this study attempts to quantify the fraction of the total porosity that is caused by joints within the rocks.

Permeability due to fracturing is another important property that can be considered by a quantitative approach. Permeability is a measure of the relative ease with which fluids pass through a porous material (Davis, 1969). Even when the value of the total porosity is very low, permeability, due largely to fracturing, can be relatively high as compared with unfractured rocks with similar total porosity values (Stearns and Friedman, 1972). As an example, different rock types of the Santa Maria District in California illustrate the importance of fracture induced permeability to the formation of sites suitable for petroleum accumulation (Regan and Hughes, 1949). The rocks in that study area consisted primarily of chert and shale, both of which had very low porosities as measured from drill cores, and were generally considered to be impermeable. The presence of abundant fractures, however, provide sufficient permeability to allow hydrocarbon accumulation to occur to the degree that oil could be produced from these rocks on a commercial scale.

The present study is not concerned with the reservoir potential of the Conasauga Group, but rather is directed toward calculating a mean value for the fracture permeability in the Southern Conasauga Belt. The permeability that is calculated has a magnitude (conductivity) and a mean direction of flow. Previous studies in the Conasauga Group suggest a primary direction of ground water flow

parallel to the strike of the strata (Webster, 1976). The flow path is thought to be primarily along bedding plane surfaces and shale partings with only a low percentage of fluid flowing at oblique angles to the strike. The strike joints, as discussed earlier, can provide a definite conduit for fluid migration within the study area. The total groundwater flow may well be a combination of the permeability along joint and bedding plane surfaces in the strata.

Overview

The Fracture Flow Modeling System (FRAFLO) is a group of computer programs designed for calculating the fracture porosity and permeability within the Southern Conasauga Belt. The model developed contains many interrelated parts illustrated in a simplified flow chart (Figure 23). Options available range from the development of three-dimensional (3-D) diagrams of elevation or porosity surfaces to a tabular listing of the calculated fracture porosity and permeability (FRAFLO). After selecting an option, geographical coordinates of the entire study area are required (TOPMAK), from which the surface elevations can be computed (BLDMAT). If the option selected is a 3-D plot of the entire area, the data would be manipulated (MATFIX) and the plot produced (PLOSOU).

Selection of a particular site of interest within the Southern Conasauga Belt can be made and the surface elevations for each coordinate extrapolated (CELL). If a 3-D plot of the surface elevations for the site of interest is required, the computer will provide this type of graphical display (PLOCEL).

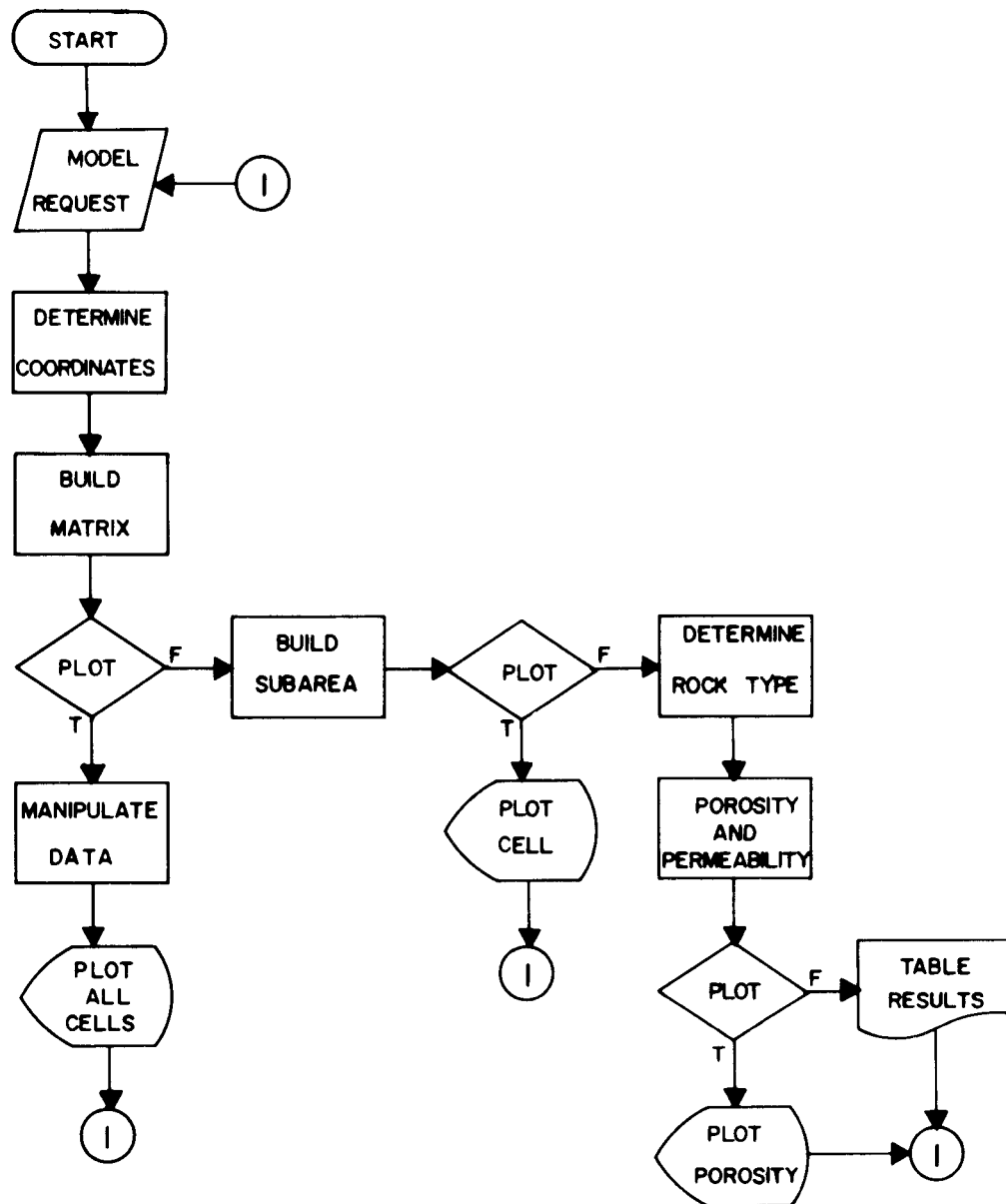


Figure 23. Generalized flow chart of the FRAFLO model.

Determination of the porosity and permeability requires entering the depth below the ground surface at the point in space where the calculation is to be performed. By selecting the nearest drill core available, the subsurface information contained in this core can be extrapolated for the selected site of interest (CORFIX). The parameters contributed from field measurements include joint orientations (ORDAT) and the mean density and length of the joints (DENLEN). The other parameters that need to be determined are the rock constituents (RCKTYP), bed thickness (THKCAL), and the size of the gap between the joint planes (GAPSET). By combining the parameters mentioned above, porosity and permeability resulting from the joints can be calculated (PORCAL). A mean vector direction of the permeability is calculated using the joint orientations (PRMVEC). The results of the porosity and permeability calculations can be displayed graphically (PLOCEL) or in a table form (TABPOR).

Spatial and Lithologic Calculations

Each subroutine will be described in detail with a discussion of required assumptions and algorithms derived. The entire model is written in FORTRAN for a Decsystem 10 computer. A complete listing of the program has been provided in Appendix A and a user guide of the model in Appendix B. A further discussion of the file structures and common variables used are listed in Appendix C and will not be discussed in the text.

Model Requested (FRAFLO)

FRAFLO is the main program for the entire computer model. The primary purpose is to determine the option requested and to call all subroutines required to produce the results.

Determine Coordinates (TOPMAK)

This subroutine is used to calculate the coordinates (latitude and longitude) and surface elevations for any point within the entire Southern Conasauga Belt.

The contoured base map was used to provide the necessary surface elevations for the model. The surface projection of the Southern Conasauga Belt was photographically enlarged, and an overlay was placed on each square of the Oak Ridge Administrative (ORA) grid. This unit square was divided into 361 subsquares each representing a surface of approximately 80.16 meters (263 feet) on a side. The surface elevations for the center of each of the subsquares was interpolated from the topographic map for the entire Southern Conasauga Belt within the reservation boundaries. These topographic data were coded and recorded in a file (STOPO.DAT) for permanent storage.

The subroutine TOPMAK reads the file STOPO.DAT and converts the coded data into latitude, longitude, and surface elevations for each subsquare. Latitude, as applied in the model, represents north-south ORA grid coordinates and the east-west ORA grid coordinates are equivalent to longitude. This data is then recorded into a temporary disk file, CONTUR.DAT, and stored for later use in the model.

Build Matrix (BLDMAT)

The coordinate and elevation data must be in a systematic form to be used in the model. This subroutine takes the data stored in the file CONTUR.DAT and builds a rectangular matrix encompassing all longitude and latitude values recorded in the area. The array created is dimensioned at 190 (longitude) by 38 (latitude) with all 38 positions of the latitude required to be filled. The range of the longitude values is from 20000 to 70000 and the latitude range is from 13000 to 23000. Latitudes located outside of the Southern Conasauga Belt, but within the rectangular matrix, are given a zero elevation value of 600. This value is required for application of the plotting subroutines. The data contained in the matrix, along with its surface elevations, are output into a new temporary file, SLALO.DAT, and the old file CONTUR.DAT is deleted.

Manipulate Data (MATFIX)

Data for a 3-dimensional plot must be manipulated in order to produce the required format for the plotting subroutine. This subroutine builds an array consisting of 190x38 elements by filling each array position with the required surface elevation for its particular location within the matrix. This results in a 3-axis coordinate system which can be graphically displayed. The elevations for each member of the array are written in a temporary file, SMAT.POT. The data stored in this file can be plotted in a 3-D diagram, or at a future time a contour plotting subroutine can be developed to produce a topographic map of the area.

Plot All Cells (PLOSOU)

This subroutine reads the file SMAT.POT into an array and outputs a 3-D surface elevation diagram of the entire Southern Conasauga Belt. This diagram has been reproduced in Figure 24 at a reduced scale. The surface elevations range from 600 feet (base map elevations are in feet) at the base to 1100 feet at the uppermost surface. The longitude is a west (0.0) to east (200.0) traverse of the rectangular grid system. The individual squares (cells) represent an 80.16 m (263 feet) length on each side. For example, the low surface elevation depicted by the cells at a longitude of 100.0 (47000) is the floodplain developed by the Clinch River.

The plotting package DISPLA (ISSCO, 1975) is required for any graphical results obtained.

Build Subarea (CELL)

Given the coordinate for a point located within the study area and the size of the subarea requested, subroutine CELL will calculate the location coordinates and surface elevations for all points within the subarea. The subroutine requires the input of the longitude and latitude values for a site of interest that is located within the Southern Conasauga Belt along with the number of divisions on the developed subarea (cell) edge. This information is used to determine the size and number of divisions of the cell edge, which has a total length of 80.16 m (263 feet) on a side. If the number of divisions requested is 10, then each subcell created will be approximately 8 m (26 feet) on a side ($80.16/10=8.16$). The minimum size that can be calculated for each subcell is 1.52 m (5 feet), which would result in

ORNL-DWG 80-10753

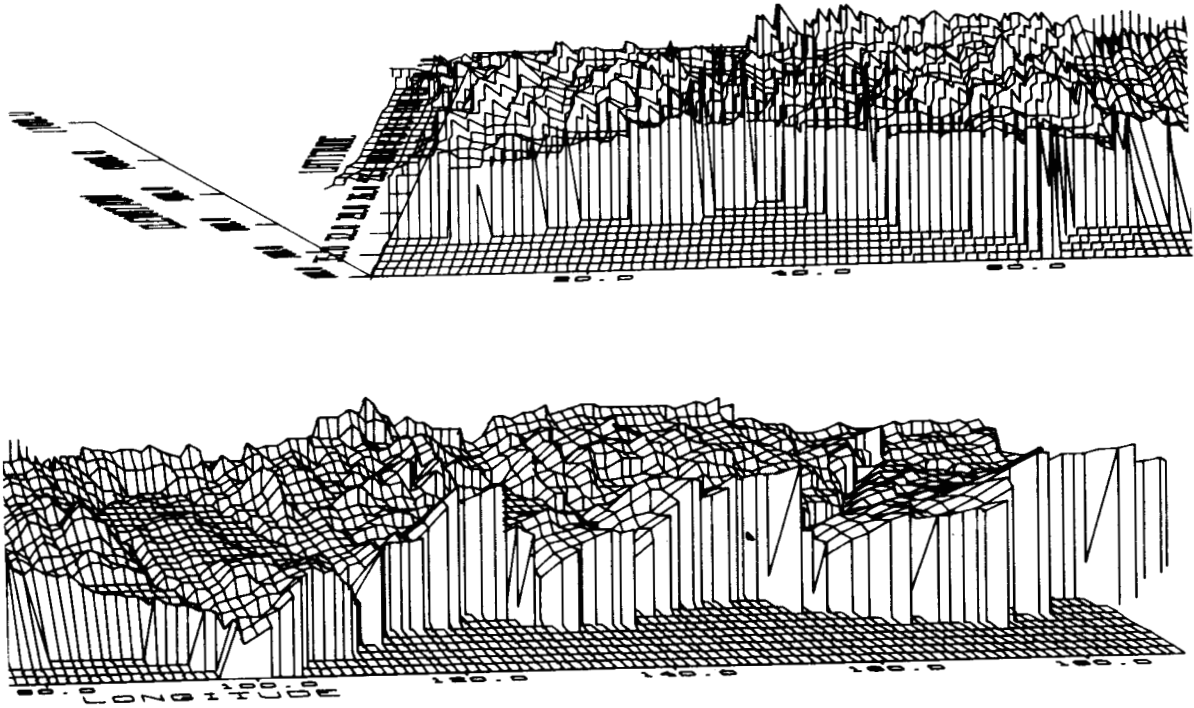


Figure 24. Surface elevation of the Southern Conasauga Belt. The vertical exaggeration is 0.017.

52 divisions.

By using an algorithm to determine all possible coordinates existing within the study area, the cell containing the point of interest is determined. This cell consists of one set of coordinates, analogous to those created by TOPMAK, in each of its four corners. The next procedure is to read the file SLALO.DAT and obtain the surface elevations for these four coordinates. This information will be used to calculate the elevation for each subcell formed.

Each subcell coordinate is calculated, and two equations, as listed below, are used for the interpolation of surface elevations for each point (Davis, 1973). The technique used has been proven effective for the creation of contour maps from data recorded in a grid pattern.

Equation 1 calculates the distance from the center of each subcell to the four corners of the cell.

$$\sum_{j=1}^4 D_j = \sum_{i=1}^4 \sqrt{(LO_i - LO)^2 + (LA_i - LA)^2} \quad (1)$$

The elevation for this newly created subcell is determined by dividing the difference between each of the elevations by the inverse distance to the four corners.

$$NEL = \frac{\sum_{i=1}^4 [EL/D_i]}{\sum_{j=1}^4 [1/D_j]} \quad (2)$$

This results in a weighted average elevation based on the elevations

of all four corners of the cell. The process is continued for each subcell with the coordinates and surface elevations written and stored in the file CELL.OUT.

Plot Cell (PLOCEL)

The surface elevation for each subcell can be plotted on a 3-D diagram representing the entire cell. Examples of the surface elevation plots were calculated for subcell increments of 15 (Figure 25) and 25 (Figure 26) divisions with a total surface of 79.25 m (260 feet) on a side. The maximum and minimum longitude, latitude, and surface elevation are determined and printed out on the plots. The longitude, at the zero value of the axis, is the minimum longitude (32236), and the maximum longitude (32496) is represented at the maximum value on the longitude axis. The same relationship exists for the plotted latitude data. The surface elevation, on the vertical axis, for each subcell coordinate was determined using the known elevation of the four corners. The vertical exaggeration can be individually calculated and will be different for each plot depending on the range of elevations in the cell.

The package DISPLA contains all of the plotter subroutine calls with their required arguments so their use will not be discussed.

Determine Rock Type (CORFIX)

The subroutine CORFIX determines the rock type, at a specified depth, from drill core data at all subcell locations. The two external inputs required for this subroutine are a drill hole number and the depth from the surface where the porosity and permeability

SURFACE ELEVATION PLOT

LONGITUDE MIN- 31184
LONGITUDE MAX- 31444
LATITUDE MIN- 19077
LATITUDE MAX- 19337

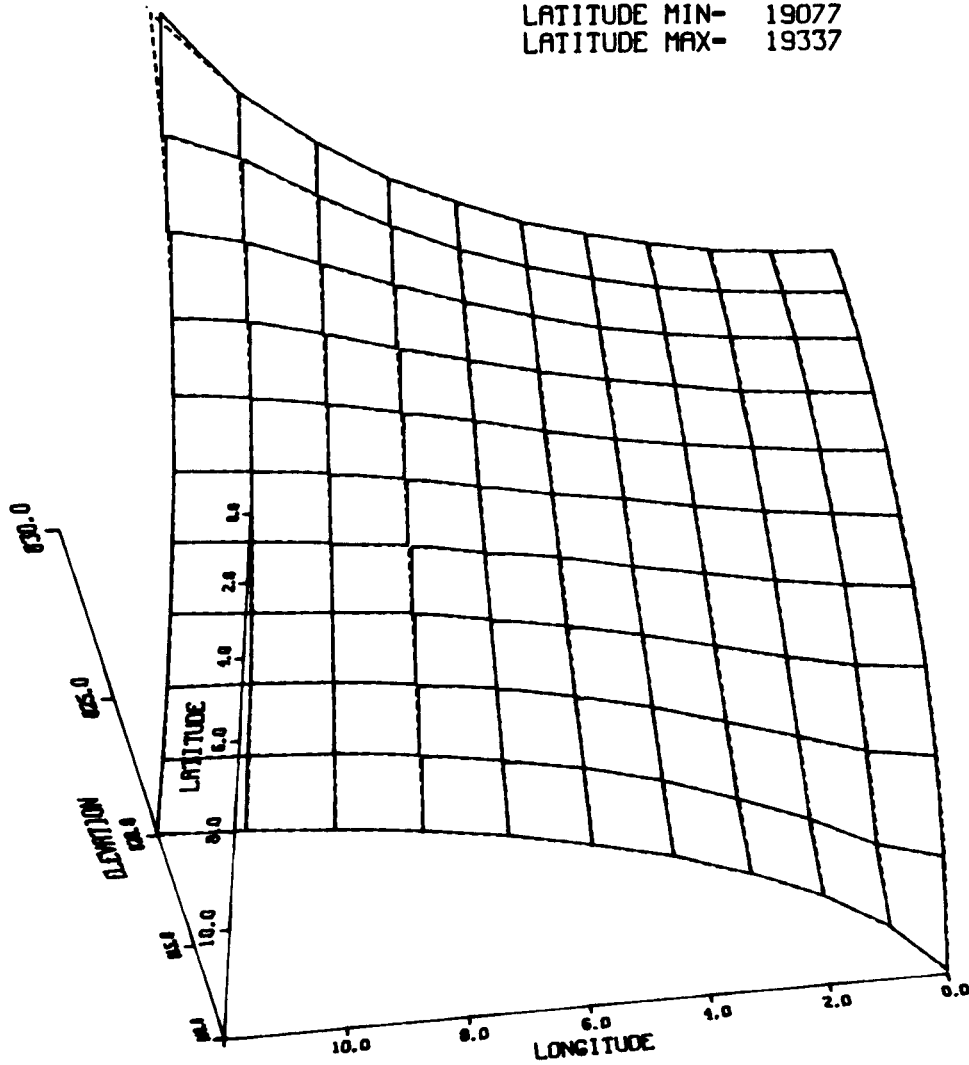


Figure 25. Cell plot of surface elevations at 100 subcell locations. The cell represents an increment value of 15.

SURFACE ELEVATION PLOT

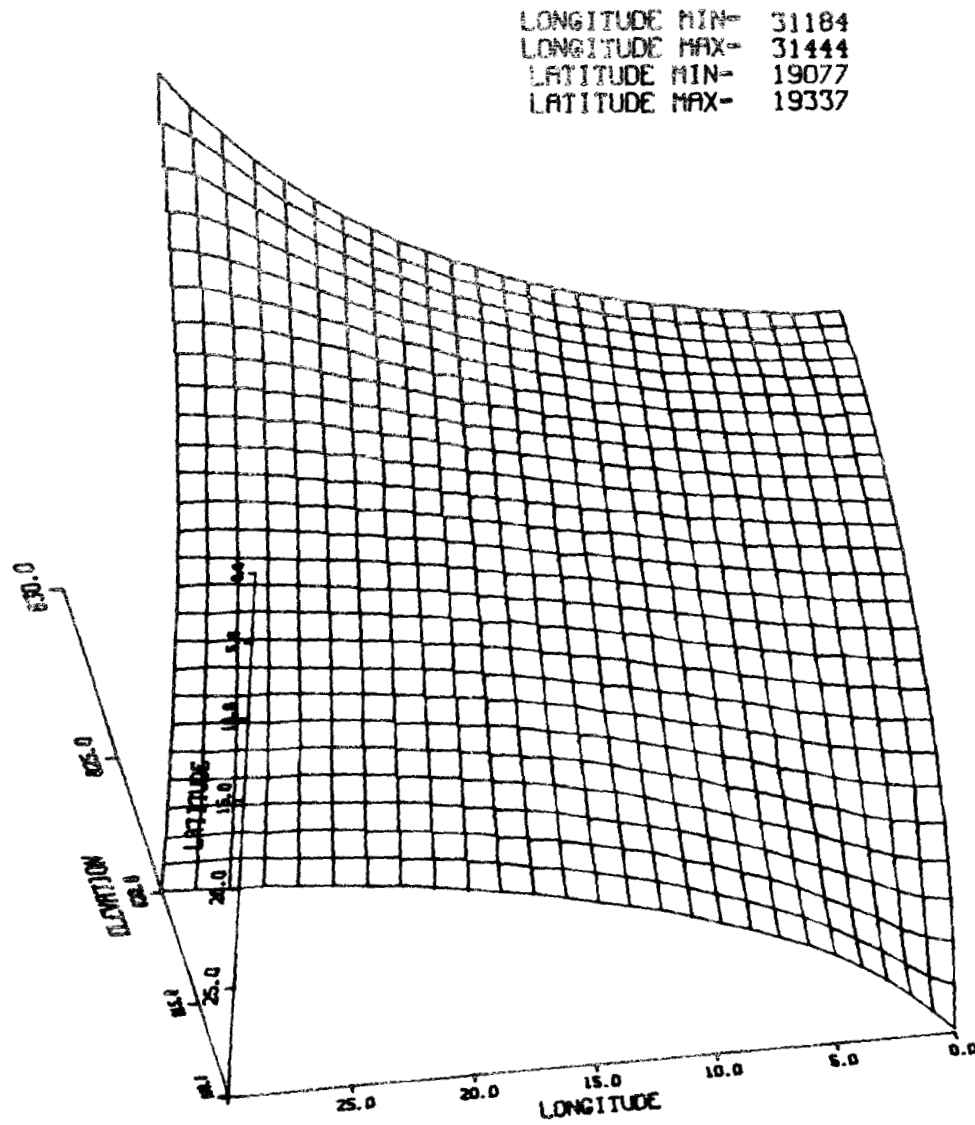


Figure 26. Cell plot of surface elevations at 676 subcell locations.
The cell represents an increment value of 25.

calculation is to be made. The Southern Conasauga Belt contains eight drill holes cored at various locations throughout the region (Figure 2, p. 6). One of the major problems existing when using the drill hole data is the lack of overlap between each section of core. This is due to the wide spacing between drill holes along with their very shallow total depth (30.48 m; 100 feet). If an attempt is made to produce a geologic column or cross section based strictly on drill core information, approximately 45 percent of the Conasauga Group in the section would be missing. This value is calculated by projecting the mean dip of the strata to the surface while assuming a lack of lithologic change along strike over the area. The absence of detailed subsurface information introduces a definite uncertainty to the results of the model.

Rock type and bed thickness are very important in fracture porosity calculations, and a potentially large error is caused by the scarcity of this data. The eight drill cores in the Southern Conasauga Belt were the only cores logged in sufficient detail for quantitative application. The logged information divides each 15.24 cm (6 inch) interval into its percentage of siltstone, shale, limestone, and glauconite. These four components will hereafter be referred to as the rocks' lithologic constituents. A few of the cores were inspected, and the accuracy of logging and interpretation checked and found to be reasonably precise, but not without some difficulties. Many of the cores were badly broken suggesting difficulty in logging of the destroyed areas; but, in several instances, data was recorded for these void areas. Some of the

samples were checked regarding the accuracy of the lithologic identification; it was found that many limestone beds were incorrectly recorded as siltstone, and the abundance of calcium carbonate in the rocks was generally underestimated.

Data from the core logs, regardless of their accuracy, were entered into the computer with the mean percentage of each lithologic constituent recorded at 30.48 cm (one foot) intervals. These data were reformatted by the computer program STRAT to produce the proper format required by the model. The results of all cores for the Southern Conasauga Belt were written in the permanent file CORE.DAT to be used in the calculations. The requested drill hole loggings are read into an array and used for all rock type determinations.

Additional assumptions were required when using the drill hole information. The surface elevations and coordinates of each drill hole were recorded primarily from logger's notes, but in some cases, it was necessary to interpret the information from the base map. Dips of the beds were recorded on logs, and a mean dip for each core was calculated. This is only an estimate of the dip of the strata, but it is believed to be accurate enough for use in the model. The drill cores used were projected to the required depth and location for lithologic constituent determination. Lithology was assumed to be constant along the strike of the rock; hence the latitude is the determining factor of the lithology calculated. This is a critical assumption that is required and results in a definite weakness in the validity of the model results. An increase in drill core information added at a later time will result in a decrease in the effect of this

broad generalization. Homogeneous lithology along strike is a necessary assumption that is used in the calculations.

The depth of interest is the subsurface depth with the surface topography considered. If the depth of interest is 4.56 m (15 feet), the calculated depth is 4.56 m below the surface topography. This implies that the surface developed is not a horizontal plane but an undulating surface which should be considered during its application.

The subcell latitude and the depth of interest are used to project the core information along the mean dip to the subsurface location. With the use of simple trigonometric functions, the lithology at this new location can be calculated. If the core is the correct length and the projection of the strata intersects the subcell location at the depth of interest, the lithology measured from the core can be recorded.

Each subcell location and surface elevation is read from the file CELL.OUT, and the projection calculation is carried out to determine if the selected drill core can provide lithologic information. If the projection results in a lack of intersection at the depth of interest, or, if the core data for the interval is missing, a missing value code of -99 is recorded for the depth and no further computations are performed for that subcell location. If the core is applicable and the data from the logs contain a measured interval and not a missing unit, the lithology is determined for the subcell location. The model calculates the amount of siltstone, shale, and limestone for a 30.48 cm (one foot) interval determined by the projection. The percentage of glauconite is combined with the

siltstone value resulting in a total percentage of siltstone.

Porosity and Permeability Calculation

The porosity and permeability are calculated by the subroutine PORCAL (see Figure 27 for flow chart). The coordinates, depth, and lithologic constituents that are used to calculate the porosity and permeability are those obtained primarily from the subroutine CORFIX.

Rock Name (RCKTYP)

This subroutine determines a name for the rock based on the percentage of its constituents supplied by CORFIX from the drill core results. The quantity of siltstone, shale, and limestone within the rock is used to calculate a lithologic name. A specific rock name is determined if the core sample contains a minimum of 50 percent of any one constituent. The rock is denoted as mixed if there is no component greater than 50 percent.

Gap Width (GAPSET)

This subroutine determines a numerical value for the joint gap width for each rock type at a specified depth. The size of the gap between joint planes is determined by a mathematical function relating the initial gap to depth. This calculation is required for each rock type with the assumption that both joint sets contain the same gap size. This assumption is forced by the lack of field data supporting any difference in gap width of each joint set. The primary parameter in the calculation of joint gap is the initial gap width. The gap width at the surface is very difficult to measure in

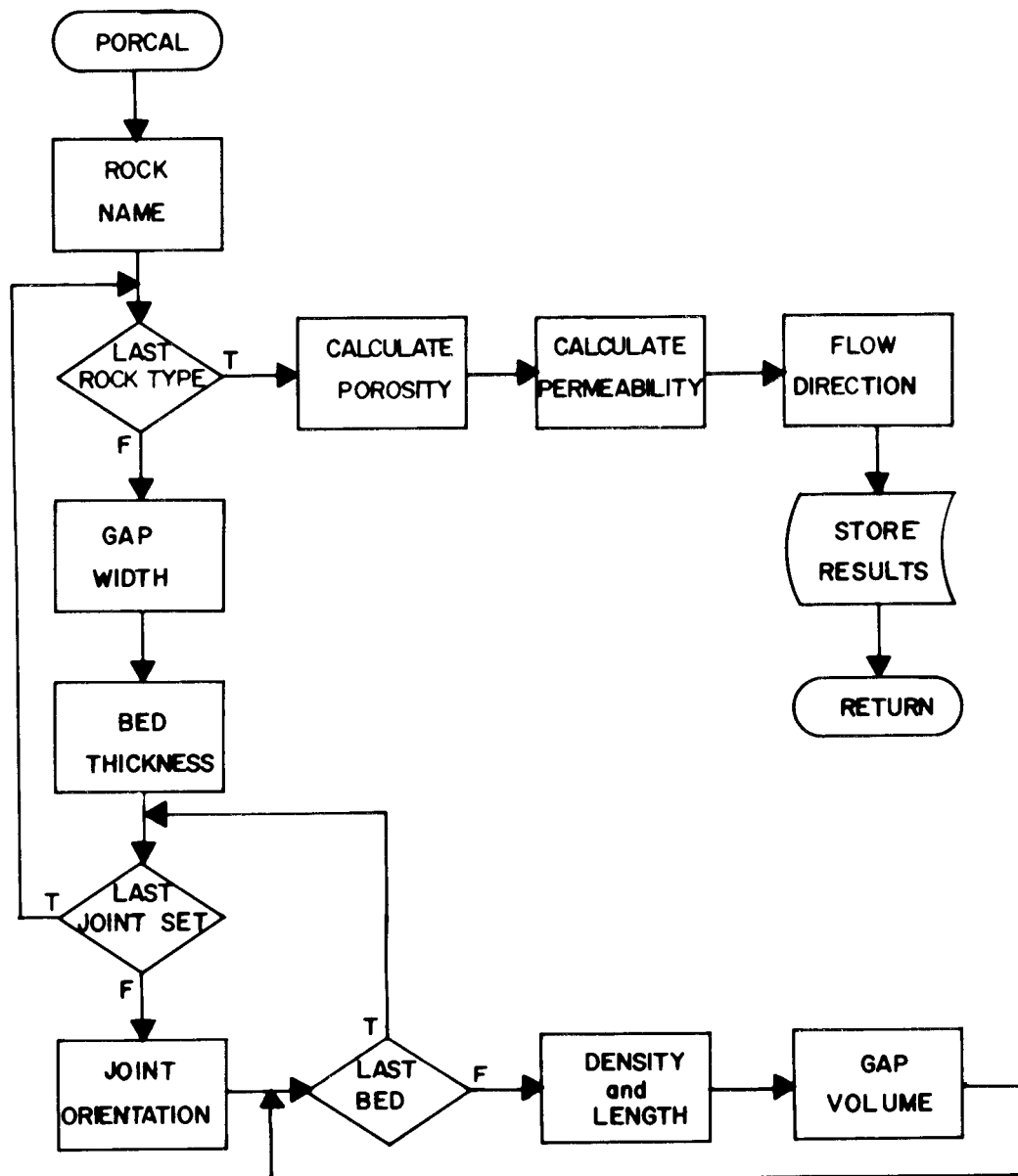


Figure 27. Simplified flow chart of the fracture porosity and permeability calculation.

the field and its determination was attempted from drill cores. The range in gap width values measured in the drill cores was 0.7 to 0.1 mm in the siltstones and from 0.2 to less than 0.1 mm in the shales. This wide range suggested that a more refined estimate of the gap width would be better determined using known measurements of conductivity recorded in the field. The relationship between the gap width and the conductivity will be discussed in a later section.

Reduction of gap width with increasing depth is another critical factor. A 1 percent decrease in gap width for each one meter increase in depth is the relation that is used (Davis, 1969). In unconsolidated sediments, this factor would be much higher and depend significantly on overburden pressures of the overlying sediments. In the consolidated sediments of the Conasauga Group, the joints are near vertical resulting in very little closure by compaction with increase in depth. A 1 percent reduction in gap at the shallow depths appears to be a valid first approximation.

Bed Thickness (THKCAL)

The subroutine THKCAL calculates a bed thickness value for each lithology of the interval length of core.

The major assumption is that the strata was initially deposited with a bed thickness that can be predicted by a mathematical distribution. Analysis of the data collected in the field suggest bed thickness may conform to a normal or t distribution (Neter et al., 1978). The different bed thickness values recorded from the density of joint measurements were plotted on a frequency diagram (Figure 28). A total of 31 different beds were measured in five

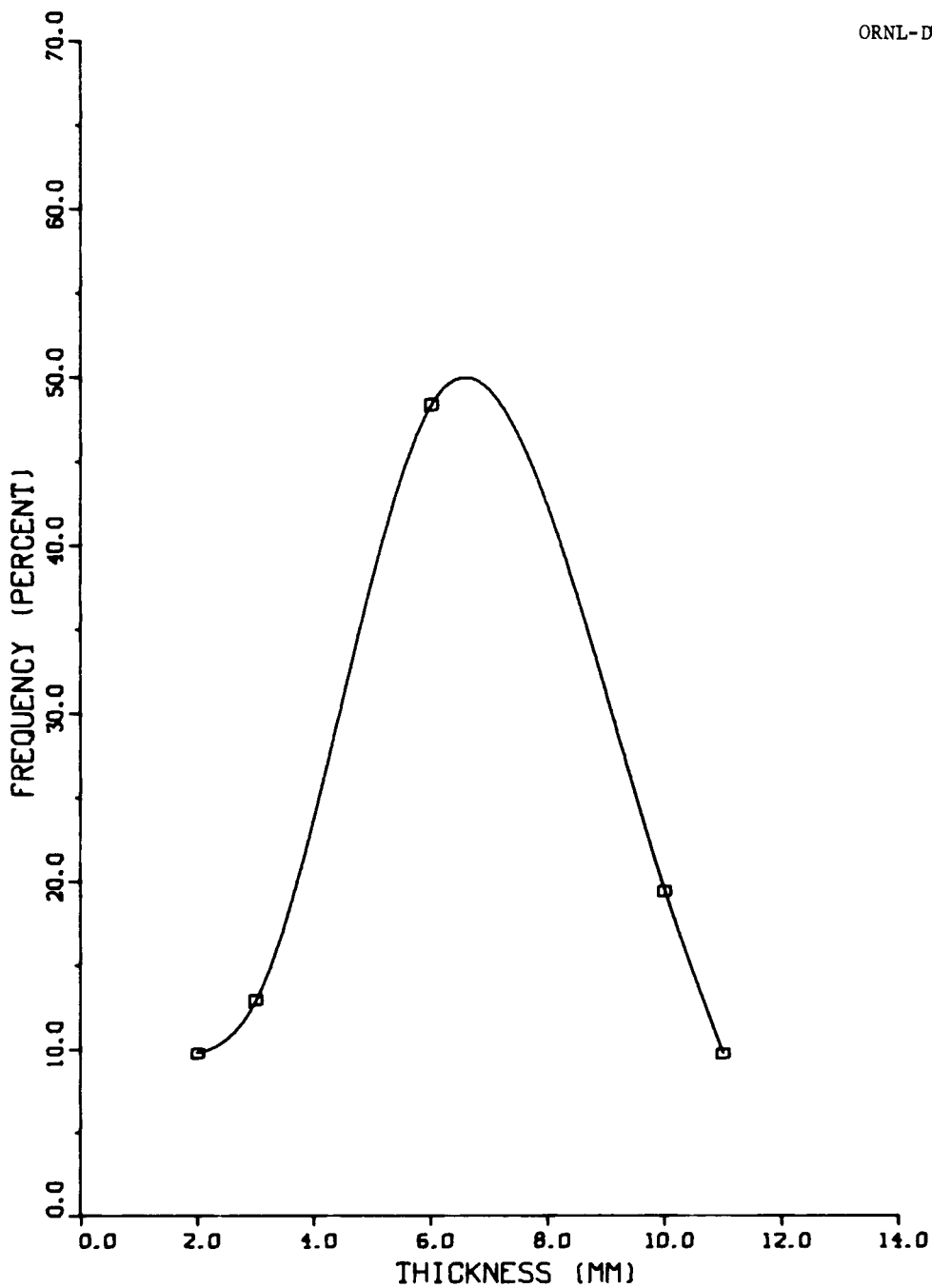


Figure 28. Frequency distribution of bed thickness values in shale beds measured within the study area.

different bed thickness intervals. The plot was created only for the shale beds due to their large abundance in the sample population. The frequency distribution curve contains a calculated mean bed thickness value of 6.48 mm (0.26 inches) with a standard deviation of 2.87. The plot appears to be closely related to a normal distribution. If this assumption is correct, two standard deviation units about the mean will result in consideration of 95.4 percent of the total population.

The subroutine uses a mean and standard deviation value for each rock type which can be initially calculated from an estimated minimum and maximum bed thickness. The total thickness of core in the calculation is the 30.48 cm (one foot) length supplied by the subroutine CORFIX. The thickness for each rock type is based on the percentage of the particular lithologic constituents present. If the total thickness of core is 30.48 cm and 50 percent of the rock consists of shale, the total thickness of the shale beds within the core would be 15.24 cm.

The fact that a normal distribution occurs is not as critical as the existence of some type of distribution. If the beds exhibited a random thickness distribution, a random number generator to predict the bed thickness values would be required and duplication of the results would be impossible.

The method used to develop the systematic relationship of creating a distribution is complex. The normal distribution curve was divided into seven equal units with the minimum (unit 1), mean (unit 4), and maximum (unit 7) bed thickness determined. The values

for the remaining units are calculated while retaining an equal bed thickness value between each unit.

The major problem in programming this distribution is to consume the entire bed thickness by subtracting the calculated unit values from the total thickness, while retaining the distribution. This is very difficult, and the procedure used only approximates a normal distribution, with various non-zero values for the calculated skewness and kurtosis as a result.

A primary factor in creating a distribution from the existing data is the initial bed thickness. It is very difficult to retain a distribution when the initial bed thickness is small. The use of thick units would alleviate this problem, allowing multiple groups of beds to be considered, resulting in the formation of a complete distribution.

The method used in the program is to consider the total bed thickness and subtract each bed thickness unit from this until the total thickness remaining is zero or less than the minimum unit thickness. The mean value in the program will always have the highest frequency. Each individual calculated bed thickness value is written into an array and used in the model.

Joint Orientation (ORDAT)

Regression analysis, using the program SAS (Barr et al., 1979), was applied to joint orientation data in an attempt to quantify the relation of strike and dip of the joints with changes in longitude. A better approximation for the orientations of the strike and a-c joints could be made if regression techniques are applied. A first-

order linear regression model was applied to the strike and dip of the joints at each location with longitude as the independent variable. Equations for the strike and dip of each joint set were determined and used in this subroutine. Given the longitude of the subcell and the joint set of interest, the mean orientation of each joint set can be determined.

Density and Length (DENLEN)

The subroutine DENLEN calculates the mean joint length and the number of joints within the subcell area for each bed thickness and rock type. The data used for this subroutine are the relationships between the joints discussed in the previous chapter. A first-order linear regression analysis was applied to the joint length and density data as a function of bed thickness for each rock type. The data for the length of joint measurements displayed very low r-square values suggesting the lack of a strong correlation between the parameters. This was discussed earlier (see p. 43); a predictive model based solely on the joint length data collected in the field would be inaccurate.

The equations developed for the joint density relationships displayed r-square values for shale of 35.8 percent and siltstone 79.4 percent. This is a reasonable correlation between the parameters, suggesting that the equations for joint density as a function of bed thickness can be used in the model.

Calculation of the predicted joint length is accomplished by using the relationship of joint length as a function of the joint density and bed thickness. These developed equations displayed

r-square values of 99.1 percent for the siltstone beds and 98.4 percent for shale. The high correlation of the regression analysis implies a very strong relationship between the parameters. Determination of the joint length by this method results in increased accuracy of the predicted results and does not reject the field measurement for joint length. The mean length and density of joints can be calculated for each rock type.

For each of the regressions, the mean value of all measurements collected was used resulting in a very small number of data points utilized in the analysis. For this reason, a first-order regression was the highest order model used in the calculations. The equations developed will predominantly explain the data and consider only a minimum amount of noise. The data for each individual joint set was examined, and very low correlations existed for either set at the same location. It was decided that the mean results of the combined joint sets would give a better estimate of the parameters.

The value for the mean joint length and the total density of joints within the subcell must be determined. The area of the subcell can be calculated, and its relationship to the area created by the joints of a mean length can be derived.

The last required parameter for the model is the total number of joints within the subcell area. This value was calculated by assuming the joints to be all oriented parallel with the sides of the subcell. The problem with this assumption is that a portion of the joint may lie outside the cell. This is not critical, however, because the actual joint lengths are very small compared to the total

size of the subcell area, and the overlap can be considered negligible. Each traverse of joints within the subcell was believed to abut against another in their joint length component. It is very difficult to determine this factor from field observations; but in a quantitative model, this assumption should predict reasonably accurate results.

All of the factors were combined and the number of joints of a mean length within the entire subcell area was calculated. This calculation is performed for each bed thickness and rock type and used in the fracture porosity and permeability determination.

Porosity and Permeability Calculation (PORCAL)

The results from the previously discussed subroutines are combined in the program for the calculation of the fracture porosity and permeability of each individual subcell. The external data obtained from subroutine CORFIX consists of the latitude and longitude of the subcell, the depth of interest, and the lithologic constituents of the core. The initial procedure is to determine a rock name for the core interval of interest (RCKTYP). The percentage of limestone is not used in the calculation, but its presence is noted and it will be considered as having an absence of fracture porosity and permeability.

The mean gap width and the volume created by the joint gap for each rock type must be determined. The gap width for each rock type is calculated by the subroutine GAPSET. The thickness of each individual bed is calculated and stored in an array (THKCAL). The individual joint set orientations (ORDAT) are determined with each

containing a volume created by the strike and dip of the joint plane. Different bed thickness values will have a different density and length of joints associated with them. The volume of the gap can be calculated from the data with individual volumes summed up for each bed, joint set, and rock type, resulting in a numerical value for the total volume contained in the joints.

The calculation of the total fracture porosity for the subcell is the ratio of the volume formed by the joints to the total volume of the cube defining the subcell. The cube volume consists of the product of the subcell length, width, and the sum total of the bed thickness values. The equation used for the porosity calculation is:

$$\theta = \frac{\sum_{LITH=1}^2 \sum_{JSET=1}^2 \sum_{j=1}^{TBEDS} [GJ_j] [LJ_j] [T_j] [NJ_j]}{[WC] [LC] [TT]}$$

The fracture permeability can be determined by initially calculating the intrinsic permeability from which the conductivity can be derived. Intrinsic permeability is defined as the permeability of a medium which is independent of the fluid properties governing the flow (Todd, 1959) and can be calculated by the following equation;

$$K = \frac{\left\{ \frac{[WC] [LC]}{TJ} \right\}^2 \theta^3}{12} \quad (4)$$

Intrinsic permeability is a function of fracture porosity and average spacing of the joints. This equation was originally designed for

spacing of joints in drill cores (Snow, 1968) and was modified for use in the calculations. Saturated hydraulic conductivity is calculated from the intrinsic permeability by considering the specific weight and the viscosity of the fluid of interest.

$$C = K \frac{\nu}{\mu} \quad (5)$$

The fluid used for the calculation is water at a temperature of 15.6° Celsius (60° Fahrenheit).

All results are stored in a file POROS.DAT with each record representing a different subcell.

Flow Direction (PRMVEC)

Determination of the mean direction of fluid flow through the joints is an important factor when predicting groundwater flow. This subroutine determines the mean direction and magnitude of flow in the combined joint sets.

Each joint orientation can be considered as a unit vector with the direction of flow related to the dip and strike of the joint plane. The joint sets, for a particular longitude, are calculated using the subroutine ORDAT. From this information, unit vectors for each joint set can be determined, resulting in a vector representation of the joint plane. The mean unit vector in three coordinate space can be derived by using vector addition of the joint sets. The magnitude of this vector as well as the direction related to the orientation of the strike and dip of the joints can be calculated. With this information, the direction of fluid migration

through the joints is estimated.

Plot Porosity (PLOCEL)

The results of the fracture porosity calculation can be output in a three-dimensional surface plot. The data are read from file POROS.DAT and stored in a variably dimensioned array. The method is analogous to the surface elevation plot with the exception of the depth of interest value recorded on the plot. An example of the porosity calculated for an increment of 10 is reproduced in Figure 29. The plot represents a depth of 4.56 m (15 feet) below the surface and display the range of porosity determined throughout the cell.

Table Results (TABPOR)

A table listing the fracture porosity and permeability calculation can be created by the subroutine TABPOR. The data is read from the file POROS.DAT and output to the line printer (Table 5). If a void was recorded in the file representing a lack of core available for the calculation, the subcell coordinates are not listed. The file POROS.DAT is not deleted so the data, contained in the file and not tabularized, can be used for alternate purposes.

Results

The calculated fracture porosity is a function of the rock type, bed thickness, joint length and density, joint orientation, and the joint gap width with each parameter affecting the calculation to a different degree. In the following discussion, an attempt will be

FRACTURE POROSITY PLOT

AT DEPTH OF 5.0 METERS

LONGITUDE MIN- 31184
LONGITUDE MAX- 31444
LATITUDE MIN- 19077
LATITUDE MAX- 19337

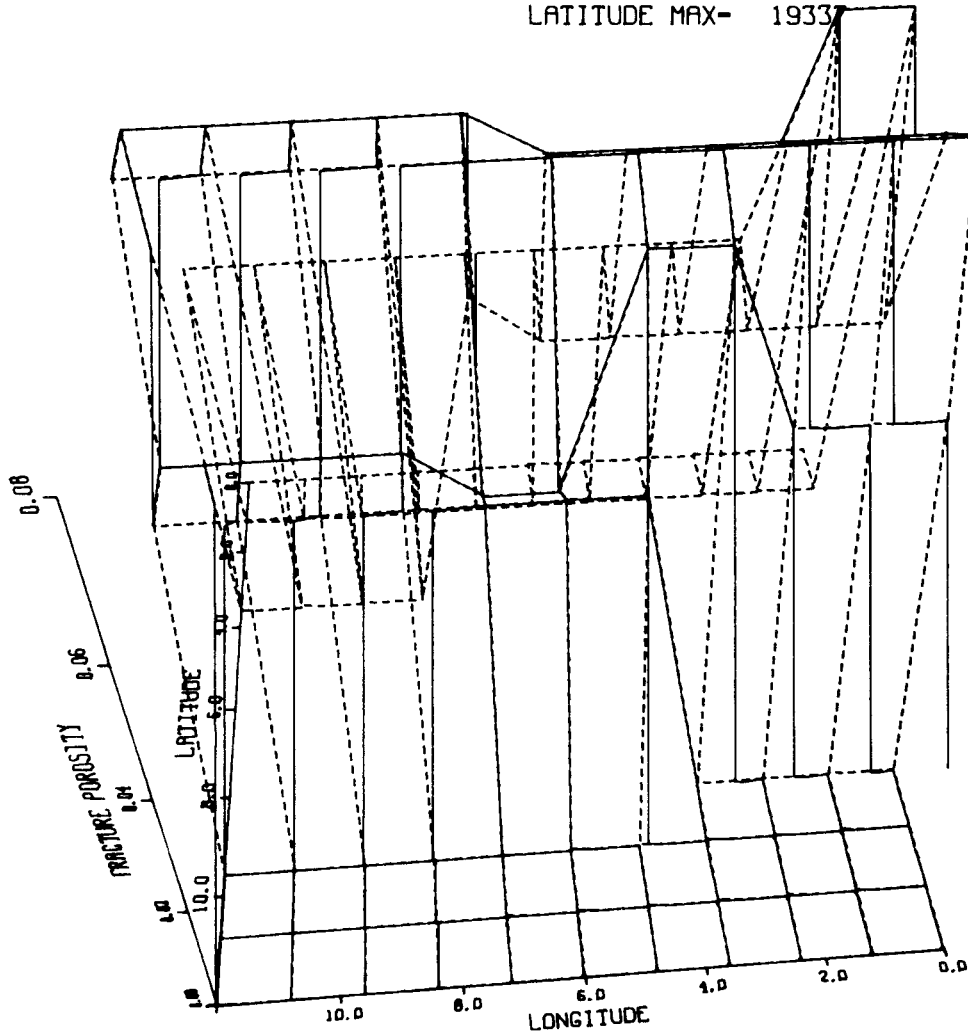


Figure 29. Fracture porosity surface calculated for each subcell location. The data is calculated for a depth of 5.0 m and 10 increments.

Table 5. Listing of the calculated fracture porosity and permeability for each subcell location at a depth of 4.57 m and surface gap width of 0.2 mm

FRACTURE POROSITY AND PERMEABILITY LISTING AT 4.57 METERS DEPTH						
SURFACE GAP WIDTH (MM) SILT- .200 SHALE- .200						
ORA GRID SYSTEM						
LONGITUDE	LATITUDE	LITHOLOGY	JOINT GAP	FRACTURE POROSITY	INTRINSIC PERMEABILITY	HYDRAULIC CONDUCTIVITY
(EAST-WEST)	(NOR-SOU)		(MM)	(PERCENT)	(DARCY)	(CM/DAY)
31184	19181	SL-SH	.1921	0.075	0.022	1.655
31184	19207	SL-SH	.1921	0.081	0.025	1.821
31184	19233	SL-SH	.1921	0.075	0.022	1.655
31184	19259	SILT	.1921	0.045	0.007	0.503
31184	19285	SILT	.1921	0.052	0.013	0.932
31210	19181	SL-SH	.1921	0.075	0.022	1.655
31210	19207	SL-SH	.1921	0.081	0.025	1.821
31210	19233	SL-SH	.1921	0.075	0.022	1.655
31210	19259	SILT	.1921	0.045	0.007	0.503
31210	19285	SILT	.1921	0.052	0.013	0.932
31236	19155	SILT	.1921	0.052	0.011	0.785
31236	19181	SL-SH	.1921	0.075	0.022	1.655
31236	19207	SL-SH	.1921	0.081	0.025	1.822
31236	19233	SL-SH	.1921	0.075	0.022	1.655
31236	19259	SILT	.1921	0.045	0.007	0.503
31236	19285	SILT	.1921	0.052	0.011	0.785
31262	19155	SILT	.1921	0.052	0.011	0.785
31262	19181	SILT	.1921	0.045	0.007	0.503
31262	19207	SL-SH	.1921	0.081	0.025	1.822
31262	19233	SL-SH	.1921	0.075	0.022	1.655
31262	19259	SILT	.1921	0.052	0.011	0.785
31262	19285	SILT	.1921	0.052	0.011	0.785
31288	19155	SILT	.1921	0.052	0.011	0.785
31288	19181	SILT	.1921	0.045	0.007	0.503
31288	19207	SL-SH	.1921	0.081	0.025	1.822
31288	19233	SL-SH	.1921	0.075	0.022	1.655
31288	19259	SILT	.1921	0.052	0.011	0.785
31288	19285	SILT	.1921	0.052	0.011	0.785
31314	19155	SILT	.1921	0.052	0.011	0.785
31314	19181	SILT	.1921	0.052	0.013	0.932
31314	19207	SL-SH	.1921	0.081	0.025	1.822
31314	19233	SL-SH	.1921	0.081	0.025	1.822
31314	19259	SILT	.1921	0.052	0.011	0.785
31314	19285	SILT	.1921	0.052	0.011	0.785
31340	19155	SILT	.1921	0.052	0.011	0.785
31340	19181	SILT	.1921	0.052	0.013	0.932
31340	19207	SL-SH	.1921	0.081	0.025	1.822
31340	19233	SL-SH	.1921	0.081	0.025	1.822
31340	19285	SILT	.1921	0.052	0.011	0.785
31366	19155	SILT	.1921	0.052	0.013	0.932
31366	19181	SILT	.1921	0.052	0.013	0.932
31366	19207	SL-SH	.1921	0.081	0.025	1.822
31366	19233	SL-SH	.1921	0.081	0.025	1.822
31366	19285	SILT	.1921	0.052	0.011	0.785
31392	19155	SILT	.1921	0.052	0.013	0.932
31392	19181	SILT	.1921	0.052	0.013	0.932
31392	19207	SL-SH	.1921	0.081	0.025	1.822
31392	19233	SILT	.2113	0.054	0.016	1.170
31392	19285	SILT	.1921	0.052	0.011	0.785
31418	19155	SILT	.1921	0.052	0.013	0.932
31418	19181	SILT	.1921	0.052	0.013	0.932
31418	19207	SL-SH	.1921	0.081	0.025	1.822
31418	19233	SILT	.2113	0.054	0.016	1.170
31418	19285	SILT	.1921	0.052	0.011	0.785
31444	19155	SILT	.1921	0.052	0.013	0.932
31444	19181	SILT	.1921	0.052	0.013	0.932
31444	19207	SL-SH	.1921	0.081	0.025	1.822
31444	19233	SILT	.2113	0.054	0.016	1.170
31444	19285	SILT	.1921	0.052	0.011	0.785

made to describe the most influential parameters in the fracture porosity and permeability calculation.

Rock type influences most of the parameters, with the individual effects between each of these parameters difficult to evaluate. The calculated model bed thickness values are unique for each rock type and contain a particular percentage of lithologic constituents. Rock constituents are assumed gradational in 10 percent interval units from a pure shale end member to a pure siltstone. A comparison between two locations containing identical lithologic constituents can be made by neglecting the bed thickness.

The relationship between the length and density of joints, as discussed in the previous chapter, is unique for a given bed thickness and rock type. A bed composed of 20 percent siltstone and 80 percent shale in two different locations has all parameters equal with the exception of the joint gap width and the joint orientation. If the gap width remains constant at each location (same depth), then the effect of joint orientation on porosity can be considered.

Variation in joint orientation with large changes in longitude has little effect on the calculated fracture porosity. This relationship can be examined by keeping all parameters constant and varying the longitude with a mean gap width of 0.1921 mm of both rock types (shale and siltstone). The fracture porosity varies approximately 0.001 percent for each 4270 m (1400 feet) change in longitude. This is considered to be a very small variation in relation to the total size of the cell.

Decrease in porosity with increasing depth is based on the joint

gap width decrease. The greatest porosity decrease of clastic sediments is soon after deposition in the upper few tens of meters depth (Reike and Chilingarian, 1974). Major processes responsible for porosity reduction are mechanical compaction and dewatering. The rocks in this study were previously lithified, deeply buried, and brought to the surface by tectonic activity. Such tectonic activity has been shown to reduce the gradient of porosity decrease with depth. Calculated fracture porosity of this study decreases by a total of 8.2 percent for each 15.2 m (50 feet) increase in depth.

The effect of joint density and length can be determined by considering the fracture porosity of various lithologies (siltstone and shale) with a fixed gap width of 0.1921 mm at 4.56 m (15 feet) depth. Under this assumption, a pure shale has a fracture porosity of 0.088 percent, and a rock consisting of 100 percent siltstone has a fracture porosity of 0.030 percent. The range in calculated porosity for each percentage of shale and siltstone is shown in Figure 30. The value for the maximum porosity is not the pure shale end member as might be expected, but is a value of 30 percent siltstone and 70 percent shale. The porosity value calculated at this point is 0.102 percent which is a 16 percent overall increase from that of the pure shale. The expected fracture porosity is believed to be higher in the shales than in the siltstone beds (Davis, 1969). The results obtained from the model can be explained by plotting the bed thickness, joint length and joint density for shale and siltstone on the same graph (Figure 31). The joint length for the shale and siltstone beds have opposite direction of slopes

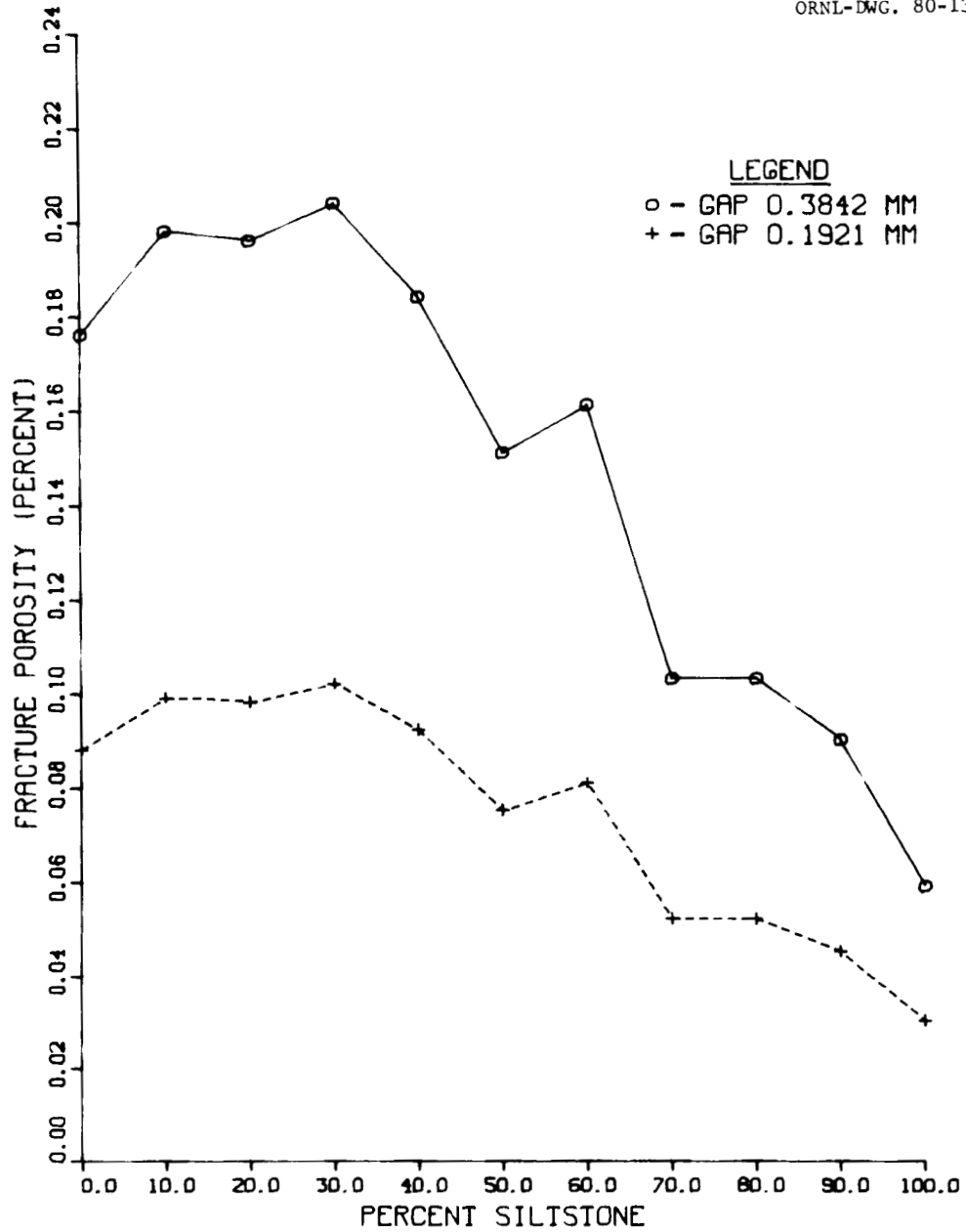


Figure 30. Calculated fracture porosity at various percentages of siltstone for joint gap widths of 0.1921 mm and 0.3842 mm.

ORNL-DWG. 80-13357

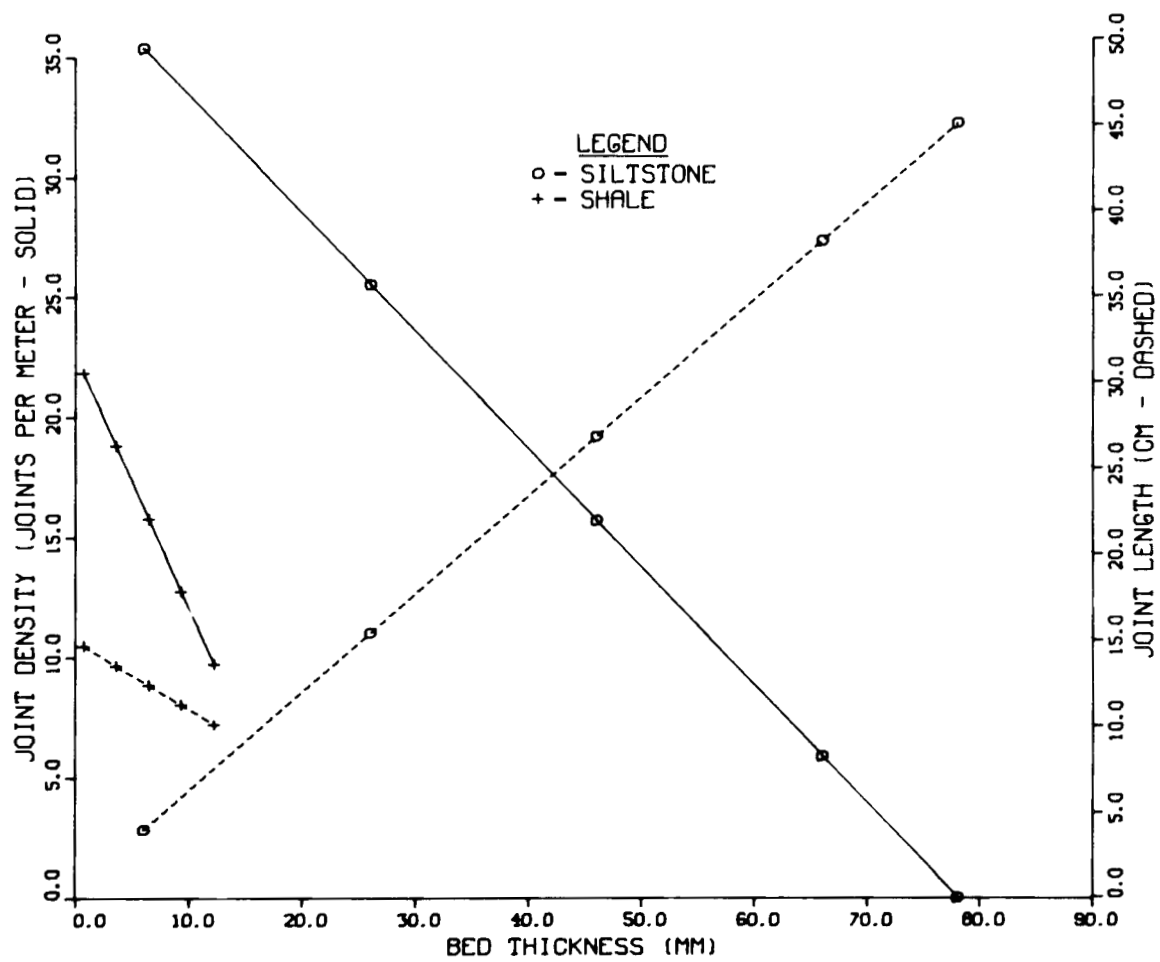


Figure 31. Variations in joint density and joint length with changes in bed thickness for shale and siltstone beds.

which will result in the thinner beds of shale containing a larger porosity value than the thick beds. The problem is in the overlap area where the bed thickness of silt is very low (less than 25 mm) and the shale beds are relatively thick (greater than 6 mm). There is a much higher density of joints in the silt than in the shale at this thickness interval which results in a large calculated void value (porosity). At a value of 30 percent silt, the total calculated bed thickness is 91 mm ($0.30 \times 304.8 = 91$); and when the bed thickness distribution is applied, the thickness values are very low. The presence of very thin siltstone beds increases the joint density along with the calculated void volume. This value is higher than exhibited in a pure shale and results in the larger values of the calculated fracture porosity. This result is probably related to the limited distribution of individual bed thickness values possible within a 304.8 mm layer, as discussed later in this section.

The value for the joint gap width can be varied and its effects on the fracture porosity noted by holding all other parameters constant. The range of gap width values, measured by Snow (1968) in the upper 9 m (30 feet) of an igneous rock body in Colorado, were from 0.075 mm to 0.4 mm. A gap width of 0.3842 mm was used in the model for both the siltstone and shale to compare its effect on the fracture porosity with the results described earlier (Figure 30). The mean fracture porosity values calculated ranged from a minimum of 0.059 percent (100 percent siltstone) to a maximum of 0.204 percent (30 percent siltstone). Comparing this data with the porosities calculated at 0.1921 mm gap width shows a doubling of the fracture

porosity with a doubling of the gap width.

The intrinsic permeability calculated by the model is affected by the same parameters as the fracture porosity. The permeability (Equation 4) considers the fracture porosity, joint length, and joint density in its calculation.

The predominant effects of the parameters on the intrinsic permeability calculation can be interpreted by using graphical techniques. Fracture porosity for joint gap widths of 0.1921 mm and 0.0961 mm (Figure 32) exhibits relationships dependent on the varying percentages of siltstone and shale. The major factor affecting the fracture porosity, as determined in the previous section, was the gap width. The calculated intrinsic permeability appears to be dependent on the lithologic constituents to a greater degree than the calculated fracture porosity. The highest porosity value, consisting of 30 percent siltstone, does not occur at the maximum permeability. The maximum permeability is at 90 percent shale and 10 percent siltstone, while the minimum permeability is 100 percent siltstone. This can be explained by using a simulation run for a gap width value of 0.1921 mm (Figure 33). However, by increasing the total bed thickness (TT), a more extensive distribution of individual bed thicknesses is allowed and a trend toward a linear relationship of fracture porosity versus lithology results. At 3.05 m (10 feet) total thickness, the relationship is nearly linear with expected values for the actual fracture porosity determined. The intrinsic permeability contains a linear relationship with a similar increase in total bed thickness.

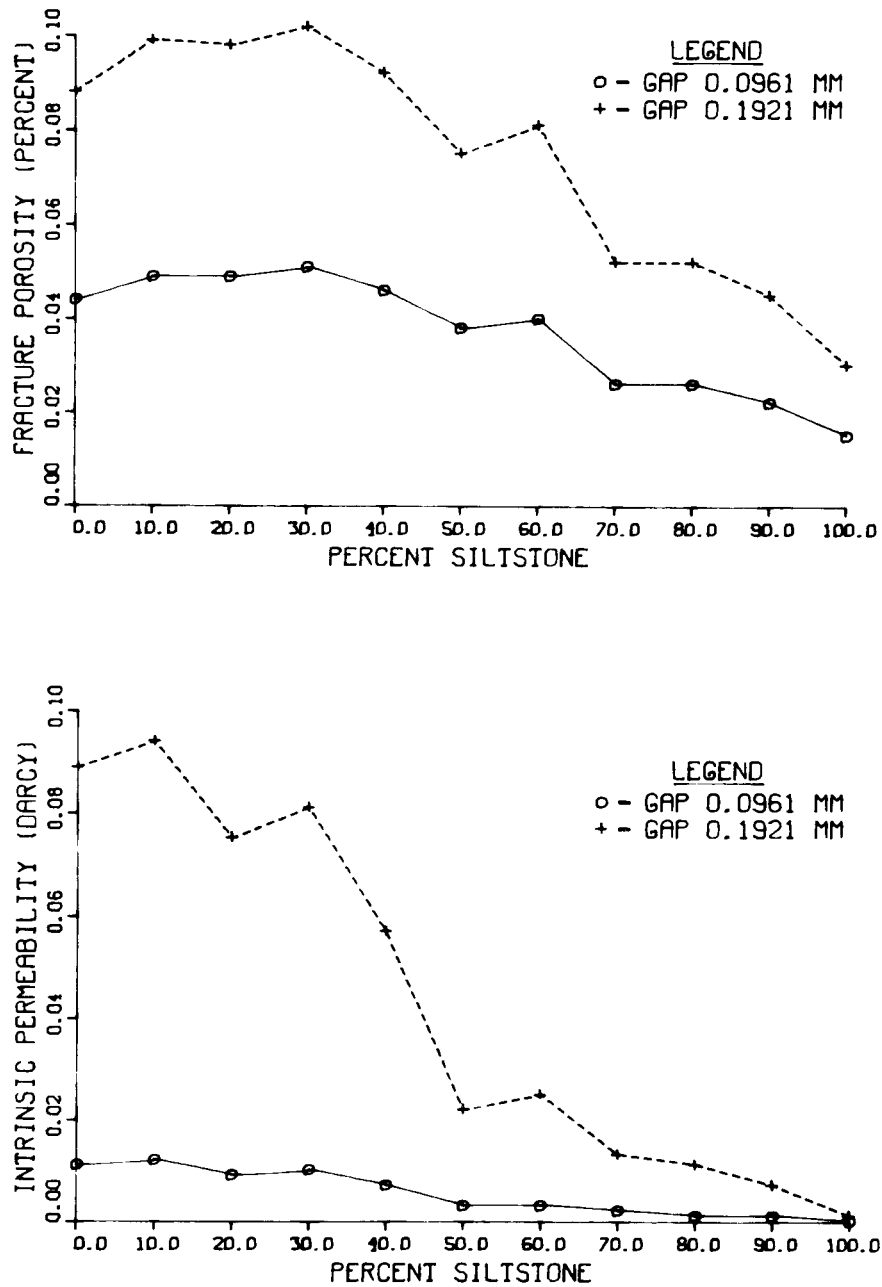


Figure 32. Variations in the calculated fracture porosity and permeability with changes in the percentage of siltstone. The joint gap widths are 0.0961 mm and 0.1921 mm.

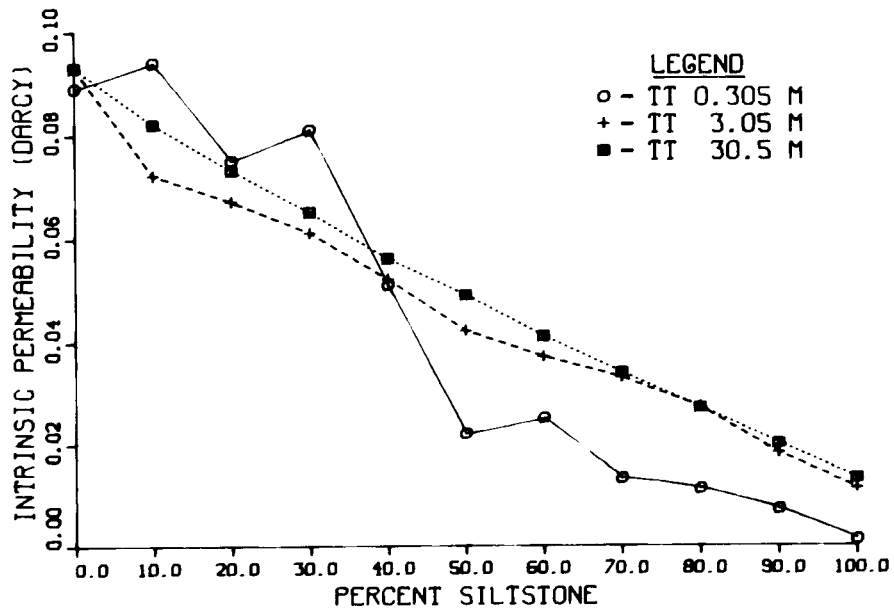
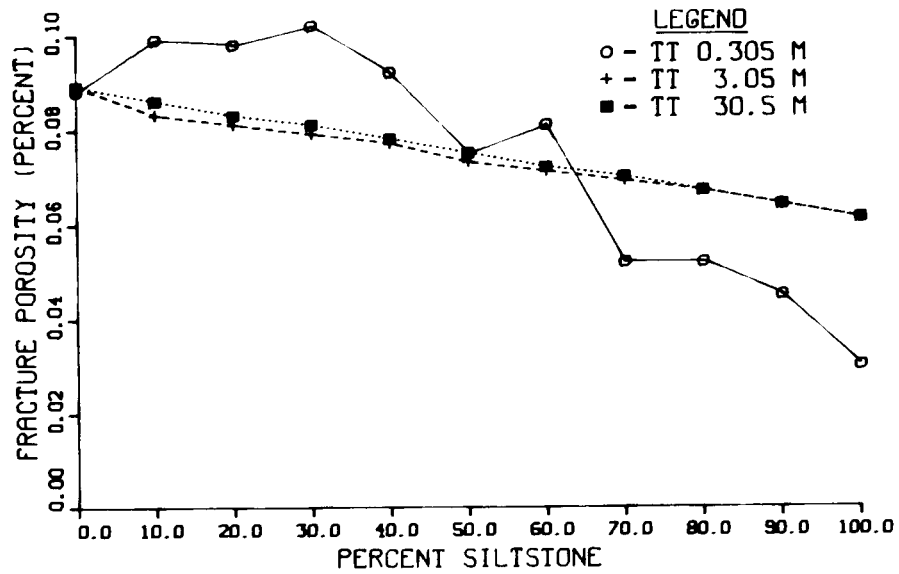


Figure 33. Effects of increasing the total bed thickness (TT) on the porosity and permeability calculation. Joint gap width is 0.1921 mm.

The results of the two graphs display the range of expected fracture porosities (0.07 percent to 0.09 percent) and intrinsic permeabilities (0.02 darcy to 0.09 darcy) that may be found at a depth of 4.57 m within the site of interest. The results imply that with an increase in shale content, the calculated intrinsic permeability increases. Joint length and density data are considered in both the permeability and porosity calculations, and this reduces the importance of bed thickness on the calculation and increases the effect of the joint length and density parameters.

The gap width of the joint is the major factor in the permeability calculation, and its effect can be illustrated by the following equation;

$$(GJ)I = (K)I^3 \quad (6)$$

Increasing the gap width by a factor (I) results in the intrinsic permeability increasing by the cube of this factor. This relationship can be illustrated by considering the permeability and lithology relationships (Figure 32). The slope of the line representing the permeability at the larger gap width is much greater than the slope representing the smaller gap width. This implies that an increase of gap width in shale beds will result in a very large increase in their permeability. The gap width for both lithologic types is doubled so that the permeability increases by a factor of approximately eight. This equation holds true for all variations in percentages of lithologic constituents. The values for the calculated intrinsic permeability are within the range of the average

permeability measured in very fine sands, silts, and clays (Viessman et al., 1972; Freeze and Cherry, 1979).

The calculated hydraulic conductivity is a multiple of the intrinsic permeability. The conductivity was measured in shale beds in the Southern Conasauga Belt (Luxmoore, 1980) and can be used to verify the value of the mean gap width. The field data, at a particular sampling location, suggested a mean value for the conductivity of 2 cm per day which translates to a surface gap width of 0.2 mm. The value of the gap used in the model for both rock types is identical, but from drill core data, the range of gap values actually measured was less than 0.2 mm in shale and 0.7 to 0.2 mm in the siltstone beds. The value for the gap required to compute measured conductivity values in the field is within the range of the gap width measured. This would suggest that a large portion of the permeability in the rocks may be due to the joints.

Observations in the field suggest that the joint gap widths in shale beds are smaller than in siltstone beds. The model can be calibrated by recording the conductivity measured in silt rich and shale rich rock types in the field and adjusting the gap width values accordingly. The gap width values derived would then result in a gradational calculated conductivity for the different rock types.

The major assumption required in the permeability calibration is the existence of continuous parallel joints containing equal gap widths along the entire length of the joint. This is the ideal case in the model and will result in the maximum value for the permeability to be calculated. If the initial gap width is assumed

to be small, the model considers this value to be the mean size of the gaps in each of the joints. The large weathered joint gaps and the filled joints are combined to form this mean gap value used in the model.

Summary

An analytical model was found to be very useful for the determination of fracture porosity and permeability in the Southern Conasauga Belt. Systematic investigations of the effects of each parameter involved in the calculation allowed the importance and influence that each individual parameter had in determining fracture porosity to be evaluated.

Joint gap width was found to have the greatest influence on the porosity and permeability calculation. An increase in the the gap width by a given amount increases the porosity by the same amount, and results in the permeability increasing by the cube of the amount. The bed thickness, joint length, and the density of the joints are closely related to the lithology of the rock. Each of these factors were found to contribute a small amount in the calculations. Variation of joint orientation with changing longitude was found to be trivial in the Southern Conasauga Belt.

Calculated fracture porosity decreased by 8.2 percent for each 15.2 m increase in depth. At a depth of 4.56 m (15 feet) from the surface, the range in porosity values was 0.03 percent to 0.10 percent with an initial surface gap value of 0.10 mm. The intrinsic permeability calculated ranged from 0.002 to 0.10 darcys for the

rocks with the identical gap width values.

Percentage of siltstone was a major factor in the degree of porosity and permeability calculated. In general, the highest values in both calculations were for 100 percent shale beds and the lowest values were the 100 percent siltstone beds with a linear relationship for the intermittent rock types.

With the use of the model, the fracture porosity and permeability can be calculated for a specific location within the Southern Conasauga Belt.

CHAPTER IV

CONCLUSION

Joint orientation analysis revealed the presence of two distinct systematic joint sets in the Southern Conasauga Belt. One set, the strike joints, are parallel to the strike of the bedding, and the second set, a-c joints, are normal to the strike joints. Joints compose a single orthogonal set present at all locations in the Southern Conasauga Belt and are believed to be related to the principal thrusting event that occurred in the region. The Northern Conasauga Belt exhibits an unpredictable joint pattern because of polyphase deformation that influenced their formation.

The analysis of the joint length and density data in siltstone suggests that joint length is directly proportional and density is inversely proportional to bed thickness. The same parameters examined in the shale beds suggest that joint density is inversely proportional to bed thickness; joint length is independent of bed thickness. The effects of surficial weathering, however, create large deviations in the measurements, as displayed in all results.

A computer model was developed to simulate in at least a semi-quantitative fashion fracture porosity and permeability for a portion of the Conasauga Group within the Southern Conasauga Belt. The most important factor in the calculation is the gap width, which is also the most difficult to measure. The gap is determined by combining permeability measurements recorded in the field with gap width data in drill cores to develop a range of values for the gap.

Increasing joint gap width by a given factor will increase the porosity by the same factor and increase the permeability by the cube of the factor. Pure shale beds generally contain the largest fracture porosity and permeability, while the pure siltstone beds have the lowest.

The results of the computer model must be used with caution. There are a few assumptions that were required with little or no supporting field evidence; and if the model is not used carefully, the results may be inaccurate. The major problematic assumptions affecting the model are listed below:

1. All data were collected from the Pumpkin Valley Shale Formation of the Conasauga Group. The joint orientation, density, and length measurements may be different in the other members within the area.

2. The collected data were all from weathered zones at surface outcrops. Field verification should be made for extrapolation to the unweathered bedrock.

3. Presence of limestone will cause serious discrepancies from the actual conditions existing within the subsurface. Data on limestone beds should be implemented at a later time for any broad area use.

4. The most important limitation of the model is the assumption of the existence of a homogeneous lithology along the strike of the strata. This can cause serious problems if attempts are made to apply the model at large distances from existing drill holes. This problem may decrease in importance with an increase in drill core information.

If the computer model is used with caution, it may provide valid numerical results for the existing subsurface fracture porosity and permeability. The same methods used in developing the model presented here should be applicable in other areas containing highly jointed rocks, but would require field verification.

LIST OF REFERENCES

- Babcock, E. A., 1973, Regional jointing in Southern Alberta: Canadian Jour. Earth Sci., v. 10, p. 1769-1781.
- Babcock, E. A., 1974, Jointing in Central Alberta Canadian Jour. Earth Sci., v. 11, p. 1181-1186.
- Babcock, E. A., 1978, Measurement of subsurface fractures from dipmeter logs: Am. Assoc. Petroleum Geologists Bull., v. 62, p. 1111-1126.
- Barr, A. J., Goodnight, J. H., Sall, J. P., Blair, W. H., and Chilko, D. M., 1979, SAS User's Guide: SAS Institute Inc., 494p.
- Curry, J. R., 1956, The analysis of two-dimensional orientation data: Jour. Geology, v. 64, p. 117-131.
- Currie, J. B., 1977, Significant geologic processes in development of fracture porosity: Am. Assoc. Petroleum Geologist Bull., v. 61, p. 1086-1089.
- Currie, J. B., and Reik, G. A., 1977, A method of distinguishing regional directions of jointing and of identifying joint sets associated with individual geologic structures: Canadian Jour. Earth Sci., v. 14, p. 1211-1228.
- Davis, S. N., 1969, Porosity and permeability of natural materials, in Flow through porous media: Dewiest, R. J. M., ed., Academic Press, New York, p. 54-90.
- Davis, S. N., and Dewiest, R. J. M., 1966, Hydrogeology: Wiley, New York, 463p.
- Davis, J. C., 1973, Statistics and data analysis in geology: Wiley, New York, 550p.
- Draper, N. R., and Smith, H., 1966, Applied regression analysis: Wiley, New York, 407p.
- Dudley, R. M., Perkins, P. C., and Evarist, G. M., 1975, Statistical tests for preferred orientation: Jour. of Geology, v. 83, p. 685-705.
- Fisher, R. A., 1953, Dispersion on a sphere: Proc. Royal Soc. London, Series A, v. 217, p. 295-305.
- Flinn, D., 1958, On tests of significance of preferred orientation in three-dimensional fabric diagrams: Jour. of Geology, v. 66, p. 526-539.

- Freeze, R. A., and Cherry, J. A., 1979, groundwater; Prentice-Hall, New Jersey, 604p.
- Harbaugh, J. W., and Bonham-Carter, G., 1970, Computer simulation in geology: Wiley, New York, 575p.
- Harris, J. F., Taylor, G. L., and Walpen, J. L., 1960, Relation of deformational fractures in sedimentary rocks to regional and local structure: Am. Assoc. Petroleum Geologists Bull., v. 44, p. 1853-1873.
- Harris, L. D., and Milici, R. C., 1977, Characteristics of thin-skinned style of deformation in the Southern Appalachians, and potential hydrocarbon traps: U.S. Geol. Survey Professional Paper 1018, 40p.
- Hatcher, R. D. Jr., 1965, Structure of the northern portion of the Dumplin Valley fault zone in East Tennessee [unp. Ph.D. thesis]: Univ. Tennessee, Knoxville.
- Hobbs, B. E., Means, W. D., and Williams, P. F., 1976, An outline of structural geology: Wiley, New York, 571p.
- Hobbs, D. W., 1972, The formation of tension joints in sedimentary rocks; an explanation: Geol. Magazine, v. 104, p. 550-556.
- Hodgson, P. A., 1961, Regional study of jointing in the Comb-Ridge-Navajo Mountain area: Am. Assoc. Petroleum Geologists Bull., v. 45, p. 1-38.
- ISSCO, 1975, Display integrated software system and plotting language; Integrated Software Systems Corporation, California.
- Jeran, P. W., and Mashey, J. R., 1970, A computer program for the stereographic analysis of coal fractures and cleats: Bureau of Mines Rept. of Inv., No. 8454, 34p.
- King, P. B., 1948, Geology of the Southern Gaudalupe Mountains; Texas: U.S. Geol. Survey Professional Paper 215, p. 114-117.
- Knoring, L. D., 1970, Correlation of joint trends with the elements of tectonic structures, in Topics in mathematical geology: Romanova, and Sarmanova, ed., Consultants Bureau, p. 43-62.
- Krumhansl, J. L., 1979, Preliminary results report Conasauga near-surface heater experiment: Sandia Laboratories SAND79-0745, New Mexico, 61p.
- Luxmoore, R. J., 1980, Personal communication: Oak Ridge National Laboratory, Oak Ridge, Tennessee.

- Mahtab, M. A., Bolstad, D. D., Alldredge, J. R., and Shanley, R. J., 1972, Analysis of fracture orientations for input to structure models of discontinuous rock: Bureau of Mines Rept. of Inv., No. 7669, 76p.
- Mahtab, M. A., Bolstad, D. D., and Kendorski, F. S., 1973, Analysis of the geometry of fractures in San Manuel Copper Mine, Arizona: Bureau of Mines Rept. of Inv., No. 7715, 24p.
- McMaster, W. M., 1963, Geologic map of the Oak Ridge Reservation, Tennessee: U. S. Atomic Energy Commission ORNL-TM-713, 23p.
- Milici, R. C., Brent, W. B., and Walker, K. R., 1973, Depositional environments in Upper Conasauga lagoon-fill sequence in Geology of Knox County, Tennessee: Tennessee Div. Geology Bull. 70, p. 138-148.
- Muecke, G. K., and Charlesworth, H. A. K., 1966, Jointing in folded Cardium Sandstone along the Bow River, Alberta: Canadian Jour. Earth Sci., v. 3, p. 579-596.
- Murray, G. H. Jr., 1968, Quantitative fracture study Spanish Pool, Mckenzie County, North Dakota: Am. Assoc. Petroleum Geologists Bull., v. 52, p. 57-65.
- Murrell, S. A. F., 1977, Natural faulting and the mechanics of brittle shear failure: Jour. Geol. Soc. London, v. 133, p. 175-189.
- Neter, J., Wasserman, W., and Whitmore, G., 1978, Applied statistics: Allyn and Bacon Inc., Boston, 743p.
- Nickelsen, R. P., and Hough, V. N. D., 1967, Jointing in the Appalachian Plateau of Pennsylvania: Geol. Soc. America Bull., v. 78, p. 609-630.
- Ossi, E. J., 1979, Mesoscopic structures and fabric within the thrust sheets between the Cumberland Escarpment and Saltville Fault [unp. MS. thesis]: Univ. Tennessee, Knoxville, 97p.
- Parker, J. M., 1942, Regional systematic jointing in slightly deformed sedimentary rocks: Geol. Soc. America Bull., v. 53, p. 381-408.
- Parsons, R. W., 1966, Permeability of idealized fractured rock: Soc of Petroleum Engineers Jour., v. 6, p. 126-136.
- Pincus, H. J., 1951, Statistical methods applied to the study of rock fractures: Geol. Soc. America Bull., v. 62, p. 81-130.
- Pirson, S. J., 1953, Performance of fractured oil reservoirs: Am. Assoc. Petroleum Geologists Bull., v. 37, p. 232-244.

- Price, N. J., 1966, Fault and joint development in brittle and semi-brittle rock: Pergamon, New York, 176p.
- Price, R. A., 1967, The tectonic significance of mesoscopic subfacies in the Southern Rocky Mountains of Alberta and British Columbia: Canadian Jour. Earth Sci., v. 4, p. 39-70.
- Regan, L. J. Jr., and Hughes, A. W., 1949, Fractured reservoirs of Santa Maria District, California: Am. Assoc. Petroleum Geologists Bull., v. 33, p. 32-51.
- Reike, H. H., and Chilingarian, G. V., 1974, Compaction of argillaceous sediments: Elsevier, New York, 424p.
- Rodgers, J., 1953, Geologic map of East Tennessee with explanatory text: Tennessee Div. of Geology Bull. 58, pt. 2, 168p.
- Roeder, D. H., Gilbert, O. E., and Witherspoon, W. D., 1978, Evolution and microscopic structure of Valley and Ridge thrust belt, Tennessee and Virginia: Univ. Tenn. Studies in Geology Number 2, 25p.
- Samman, N. F., 1975, Sedimentation and stratigraphy of the Rome Formation in East Tennessee [unp. Ph.D. thesis]: Univ. Tennessee, Knoxville, 337p.
- Snow, D. T., 1968, Rock fracture spacings, openings, and porosities: Am. Soc. Civil Engineers Proc., Jour. Soil Mechanics and Found. Div., v. 94, p. 73-91.
- Spencer, E. w., 1959, Geologic evolution of the Beartooth Mountains., Montana and Wyoming; pt. 2 (fracture patterns): Geol. Soc. America Bull., v. 70, p. 467-508.
- Stauffer, M. R., 1966, An empirical-statistical study of three-dimensional fabric diagrams as used in structural analysis: Canadian Jour. Earth Sci., v. 3, p. 473-498.
- Stearns, D. W., and Friedman, M., 1972, Reservoirs in fractured rock in Stratigraphic oil and gas fields: Am. Assoc. Petroleum Geologists Mem. 16., p. 82-106.
- Todd, D. K., 1959, Ground water hydrology: Wiley, New York, 336p.
- Viessman, W., Harbaugh, T. E., and Knapp, J. W., 1972, Introduction to hydrology: Intext Educational, New York, 415p.
- Vistellius, A. B., 1966, Structural diagrams: Pergamon, New York, 178p.
- Watson, G. S., 1966, The statistics of orientation data: Jour. Geology, v. 74, p. 786-797.

Webster, D, 1976, A review of hydrologic and geologic condition related to the radioactive solid-waste burial grounds at Oak Ridge National Laboratory, Tennessee: U.S. Geol. Survey Open-File Rept. 76-727, p. 15-19.

Winchell, H., 1937, A new method of interpretation of petrofabric diagrams: Am. Mineralogist, v. 22, p. 15-36.

APPENDIX A
FORTRAN PROGRAM

APPENDIX A
FORTRAN PROGRAM

```

00010      PROGRAM FRAFLO
00020
00030      C      FRACTURE FLOW MODELING SYSTEM
00040      C      MAINLINE PROGRAM WHICH CALCULATES THE FRACTURE
00050      C      POROSITY AND PERMEABILITY OF ROCKS.
00060      C      FOR USERS GUIDE AND ANY I/O INFORMATION AND
00070      C      SUBROUTINES REQUIRED FOR LOADING.. SEE ;
00080      C      SLEDZ AND HUFF (1980).. ORNL PUBLICATION OR
00090      C      SLEDZ (1980)..MS THESIS AT UNIVERSITY OF TENNESSEE
00100      C      WRITTEN BY JIM SLEDZ 3/21/80
00110      C      MODIFIED BY JIM SLEDZ 6/29/80
00120
00130      COMMON/KEEP/INCR,DEPTH,SILGAP,SHAGAP
00140      COMMON/WORK/NPRIN,IOTTY,INTTY,IUNIT1,IUNIT2,IUNIT3
00150
00160      C      MAX DIMENSION FOR PLOTS (PLOCEL)
00170
00180      DIMENSION ARAY(53,53),IWORK(220)
00190
00200      DATA IUNIT1/20/,IUNIT2/21/,IUNIT3/22/
00210      DATA NPRIN/6/,KSWTH/0/,IOTTY/5/,INTTY/5/
00220
00230      WRITE(IOTTY,1000)
00240      1000  FORMAT(//' WELCOME TO THE FRACTURE FLOW MODELING SYSTEM'//)
00250
00260      KNT=0
00270      10  CONTINUE
00280      WRITE(IOTTY,1001)
00290      1001  FORMAT(' OPTION; G'S)
00300      READ(INTTY,1002,ERR=20) IANS
00310      1002  FORMAT(I2)
00320
00330      IF(IANS.LT.0) GO TO 999
00340      IF(IANS.GE.1.AND.IANS.LE.4) GO TO 50
00350
00360      20  CALL ERROR(1,$10)
00370
00380      C      COMPLETE SURFACE 3-D
00390
00400      50  IF(KNT.GT.0) GO TO 55
00410      KNT=KNT+1
00420      CALL TOPMAK
00430      CALL BLDMAT
00440      55  IF(IANS.GT.1) GO TO 100
00450      CALL MATFIX
00460      C      CALL PLOSOU
00470      KSWTH=-1
00480      GO TO 10
00490
00500      C      SURFACE 3-D OF CELL
00510
00520      100  CALL CELL(LAT,IRAYDM,IPLODM)
00530      IF(IANS.GT.2) GO TO 150
00540      CALL PLOCEL(IWORK,IRAYDM,ARAY,IPLODM,0)
00550      KSWTH=-1
00560      GO TO 10
00570
00580      C      CELL FRACTURE POROSITY
00590
00600      150  CALL CORFIX

```

```

00610      IF(IANS.EQ.4) CALL TABPOR($10)
00620      CALL PLOCEL(IWORK,IPAYDM,ARAY,IPLODM,1)
00630      KSWTH=-1
00640      GO TO 10
00650
00660 C      END IT ALL
00670
00680 999  CONTINUE
00690      IF(KSWTH.LT.0) CALL DONEPL
00700      OPEN(UNIT=IUNIT1,FILE='SLALO.DAT')
00710      CLOSE(UNIT=IUNIT1,DISPOSE='DELETE')
00720      CALL EXIT
00730      END
00740
00750
00760
00770      SUBROUTINE ERRCR(N,*)
00780
00790 C      SUBROUTINE OF ERROR COMMANDS
00800 C      WRITTEN BY JIM SLEDZ 3/21/80
00810 C      MODIFIED BY JIM SLEDZ 7/9/80
00820
00830      COMMON/WORK/NPRIN,IOTTY,INTTY
00840
00850      IF(N.EQ.1) WRITE(IOTTY,1000)
00860      IF(N.EQ.2) WRITE(IOTTY,1001)
00870      IF(N.EQ.3) WRITE(IOTTY,1002)
00880      IF(N.EQ.4) WRITE(IOTTY,1003)
00890
00900      RETURN 1
00910
00920 1000  FORMAT(' AVAILABLE OPTIONS ARE;'/,
00930 1 ' 1 COMPLETE SURFACE 3-D',/,
00940 2 ' 2 CELL SURFACE 3-D',/,
00950 4 ' 3 CELL FRACTURE POROSITY 3-D',/,
00960 5 ' 4 CELL FRACTURE POROSITY TABLE',/,
00970 7 ' -1 END',/)
00980 1001  FORMAT(' AVAILABLE CORES ARE;'/,1X,
00990 1 '
01000 2 '1 - OR12 - (30870,19315)'/,1X,
01010 3 '2 - OR13 - (31397,19289)'/,1X,
01020 4 '3 - OR14 - (32240,19001)'/,1X,
01030 5 '4 - OR15 - (35711,18373)'/,1X,
01040 6 '5 - OR17 - (35922,16976)'/,1X,
01050 7 '6 - OR18 - (35843,17846)'/,1X,
01060 8 '7 - OR19 - (36528,16845)'/,1X,
01070 9 '8 - OR20 - (35553,17582)'/)
01080 1002  FORMAT(/,' ** LATITUDE OUT OF RANGE...REENTER **'/)
01090 1003  FORMAT(/,' ** LONGITUDE OUT OF RANGE...REENTER **'/)
01100
01110      END
01120
01130
01140
01150      SUBROUTINE TOFMAK
01160
01170 C      SUB USED TO CCNVERT DATA RECORDED FROM TOPO
01180 C      MAP TO X,Y,Z COORDINATES.
01190 C      WRITTEN BY JIM SLEDZ 2/18/80
01200 C      MODIFIED BY JIM SLEDZ 5/7/80

```

```

01210
01220      COMMON/WORK/NFRIN,IOTTY,INTTY,IUNIT1,IUNIT2
01230      DIMENSION IRAY(31)
01240
01250      OPEN(UNIT=IUNIT1,FILE='STOP0.DAT',ACCESS='SEQIN')
01260      OPEN(UNIT=IUNIT2,FILE='CENTUR.DAT',ACCESS='SEQOUT')
01270
01280      C      READ LATITUDE, LONGITUDE FOR EACH ELEVATION
01290
01300      10      READ(IUNIT1,100,END=99) IRAY
01310
01320      C      CALCULATE LONGITUDE AND LATITUDE
01330
01340      LONG=(IRAY(3)*1000+132)+(IRAY(4)*263)
01350      LAT=(IRAY(1)*1000+132)+(IRAY(2)*263)
01360
01370      C      CALC ELEVATION
01380
01390      DO 25 J=5,31
01400      IF(IRAY(J).EQ.0) GO TO 10
01410      IF(IRAY(J).LT.20) IRAY(J)=((IRAY(J)-10)*10)+1000
01420      IF(IRAY(J).LT.30) IRAY(J)=((IRAY(J)-20)*10)+1100
01430      IF(IRAY(J).LT.100) IRAY(J)=IRAY(J)*10
01440
01450      C      WRITE ALL INFC
01460
01470      WRITE(IUNIT2,101) LONG,LAT,IRAY(J)
01480      IRAY(2)=IRAY(2)+1
01490      IF(IRAY(2).LE.18) LAT=LAT+263
01500      IF(IRAY(2).GT.18) LAT=((IRAY(1)+5)*1000+132)+((IRAY(2)
01510      1      -19)*263)
01520      25      CONTINUE
01530
01540      99      CLOSE(UNIT=IUNIT1)
01550      CLOSE(UNIT=IUNIT2)
01560
01570      RETURN
01580
01590      100     FORMAT(3I12)
01600      101     FORMAT(2(I5,2X),I4)
01610
01620      END
01630
01640
01650
01660      SUBROUTINE BLOMAT
01670
01680      C      SUB TO FILL 3E CELLS WITH AN ELEVATION USING THE
01690      C      OUTPUT OF *TOFMAK*.
01700      C      SUB USES AN ELEVATION OF 600 WHEN COORDINATES
01710      C      LIE OUTSIDE THE STUDY AREA.
01720      C      WRITTEN BY JIM SLEDZ 3/5/80
01730      C      MODIFIED BY JIM SLEDZ 5/7/80
01740
01750      COMMON/WORK/NFRIN,IOTTY,INTTY,IUNIT1,IUNIT2,IUNIT3
01760      DIMENSION IRAY(38)
01770
01780      DATA JKNT/0/,KN1/0/,J/0/,JLONG/69866/,IKEY/0/
01790
01800      OPEN(UNIT=IUNIT2,FILE='CONTUR.DAT',ACCESS='SEQIN')

```

```

01810      OPEN(UNIT=IUNIT3,FILE='SLALQ.DAT',ACCESS='SEQINOUT')
01820
01830      C      ALL POSSIBLE LATITUDES
01840
01850          DO 5 J0=12,50
01860          J11=J0-11
01870          IF(J0.LE.18) IRAY(J11)=10132+(J0*263)
01880          IF(J0.GT.18.AND.J0.LE.37) IPAY(J11)=15132+((J0-19)*263)
01890          IF(J0.GT.37) IRAY(J11)=20132+((J0-38)*263)
01900      5      CONTINUE
01910
01920      10     J=J+1
01930
01940      C      READ IN DATA
01950
01960          READ(IUNIT2,101,END=98) LONG,LAT,I
01970          IF(LONG.EQ.JLCNG) GO TO 12
01980          IF(J.GT.38) GO TO 11
01990      7      DO 11 KK=J,38
02000          WRITE(IUNIT3,101) JLONG,IRAY(KK),IZERO
02010          JKNT=JKNT+1
02020      11     CONTINUE
02030          IF(IKEY.EQ.1) GO TO 99
02040          J=1
02050      12     KNT=KNT+1
02060      101    FORMAT(2(I5.2X),I4)
02070
02080      C      CHECK FOR LATITUDE MATCH
02090
02100      15     IF(IRAY(J).EQ.LAT.OP.J.GE.38) GO TO 25
02110
02120      C      ZERO ELEVATION AT 600 FEET
02130
02140          IZERO=600
02150          ILAT=IRAY(J)
02160
02170      C      WRITE BASE LINE DATA
02180
02190          WRITE(IUNIT3,101) LONG,ILAT,IZERO
02200          J=J+1
02210          JKNT=JKNT+1
02220          GO TO 15
02230
02240      C      WRITE ACTUAL DATA
02250
02260      25     WRITE(IUNIT3,101) LONG,LAT,I
02270          JLONG=LONG
02280          JKNT=JKNT+1
02290          GO TO 10
02300
02310      C      FINISH
02320
02330      98     CLOSE(UNIT=IUNIT2,DISPOSE='DELETE')
02340          IKEY=1
02350          GO TO 7
02360      99     CLOSE(UNIT=IUNIT3)
02370          RETURN
02380          END
02390
02400

```

```

02410
02420      SUBROUTINE MATFIX
02430
02440      C      DESIGNED TO ARRANGE DATA FOR 3-D PLOTTING FROM DATA
02450      C      TAKEN FROM 'BLDMAT.MDL'
02460      C      WRITTEN BY JIM SLEDZ 3/5/80
02470      C      MODIFIED BY JIM SLEDZ 5/7/80
02480
02490      CCOMMON/WORK/NFRIN,IQTTY,INTTY,IUNIT1,IUNIT2
02500      DIMENSION IRAY(190,38)
02510
02520      OPEN(UNIT=IUNIT1,FILE='SLALO.DAT',ACCESS='SEQIN')
02530      OPEN(UNIT=IUNIT2,FILE='SMAT.POT',ACCESS='SEQOUT')
02540
02550      C      SET UP MATRIX - LONG,LAT BY ELEVATION
02560
02570      DO 20 LONG=1,190
02580      DO 10 LAT=1,38
02590      READ(IUNIT1,100) IELAV
02600      100  FORMAT(14X,I4)
02610      IRAY(LONG,LAT)=IELAV
02620      10  CONTINUE
02630      20  CONTINUE
02640
02650      C      WRITE MATRIX IN NEW FORMAT TO DISK
02660
02670      DO 40 LONG=1,190
02680      WRITE(IUNIT2,101) (IRAY(LONG,LAT),LAT=1,38)
02690      101  FORMAT(19I4,/,15I4)
02700      40  CONTINUE
02710      CLOSE(UNIT=IUNIT1)
02720      CLOSE(UNIT=IUNIT2)
02730      RETURN
02740      END
02750
02760
02770
02780      SUBROUTINE PLOSCU
02790
02800      C      READS ELEVATION DATA FROM FILE 'SMAT.POT', AFTER
02810      C      PROCESSING BY MATFIX, AND MAKES A 3-D PLOT OF IT
02820      C      WRITTEN BY JIM SLEDZ 3/5/80
02830      C      MODIFIED BY JIM SLEDZ 5/7/80
02840
02850      CCOMMON/WORK/NFRIN,IQTTY,INTTY,IUNIT1
02860      DIMENSION ZMAT(190,38),IWORK(1000)
02870
02880      C      READ ELEVATION DATA FROM FILE
02890
02900      OPEN(UNIT=IUNIT1,FILE='SMAT.POT',ACCESS='SEQIN')
02910      DO 20 LONG=1,190
02920      READ(IUNIT1,100) (ZMAT(LONG,LAT),LAT=38,1,-1)
02930      100  FORMAT(19F4.0,/,19F4.0)
02940      20  CONTINUE
02950      CLOSE(UNIT=IUNIT1,DISPOSE='DELETE')
02960
02970      C      PLOT IN 3-D
02980
02990      CALL CALCMP
03000      CALL BGNPL(-1)

```

```

03010      CALL BSCALE(5.,1.)
03020      CALL NOBRDP
03030      CALL PAGE(110,11)
03040      CALL TITL3D('SOUTHERN CONASAUGA BELT',23,10.,9.)
03050      CALL AXES3D('LONGITUDE',9,'LATITUDE',8,'ELEVATION',9,10.,8.,6.)
03060      CALL VUANGL(85.,45.,20.)
03070      CALL GRAF3D(190.,20.,0.,0.,3.,38.,600.,100.,1100.)
03080      CALL SURMAT(ZMAT,1,190,1,38,IWORK)
03090      CALL ENDPL(0)
03100      RETURN
03110      END
03120
03130
03140
03150      SUBROUTINE CELL(LATIT,IDIMEN,MDIMEN)
03160
03170      C      GIVEN THE MINIMUM LATITUDE AND LONGITUDE FOR CELL AND
03180      C      THE NUMBER OF DIVISIONS PER EDGE OF CELL, WILL CALC.
03190      C      THE COORDINATES AND ELEVATIONS FORMING THE CELL.
03200      C      OUTPUTS RESULTS TO FILE CELL.OUT
03210      C      WRITTEN BY JIM SLEDZ 3/6/80
03220      C      MODIFIED BY JIM SLEDZ 7/20/80
03230
03240      COMMON/KEEP/INCRE
03250      COMMON/WORK/NPRIN,IOTTY,INTTY,IUNIT1
03260      DIMENSION IEL(4),DIST(4)
03270      DATA IEL/4*0/
03280
03290      C      INPUT PARAMETERS, LATITUDE AND LONGITUDE IS MIN. OF CELL
03300
03310      1      CONTINUE
03320      WRITE(IOTTY,1000)
03330      1000  FORMAT(' COORDINATES ARE ORA GRID SYSTEM',,' LATITUDE; '$)
03340      READ(INTTY,1001) LATIT
03350      1001  FORMAT(I5)
03360      IF(LATIT.LT.0.OR.LATIT.GT.20000) CALL ERROR(3,$1)
03370      2      CONTINUE
03380      WRITE(IOTTY,1002)
03390      1002  FORMAT(' LONGITUDE; '$)
03400      READ(INTTY,1001) LONG
03410      IF(LONG.LT.20000.OR.LONG.GT.70000) CALL ERROR(4,$2)
03420      WRITE(IOTTY,1003)
03430      1003  FORMAT(' DIVISIONS ON CELL EDGE ; '$)
03440      READ(INTTY,1001) LDIV
03450      INCRE=263/LDIV
03460
03470      C      CELL DIVISIONS OF 5 FEET IS MAX.
03480
03490      IF(INCRE.GT.52) INCRE=52
03500
03510      C      FIND LONGITUDE BY STARTING AT 20132 AND WORK THE WAY UP
03520
03530      DO 3 J=20,65,5
03540      DO 4 K=1,19
03550      KEYLOG=(J*1000+132)+((K-1)*263)
03560
03570      C      FIND THE LOWER AND UPPER LONGITUDES
03580
03590      IF(KEYLOG.GT.LONG) GO TO 15
03600      LONCN=KEYLOG

```

```

03610      4      CONTINUE
03620      3      CONTINUE
03630     15      LONUP=KEYLOG
03640
03650      C      FIND THE UPPER AND LOWER LATITUDES
03660
03670          DO 30 JJ=10,25,5
03680          DO 35 KK=1,19
03690          KEYLAT=(JJ*1000+132)+((KK-1)*263)
03700          IF(KEYLAT.GT.LATIT) GO TO 50
03710          LATDN=KEYLAT
03720     35      CONTINUE
03730     30      CONTINUE
03740     50      LATUP=KEYLAT
03750
03760      C      FIND THE ELEVATIONS FOR THE LOWER AND UPPER LONG AND LAT
03770
03780          OPEN(UNIT=IUNIT1,FILE='SLALO.DAT',ACCESS='SEQIN')
03790     45      READ(IUNIT1,1005,END=51) ILONG,ILAT,IELEV
03800     1005    FORMAT(2(I5,2X),I4)
03810
03820      C      FOUR CORNERS OF CELL ARE 4,2,1,3 (CLOCK-UPPER LEFT-START)
03830
03840          IF(ILONG.EQ.LONDN.AND.ILAT.EQ.LATDN) IEL(1)=IELEV
03850          IF(ILONG.EQ.LONDN.AND.ILAT.EQ.LATUP) IEL(2)=IELEV
03860          IF(ILONG.EQ.LONUP.AND.ILAT.EQ.LATDN) IEL(3)=IELEV
03870          IF(ILONG.EQ.LONUP.AND.ILAT.EQ.LATUP) IEL(4)=IELEV
03880          GO TO 45
03890     51      CLOSE(UNIT=IUNIT1)
03900
03910      C      CALCULATE THE EXTRAPOLATED ELEVATIONS FOR THE CELL (DAVIS-P.316)
03920
03930          OPEN(UNIT=IUNIT1,FILE='CELL.OUT',ACCESS='SEQOUT')
03940          KNT=0
03950          DO 75 J=LONDN,LONUP,INCRE
03960          KNT=KNT+1
03970          DO 60 K=LATDN,LATUP,INCRE
03980
03990      C      INCREMENTAL DISTANCE OF POINT (J,K) TO EACH CORNER
04000
04010          DIST(1)=((LONDN-J)**2+(LATDN-K)**2)**0.5
04020          DIST(2)=((LONDN-J)**2+(LATUP-K)**2)**0.5
04030          DIST(3)=((LONUP-J)**2+(LATDN-K)**2)**0.5
04040          DIST(4)=((LONUP-J)**2+(LATUP-K)**2)**0.5
04050
04060
04070      C      CHECK IF DIVIDING BY ZERO
04080
04090          DO 52 JD=1,4
04100          IF(DIST(JD).EQ.0.) DIST(JD)=1.
04110     52      CONTINUE
04120
04130      C      TOTAL ELEVATION
04140
04150          TELEV=IEL(1)/DIST(1)+IEL(2)/DIST(2)+IEL(3)/DIST(3)+
04160     1      IEL(4)/DIST(4)
04170          RECDIS=1./DIST(1)+1./DIST(2)+1./DIST(3)+1./DIST(4)
04180
04190      C      NEW ELEVATION
04200

```

```

04210      ANEL=TELEV/PECCIS
04220      WRITE(IUNIT1,1006) J,K,ANEL
04230      100E  FORMAT(2(I5,2X),F7.1)
04240      60   CONTINUE
04250      75   CONTINUE
04260      CLOSE(UNIT=IUNIT1)
04270
04280      C      DIMENSION SETUP FOR 3-D PLOT
04290
04300      JINC=KNT
04310      IDIMEN=(JINC)*4+5
04320      MDIMEN=JINC
04330      RETURN
04340      END
04350
04360
04370
04380      SUBROUTINE PLOC(ARWK,M,ARY,N,KEY)
04390
04400      C      PLOTS ANY CELL USING DIMENSIONS NXN INTO A 3-D
04410      C      PLOT OVER A 6XE INCH AREA
04420      C      KEY GT ZERO FOR FRACTURE POROSITY PLOT
04430      C      WRITTEN BY JIM SLEDZ 3/25/80
04440      C      MODIFIED BY JIM SLEDZ 6/29/80
04450
04460      COMMON/KEEP/INCR,DEPTH
04470      COMMON/WORK/NFRIN,IOTTY,INTTY,IUNIT1
04480      DIMENSION ARY(1:N,1:N),ARWK(1:M),IPAK(150)
04490      DATA IPLT/-1/
04500
04510      IF(KEY.EQ.0) OPEN(UNIT=IUNIT1,FILE='CELL.OUT',ACCESS='SEQIN')
04520      IF(KEY.GT.0) OPEN(UNIT=IUNIT1,FILE='POROS.DAT',ACCESS='SEQIN')
04530      JOMIN=100000
04540      JOMAX=0
04550      JAMIN=100000
04560      JAMAX=0
04570      EMAX=0.0
04580      EMIN=10000.
04590
04600      C      INCREMENT OF PLOTTING CELL
04610
04620      APNT=FLOAT(N)
04630      IPLT=IPLT+1
04640
04650      C      READ DATA TO BE PLOTTED AND FILL ARY WITH ELEVATIONS
04660
04670      DO 20 LONG=1,N
04680      DO 15 LAT=N,1,-1
04690      IF(KEY.EQ.0) READ(IUNIT1,100) JO,JA,ARY(LONG,LAT)
04700      IF(KEY.GT.0) READ(IUNIT1,101) JO,JA,ARY(LONG,LAT)
04710      101  FORMAT(2(I5,1X),23X,F6.3)
04720      100  FORMAT(2(I5,2X),F7.1)
04730
04740      C      CALCULATE MAX AND MIN OF LONG AND LAT
04750
04760      ELEV=ARY(LONG,LAT)
04770      IF(JO.GT.JOMAX) JOMAX=JO
04780      IF(JO.LT.JOMIN) JOMIN=JO
04790      IF(JA.GT.JAMAX) JAMAX=JA
04800      IF(JA.LT.JAMIN) JAMIN=JA

```

```

04810         IF(EMIN.GT.ELEV) EMIN=ELEV
04820         IF(EMAX.LT.ELEV) EMAX=ELEV
04830     15     CONTINUE
04840     20     CONTINUE
04850         CLOSE(UNIT=IUNIT1)
04860
04870     C      3-D PLOT
04880
04890         CALL CALCMP
04900         CALL BGNPL(IPL1)
04910         CALL NOBPDP
04920         CALL PAGE(15,11)
04930         IF(KEY.GT.0) GO TO 25
04940         CALL TITL3D('SURFACE ELEVATION PLOT',22,10.,9.)
04950         CALL AXES3D('LONGITUDE',9,'LATITUDE',
04960     1      8,'ELEVATION',9,9.,9.,9.)
04970         GO TO 30
04980     25     CALL TITL3D('FRACTURE POROSITY PLOT',22,10.,9.)
04990         CALL AXES3D('LONGITUDE',9,'LATITUDE',
05000     1      8,'FRACTURE PCROSITY',17,9.,9.,9.)
05010         CALL MESSAG('AT DEPTH OF ',12,4.0,8,9)
05020         CALL REALNO(DEPTH,1,'ABUT','ABUT')
05030         CALL MESSAG(' METERS',7,'ABUT','ABUT')
05040     30     CALL VUANGL(85.,45.,20.)
05050         CALL GRAF3D(0.,'SCALE',APNT,0.,'SCALE',EMIN,'SCALE',EMAX)
05060         CALL SURMAT(ARRAY,1,N,1,N,AWORK)
05070         IF(N.GE.20) GO TO 35
05080         CALL DASH
05090         CALL NOHIDE
05100         CALL SURMAT(ARRAY,1,N,1,N,AWORK)
05110
05120     C      SET UP LEGEND CN PLOT
05130
05140     35     MAXLIN=LINEST(IPAK,150,20)
05150         CALL LINES('LONGITUDE MIN= $',IPAK,1)
05160         CALL LINES('LONGITUDE MAX= $',IPAK,2)
05170         CALL LINES('LATITUDE MIN= $',IPAK,3)
05180         CALL LINES('LATITUDE MAX= $',IPAK,4)
05190         CALL STORY(IPAK,4,4.5,7,9)
05200         CALL INTNO(JOMIN,6.4,8.5)
05210         CALL INTNO(JOMAX,6.4,8.3)
05220         CALL INTNO(JAMIN,6.4,8.1)
05230         CALL INTNO(JAMAX,6.4,7.9)
05240         CALL ENDPL(IPL1)
05250         RETURN
05260         END
05270
05280
05290
05300         SUBROUTINE COFFIX
05310
05320     C      CALCULATE IF COFE FIT WITHIN A CELL -- READ DATA NECESSARY
05330     C      FROM 'CORE.DAT' EXTRAPOLATING SECTION TO INTERSECT AT
05340     C      REQUESTED DEPTH
05350     C      DEPTH = DEPTH OF INTEREST
05360     C      IROCK= % OF LITHOLOGY
05370     C      WRITTEN BY JIM SLEDZ 3/5/80
05380     C      MODIFIED BY JIM SLEDZ 7/7/80
05390
05400         COMMON/KEEP/INCRE,DEPTH

```

```

05410      COMMON/WORK/NFRIN,IOTTY,INTTY,IUNIT1,IUNIT2,IUNIT3
05420      DIMENSION ICORE(8,7),IVALUE(200),IROCK(3),THK(100)
05430
05440      C      CORE IN THE FORM; LONG,LAT,SURFACE,BASE,DIP,LENGTH,FILE LOC
05450      C      CORES ARE IN FILE AS; OR12.COR,OR13.COR,OR14.COR,
05460      C      OR15.COR,OR17.COR,OR18.COR,OR19.COR,OR20.COR
05470
05480      DATA (ICORE(1,J),J=1,7)/30870,19315,815,716,33,99,1/
05490      DATA (ICORE(2,J),J=1,7)/31397,19289,824,725,30,99,100/
05500      DATA (ICORE(3,J),J=1,7)/32240,19001,840,741,33,99,199/
05510      DATA (ICORE(4,J),J=1,7)/35711,18373,872,773,29,99,298/
05520      DATA (ICORE(5,J),J=1,7)/35922,16976,840,741,39,99,397/
05530      DATA (ICORE(6,J),J=1,7)/35843,17846,865,731,29,134,496/
05540      DATA (ICORE(7,J),J=1,7)/36528,16845,879,779,43,100,630/
05550      DATA (ICORE(8,J),J=1,7)/35553,17582,870,770,27,100,730/
05560
05570      C      INPUT CORE NUMBER
05580
05590      2      CONTINUE
05600      WRITE(IOTTY,1005)
05610      1005  FORMAT(' DRILL HOLE NUMBER (1-8); '$)
05620      READ(INTTY,1006) IHOLE
05630      IF(IHOLE.LT.1.OR.IHOLE.GT.8) CALL ERROR(2,$2)
05640      1006  FORMAT(I1)
05650      WRITE(IOTTY,1007)
05660      1007  FORMAT(' DEPTH (METERS) OF INTEREST ; '$)
05670      READ(INTTY,1008) DEPTH
05680      1008  FORMAT(F7.2)
05690      C      CHANGE DEPTH TO FEET
05700
05710      DEP=DEPTH*3.28
05720      KEYDEP=IFIX(DEP)
05730      IF(DEP-KEYDEP.GT.0.5) KEYDEP=KEYDEP+1
05740
05750      C      DETERMINE LOCATION OF CORE OF INTEREST
05760
05770      OPEN(UNIT=IUNIT2,FILE='CORE.DAT',ACCESS='SEQIN')
05780      DO 5 J=1,ICORE(IHOLE,7)
05790      READ(IUNIT2,1004) TST
05800      5      CONTINUE
05810
05820      C      READ ENTIRE CORE INTO AN ARAY
05830
05840      DO 7 J=1,ICORE(IHOLE,6)
05850      READ(IUNIT2,1004) IVALUE(J)
05860      7      CONTINUE
05870      1004  FORMAT(3X,I8)
05880      CLOSE(UNIT=IUNIT2)
05890
05900      C      CALCULATE DISTANCE FROM BASE OF CORE TO SURFACE
05910
05920      ICORLN=ICORE(IHOLE,6)
05930      DIP=ICORE(IHOLE,5)
05940      SLOPE=ICORLN/COSD(DIP)
05950
05960      C      CALCULATE TOTAL SURFACE LENGTH (PROJECTION)
05970
05980      TLENGT=SLOPE*SIND(DIP)
05990
06000      C      DATA FROM DESIRED CELL

```

```

06010
06020      OPEN(UNIT=IUNIT2,FILE='POROS.DAT',ACCESS='SEQOUT')
06030      OPEN(UNIT=IUNIT1,FILE='CELL.OUT',ACCESS='SEQIN')
06040      10  READ(IUNIT1,1001,END=90) LONG,LAT,TELEV
06050      1001 FORMAT(2(I5,2X),F7.1)
06060
06070      C      NOT REPRESENTED BY THE CORE
06080
06090      IF(ICORE(IHOLE,2).LE.LAT) GO TO 20
06100
06110      C      CALCULATE DISTANCE BETWEEN 2 POINTS
06120
06130      TPDIST=ICORE(IHOLE,2)-LAT
06140
06150      C      ELEVATION OF CUR INTEREST
06160
06170      PTELEV=IFIX(TELEV)-KEYDEP
06180
06190      C      DETERMINE NEW TOP AND BOTTOM OF CORE
06200
06210      CORTOP=(TPDIST*SIND(DIP))/COSD(DIP)+ICORE(IHOLE,3)
06220      CORBAS=CORTOP-ICORLN
06230
06240      C      POINT OUT OF RANGE
06250
06260      IF(CORTOP.LT.FTELEV.AND.CORBAS.GT.PTELEV) GO TO 50
06270      IDIST=CORTOP-FTELEV
06280      GO TO 23
06290
06300      C      DISTANCE FROM LAT TO FURTHEST CORE LAT.
06310
06320      20      SLENGT=ABS(LAT-ICORE(IHOLE,2))
06330
06340      C      DEPTH OF CORE WHEN PROJECTED TO SURFACE
06350
06360      NDEPTH=(ICORLN*(TLENGT-SLENGT))/TLENGT
06370      NEWSUR=ICORE(IHOLE,3)+(ICORLN-NDEPTH)
06380      IDIST=NEWSUR-IELEVA+KEYDEP
06390
06400      C      CORE NOT REPRESENTED
06410
06420      23      IF(IDIST.LE.0.OR.IDIST.GT.ICORLN) GO TO 50
06430
06440      C      CALCULATE % OF EACH LITHOLOGY FROM CORE
06450      C      DATA IN THE FORM OF 87654321
06460
06470      ISILT=IVALUE(IDIST)/1000000
06480      ISTEP1=IVALUE(IDIST)-(ISILT*1000000)
06490      ISHAL=ISTEP1/10000
06500      ISTEP1=ISTEP1-(ISHAL*10000)
06510      IGLAUC=ISTEP1/100
06520      ILS=ISTEP1-(IGLAUC*100)
06530      IROCK(1)=ISILT+IGLAUC
06540      IROCK(2)=ISHAL
06550      IROCK(3)=ILS
06560      IF(IROCK(1).EQ.0.AND.IROCK(2).EQ.0.AND.IROCK(3).EQ.0) GO TO 50
06570
06580      C      CALCULATE POROSITY AND PERMEABILITY
06590
06600      ADEP=DEPTH

```

```

06610      GO TO 55
06620      50  ADEP=-99.
06630      55  CONTINUE
06640      CALL PORCAL(LCNG,LAT,ADEP,THOLE,IROCK)
06650      GO TO 10
06660
06670      C    FINISH
06680
06690      90  CLOSE(UNIT=IUNIT1,DISPOSE='DELETE')
06700      CLOSE(UNIT=IUNIT2)
06710      RETURN
06720      END
06730
06740
06750
06760      SUBROUTINE RCKTYP(IROCK,LNAM)
06770      C    DETERMINES TYPE OF ROCK BASED ON PERCENTAGE OF CONSTITUENTS
06780      C    WRITTEN BY JIM SLEDZ 3/5/80
06790      C    MODIFIED BY JIM SLEDZ 5/7/80
06800
06810      DIMENSION IROCK(3),LITH(7)
06820
06830      DATA (LITH(J),J=1,7)/'SILT ','SHALE','LIME ','
06840      1  'SL-SH','SL-L','SH-LS','MIXED'/
06850
06860      C    CHECK IF ROCK CONTAINS AT LEAST 70% OF ONE COMPONENT
06870
06880      DO 10 J=1,3
06890      IF(IROCK(J).GE.7) GO TO 15
06900      10  CONTINUE
06910      GO TO 25
06920      15  LNAM=LITH(J)
06930      RETURN
06940
06950      C    ROCK CONTAINS BETWEEN 50 & 70% OF COMPONENTS
06960
06970      25  LNAM=LITH(1)
06980      IF(IROCK(1).LT.5) GO TO 30
06990      IF(IROCK(2).GE.3) LNAM=LITH(4)
07000      IF(IROCK(3).GE.3) LNAM=LITH(5)
07010      RETURN
07020      30  LNAM=LITH(2)
07030      IF(IROCK(2).LT.5) GO TO 35
07040      IF(IROCK(3).GE.3) LNAM=LITH(6)
07050      RETURN
07060
07070      C    ROCK A MIXTURE OF ALL COMPONENTS
07080
07090      35  LNAM=LITH(3)
07100      IF(IROCK(3).LT.5) LNAM=LITH(7)
07110      RETURN
07120      END
07130
07140
07150
07160      SUBROUTINE GAPSET(LNUM,SUMGAP)
07170
07180      C    SUB TO DETERMINE THE WIDTH OF THE GAP FOR A GIVEN
07190      C    ROCK TYPE AND DEPTH.
07200      C    WRITTEN BY JIM SLEDZ 2/22/80

```

```

07210 C      MODIFIED BY JIM SLEDZ 7/9/80
07220
07230      COMMON/KEEP/(INCR,DEPTH,SILGAP,SHAGAP
07240      DIMENSION SGAP(2),GAPJNT(2)
07250
07260 C      GAP STARTING WICHTH -- UNITS ARE IN MM
07270 C      GAPS ARE FOR SILT,SHALE
07280
07290      DATA (SGAP(J),J=1,2)/0.2,0.2/
07300
07310 C      EQUATIONS FOR GAP WIDTH RELATED TO DEPTH
07320 C      1% DECREASE WITH EACH 1 METER DEPTH (DAVIS,1969)
07330
07340      DATA GAPJNT/0.01,0.01/
07350
07360      IDEP=IFIX(DEPTH)
07370
07380 C      CALCULATE NEW GAP AT DEPTH KEYDEP
07390
07400      SILGAP=SGAP(1)
07410      SHAGAP=SGAP(2)
07420      SUMGAP=SGAP(LNUM)
07430      DO 10 J=1,IDEP
07440      SUMGAP=SUMGAP-SUMGAP*GAPJNT(LNUM)
07450 10      CONTINUE
07460      IF(SUMGAP.LT.C.) SUMGAP=0.
07470
07480      RETURN
07490      END
07500
07510
07520
07530      SUBROUTINE ORDAT(LONG,N,STR,DIP)
07540
07550 C      CALCULATES STRIKE AND DIP OF JOINT SET (N) GIVEN
07560 C      LONGITUDE... EQUATION IS OF THE FORM B0+B1X FOR
07570 C      STRIKE,DIP BY REGRESION
07580 C      STRIKE USED IS EX. N45E-45 AND N45W-135.
07590 C      THE TWO MAJOR JOINT SETS ARE USED IN THE CALCULATIONS
07600 C      WRITTEN BY JIM SLEDZ 2/22/80
07610 C      MODIFIED BY JIM SLEDZ 4/1/80
07620
07630      DIMENSION SETJNT(2,4)
07640
07650      DATA (SETJNT(1,J),J=1,4)/155.12163,-0.0003453,60.557303,0.0003849/
07660      DATA (SETJNT(2,J),J=1,4)/62.179405,-.0001854,82.4180489,
07670 1 - .00040312/
07680
07690 C      CALC STRIKE AND DIP
07700
07710      VARSTR=SETJNT(N,1)+SETJNT(N,2)*LONG
07720      VARDIP=SETJNT(N,3)+SETJNT(N,4)*LONG
07730
07740      STR=VARSTR
07750      IF(VARSTR.GT.180.) STR=VARSTR-180.
07760      DIP=VARDIP
07770
07780      RETURN
07790      END
07800

```

```

07E10
07E20
07E30      SUBROUTINE THKCAL(TMAX,LITH,THK,JTOT)
07E40
07E50      C      SUB TO CALCULATE BED THICKNESS BASED ON THE MEAN AND STD
07E60      C      DEV. OF THICKNESS. SUB ASSUMES A NORMAL DISTRIBUTION OF
07E70      C      THICKNESS. TMAX IS THE MAX THICKNESS OF LITHOLOGY (LITH)
07E80      C      FOR BEDDING DETERMINATION. THK IS AN ARRAY OF BED THICKNESS
07E90      C      AND JTOT IS THE NUMBER OF BEDS USED
07900      C      WRITTEN BY JIM SLEDZ 3/30/80
07910      C      MODIFIED BY JIM SLEDZ 5/7/80
07920
07930      DIMENSION TMNSTD(3,2),SUMTHK(7),THK(100)
07940
07950      C      DATA IS MEAN,STD-DEV FOR SILT,SHALE,LIMESTONE
07960      C      LS ASSUME AS MEAN=6",MIN.=3"
07970
07980      DATA (TMNSTD(1,J),J=1,2)/46.00,20.00/
07990      DATA (TMNSTD(2,J),J=1,2)/6.48,2.87/
08000      DATA (TMNSTD(3,J),J=1,2)/152.4,72.39/
08010
08020
08030      THICK=TMAX
08040      TSUM=0.0
08050      JKNT=1
08060      JTOT=0
08070
08080      C      FILL ARAY WITH ZERO'S
08090
08100      DO 5 JZ=1,100
08110      THK(JZ)=0.0
08120      5      CONTINUE
08130
08140      C      THICKNESS IS MEAN PLUS AND MINUS 2 STD.DEV UNITS (95.4% OF POP.)
08150      C      AND THIS DIVIDED INTO 6 UNITS
08160
08170      TMPLUS=TMNSTD(LITH,1)+2.*TMNSTD(LITH,2)
08180      TMMIN=TMNSTD(LITH,1)-2.*TMNSTD(LITH,2)
08190      CTHK=(TMPLUS-TMMIN)/6.0
08200      SUMTHK(1)=TMMIN
08210      SUM=TMMIN
08220
08230      C      FILL IN INCREMENTS AT MIN=1,MEAN=4,MAX=7
08240
08250      DO 10 J=2,7
08260      SUMTHK(J)=SUM+CTHK
08270      SUM=SUMTHK(J)
08280      TSUM=SUM+TSUM
08290      10      CONTINUE
08300
08310      C      CHECK IF THICKNESS IS ENOUGH FOR COMPLETE DISTRIB.
08320
08330      12      TLEFT=THICK-TSUM
08340      IF(TLEFT.LT.0.0) GO TO 35
08350
08360      C      FILL IN WITH CYCLE OF COMPLETE DISTRIBUTION
08370
08380      DO 15 J=1,7
08390      THICK=THICK-S(MTHK(J)
08400      THK(JKNT)=SUMTHK(J)

```

```

08410      JKNT=JKNT+1
08420      15      CONTINUE
08430      GO TO 12
08440
08450      C      TRY MEAN,MIN, AND MAX
08460
08470      35      INUM=4
08480      40      TLEFT=THICK-SUMTHK(INUM)
08490
08500      C      NO THICKNESS LEFT....KEEP TRYING
08510
08520      IF(TLEFT.LT.0.0) GO TO 75
08530      THICK=TLEFT
08540      THK(JKNT)=SUMTHK(INUM)
08550      JKNT=JKNT+1
08560      IF(INUM.EQ.7) GO TO 75
08570      INUM=INUM-3
08580      IF(INUM.LT.0) INUM=7
08590      GO TO 40
08600
08610      C      TRY TO FILL IN MORE THICKNESS UNITS STARTING AT MAX.
08620
08630      75      DO 80 J2=7,1,-1
08640      TLEFT=THICK-SUMTHK(J2)
08650
08660      C      TO LARGE....KEEP TRYING
08670
08680      IF(TLEFT.LT.0.0) GO TO 80
08690      THICK=TLEFT
08700      THK(JKNT)=SUMTHK(J2)
08710      JKNT=JKNT+1
08720      80      CONTINUE
08730
08740      C      STILL HAVE AVAILABLE BED THICKNESS LEFT
08750
08760      IF(THICK.GE.TMIN) GO TO 75
08770      JTOT=JKNT-1
08780      RETURN
08790      END
08800
08810
08820
08830      SUBROUTINE DENLEN(ILITH,THICK,TJNTS,TJLEN)
08840
08850      C      SUB TO CALC JCINT DENSITY AND LENGTH BASED ON
08860      C      BED THICKNESS AND LITHOLOGY
08870      C      UNITS ARE IN CM.
08880      C      TJNTS= NO. OF JOINTS IN AREA OF A SQUARE INCRE X INCRE
08890      C      TJLEN=LENGTH OF EACH OF THESE JOINTS
08900      C      WRITTEN BY JIM SLEDZ 3/30/80
08910      C      MODIFIED BY JIM SLEDZ 6/29/80
08920
08930      COMMON/KEEP/INCRE
08940      DIMENSION TODEN(2,2),TOSUM(2,3)
08950
08960      C      DATA IN SILT, SHALE
08970
08980      C      REGRESSION IS DEN=B0+B1(THICK)
08990
09000      DATA (TODEN(1,J),J=1,2)/38.33324,-0.49109/  RSQUARE=79.4%

```

```

09010      DATA (TODEN(2,J),J=1,2)/22.56117,-1.05362/  RSQUARE=35.8%
09020
09030      C      REGRESSION IS JLEN=B0+B1(DEN)+B2(THICK)
09040
09050      DATA (TOSUM(1,J),J=1,3)/-0.75308,0.03284,0.586381/  RS=99.1%
09060      DATA (TOSUM(2,J),J=1,3)/10.51226,0.188671,-0.196341/  RS=98.4%
09070
09080      C      CALCULATE DENSITY FROM THICKNESS
09090
09100      10     CMINCR=INCRE*12*2.54
09110      SJDEN=TODEN(ILITH,1)+TODEN(ILITH,2)*THICK
09120
09130      C      CALCULATE LENGTH FROM ABOVE
09140
09150      TJLEN=TOSUM(ILITH,1)+TOSUM(ILITH,2)*SJDEN
09160      1      +TOSUM(ILITH,3)*THICK
09170
09180      C      CHANGE UNITS TO CM
09190
09200      TJDEN=SJDEN/10.
09210      IF(TJDEN.LT.0) TJDEN=0
09220
09230      C      AREA OF JOINTS AND TOTAL AREA OF CELL
09240
09250      AREAJ=TJLEN*CMINCR
09260      TAREA=CMINCR*CMINCR
09270
09280      C      NUMBER OF JOINT AREAS IN TOTAL AREA
09290
09300      AREASJ=TAREA/AREAJ
09310
09320      C      JOINTS PER AREA
09330
09340      AREAPJ=CMINCR*TJDEN
09350
09360      C      TOTAL NUMBER OF JOINTS IN AREA
09370
09380      TJNTS=AREASJ*AREAPJ
09390
09400      IF(TJNTS.LT.0.) TJNTS=1.
09410      IF(TJLEN.LT.0.) TJLEN=1.
09420      RETURN
09430      END
09440
09450
09460
09470      SUBROUTINE PRMVEC(JSET, LONG, THICK, TOTLEN, VDIRX, VDIRY, VDIRZ) .
09480
09490      C      CALCULATES THE MEAN DIRECTION VECTORS FROM EACH
09500      C      JOINT SET FOR A TOTAL OF 5 POSSIBLE JOINT SETS
09510      C      WRITTEN BY JIM SLEDZ 4/19/80
09520      C      MODIFIED BY JIM SLEDZ 6/21/80
09530
09540      DIMENSION VECX(5),VECY(5),VE CZ(5)
09550      SVECX=0.0
09560      SVECY=0.0
09570      SVE CZ=0.0
09580      DO 10 J=1,JSET
09590      JNT=J
09600      CALL OPDAT(LONG,JNT,STRIK,DIP)

```

```

09610
09620 C      VECTOR REPRESENTATION OF JOINT PLANE
09630
09640      VECX(JNT)=TOTLEN*SIND(90.-STRIK)
09650 C      VECY(JNT)=TOTLEN/COSD(90.-STRIK)
09660      VECZ(JNT)=THICK*SIND(90.-DIP)
09670   10      CONTINUE
09680
09690 C      VECTOR COMPONENTS OF THE SUM OF THE JOINT PLANES
09700
09710      DO 15 K=1,JSET
09720      SVECX=SVECX+VECX(K)
09730      SVECY=SVECY+VECY(K)
09740      SVE CZ=SVE CZ+VE CZ(K)
09750   15      CONTINUE
09760
09770 C      VECTOR MAGNITUDE AND DIRECTON CALCULATED WITH UNITS
09780 C      CHANGED TO DEGREES
09790
09800      VECMAG=SQRT(SVECX**2+SVECY**2+SVE CZ**2)
09810      VDIRX=180.*(SVECX/VECMAG)/3.1428
09820      VDIRY=180.*(SVECY/VECMAG)/3.1428
09830      VDIRZ=180.*(SVE CZ/VECMAG)/3.1428
09840      RETURN
09850      END
09860
09870
09880
09890      SUBROUTINE POF CAL(LONG,LAT,ZDEPTH,IHOLE,IROCK)
09900
09910 C      CALCULATES TOTAL FRACTURE POROSITY
09920 C      GIVEN THE LATITUDE AND ROCK CONSTITUENTS (FROM PIRSON,1975)
09930 C      WRITTEN BY JIM SLEDZ 3/5/80
09940 C      MODIFIED BY JIM SLEDZ 6/29/80
09950
09960      COMMON/KEEP/INCRE
09970      COMMON/WORK/NFRIN,INTTY,IOTTY,IUNIT1,IUNIT2
09980      DIMENSION IROCK(3),THK(100)
09990      CUBLIN=INCRE
10000      CUBWID=INCRE
10010
10020 C      THICKNESS IN MM
10030
10040      TMAX=12.*25.4
10050
10060 C      FLUID IS WATER (60 DEG. F) DATA TAKEN FROM CHOW(1964)
10070
10080      VISCOS=2.359E-5          LB SEC/FT**2
10090      SPEFWT=62.366          LB/FT**3
10100      WATER=SPEFWT/VISCOS
10110
10120      IF(ZDEPTH.LT.0) GO TO 50
10130
10140 C      DETERMINE ROCK NAME
10150
10160      CALL RCKTYP(IROCK,LNAM)
10170
10180 C      RESET ALL VARIABLES
10190
10200      THKTOT=0.0

```

```

10210      VOLGAP=0.0
10220      TFPOR=0.0
10230      AVGAP=0.0
10240      BJLEN=0.0
10250      DENTOT=0.0
10260      NBEDS=0
10270
10280      C      CALCULATE FOR EACH LITHOLOGY TYPE
10290
10300      DO 30 JT=1,2
10310      LITHYP=JT
10320      IF(IROCK(LITHYP).LE.0) GO TO 30
10330      CALL GAPSET(LITHYP,TGAP)
10340      AGAP=VGAP/304.8
10350
10360      C      CALCULATE THICKNESS AND GAP FOR EACH BED BASED ON % LITH
10370
10380      THICK=(FLOAT(IROCK(LITHYP))*0.1)*TMAX
10390      CALL THKCAL(THICK,LITHYP,THK,JTOT)
10400      AVGAP=AVGAP+(AGAP*(FLOAT(IROCK(LITHYP))*0.1))
10410      NBEDS=JTOT+NBEDS
10420
10430      C      CALCULATE FOR EACH JOINT SET
10440
10450      DO 10 J=1,2
10460      JSET=J
10470      CALL ORDAT(LONG,JSET,STR,DIP)
10480
10490      C      EACH BED TYPE
10500
10510      DO 5 KO=1,JTOT
10520      CALL DENLEN(LITHYP,THK(KO),TDEN,TJLEN)
10530
10540      C      CHANGE ALL UNITS TO FEET
10550
10560      ATHIK=THK(KO)/304.8
10570      AJLEN=TJLEN/30.48
10580      ADEN=TDEN/30.48
10590      BJLEN=AJLEN+BJLEN
10600      DENTOT=DENTOT+ADEN
10610
10620      C      CALCULATE VOLUME OF INDIVIDUAL JOINT GAP
10630
10640      VOLJNT=AGAP*AJLEN*(ATHIK/COSD(90.-DIP))
10650      VOLGAP=VOLJNT*ADEN+VOLGAP
10660      THKTOT=THKTOT+ATHIK
10670      5      CONTINUE
10680      10     CONTINUE
10690      30     CONTINUE
10700
10710      C      TOTAL FRACTURE POROSITY
10720
10730      TFPGR=VOLGAP/(CUBLIN*CUBWID*THKTOT)*100.
10740      AVGGAP=AVGAP*304.8
10750
10760      C      PERMEABILITY AND CONDUCTIVITY BASED ON SNOW (1968)
10770
10780      TJPBED=DENTOT/FLOAT(NBEDS)
10790      TPERM=((CUBLIN*CUBWID/TJPBED)**2*((TFPOR/100.)**3))/12.
10800      TDARCY=TPERM/1.062E-11

```

```

10810      TCOND=TPERM*WATER
10820      TCMDAY=TCOND*2633472.0
10830
10840      C      PERMEABILITY DIRECTION VECTORS
10850
10860      CALL PRMVEC(JSET, LONG, THKTOT, BJLEN, VX, VY, VZ)
10870
10880      C      WRITE TO FILE
10890
10900      WRITE(IUNIT2, 1001) LONG, LAT, LNAM, ZDEPTH, IHOLE
10910      1      ,AVGGAP, TFPOR, TDARCY, TCMDAY, VX, VY, VZ, (IROCK(J), J=1, 3)
10920      RETURN
10930
10940      C      NO DATA FOR POROSITY CALCULATION
10950
10960      50      LNAM='VOID '
10970      WRITE(IUNIT2, 1001) LONG, LAT, LNAM
10980      1001  FORMAT(2(I5, 1X), A5, 1X, F7.2, 1X, I2, 1X, F5.4, 3(1X, F6.3),
10990      1      3(1X, F6.2), 3(1X, I2))
11000      RETURN
11010      END
11020
11030
11040
11050      SUBROUTINE TAEPOR(*)
11060
11070      C      SUB TO PRINT CUT FRACTURE POROSITY DATA FROM FILE 'POROS.DAT'
11080      C      WRITTEN BY JIM SLEDZ 3/30/80
11090      C      MODIFIED BY JIM SLEDZ 7/11/80
11100
11110      COMMON/KEEP/INCRE, DEPTH, SILGAP, SHAGAP
11120      COMMON/WORK/NPRIN, IOTTY, INTTY, IUNIT1
11130
11140      OPEN(UNIT=IUNIT1, FILE='POROS.DAT', ACCESS='SEQIN')
11150
11160      C      PRINT HEADING
11170
11180      WRITE(NPRIN, 1000) DEPTH, SILGAP, SHAGAP
11190      1000  FORMAT('1', //, 10X, 'FRACTURE POROSITY AND PERMEABILITY LISTING'
11200      1      , 1X, 'AT ', F7.2, 1X, 'METERS DEPTH', //,
11210      2      13X, 'SURFACE GAP WIDTH (MM)', 2X, 'SILT- ', F5.3, 3X, 'SHALE- ',
11220      3      F5.3, ///, 3X, ' ORA GRID SYSTEM', 15X
11230      9      , 'JOINT', 2X, 'FRACTURE', 4X, 'INTRINSIC', 5X, 'HYDRAULIC', /
11240      2      2X, 'LONGITUDE', 2X, 'LATITUDE', 2X, 'LITHOLOGY', 3X, 'GAP', 3X,
11250      3      'POROSITY', 3X, 'PERMEABILITY'
11260      4      , 2X, 'CONDUCTIVITY', /
11270      5      , 1X, '(EAST-WEST) (NOR-SOU)', 13X
11280      8      , '(MM)', 2X, '(PERCENT)', 4X, '(DARCY)', 7X, '(CM/DAY)',
11290      6      /, 1X, 78(' - '))
11300
11310      C      ALL DATA FOLLOWS
11320
11330      10      READ(IUNIT1, 1001, END=99) LONG, LAT, RCK, AGAP, TPOR, TPER, TCON
11340      IF(RCK.NE. 'VOID ') WRITE(NPRIN, 1002) LONG, LAT, RCK, AGAP, TPOR
11350      1      , TPER, TCON
11360      1001  FORMAT(2(I5, 1X), A5, 12X, F5.4, 3(1X, F6.3))
11370      1002  FORMAT(3X, I5, 6X, I5, 6X, A5, 4X, F5.4, 2X, F6.3, 7X, F6.3, 8X, F6.3)
11380      GO TO 10
11390
11400      99      CLOSE(UNIT=IUNIT1)
11410      RETURN 1
11420      END

```

APPENDIX B
USER'S GUIDE

APPENDIX B

USER'S GUIDE

The user input that is required for the Fracture Flow Modeling System (FRAFLO) will be discussed below. The user should be familiar with all calculations and terminology involved prior to using the system.

The program is designed to operate from a remote terminal of a Digital (DEC) System KL-10 computer at Oak Ridge National Laboratory facility. This program may be run in batch mode with minor modifications, and the user should consult programming assistance for these changes.

To initialize the program from the monitor mode, the user types in the command:

```
.RUN FRAFLO
```

Upon the execution of this statement, the program will respond with:

```
WELCOME TO THE FRACTURE FLOW MODELING SYSTEM
```

```
OPTION:
```

The option mode is the point in the program where any of the operations may be requested. The user is placed in this mode upon program initialization and after execution of a selected option. The options available are displayed by input of a carriage return:

```
OPTION;  
AVAILABLE OPTIONS ARE;  
1 COMPLETE SURFACE 3-D  
2 CELL SURFACE 3-D  
3 CELL FRACTURE POROSITY 3-D  
4 CELL FRACTURE POROSITY TABLE  
-1 END
```

Each option will be individually discussed along with any input required for the execution of a request. A negative integer as an option will result in the termination of the program and restoring the user to the monitor mode.

Option=1

The selection of this option produces a complete three-dimensional diagram of the surface elevations for the entire Southern Conasauga Belt (Figure 24, p. 64). This diagram displays all of the available cells that may be created by the program. The only other input requested is a file name for the generated plot file:

```
ENTER NAME FOR POP FILE.  
(EXTENSION .POP WILL BE ADDED)
```

The name can be any six alpha-numeric characters with the default value of FOR24 used if no name is entered (carriage return). Upon completion, the plot file will be written onto the users disk area and the user will be returned to the option mode.

Option=2

A three-dimensional plot of surface elevations for an individual cell can be produced with option 2 (Figure 25, p. 67). After this

selection, the program will request the user to input a set of location coordinates and the size of the cell to be created;

COORDINATES ARE ORA GRID SYSTEM
LATITUDE;
LONGITUDE;
DIVISIONS ON CELL EDGE ;

The cell coordinates are any coordinates within the Southern Conasauga Belt. These are based on the ORA Grid System with the latitude representing the north-south coordinates and longitude, the east-west coordinates. The latitude values can be any value within the range of 0 to 20000 and the range of allowable longitude values are from 20000 to 70000. The input of a coordinate outside either range will result in the error;

LONGITUDE OUT OF RANGE.....REENTER
OR
LATITUDE OUT OF RANGE.....REENTER

The divisions on a cell edge are based on the number of divisions of the total cell edge length of 80.16 m (263 feet). The number input is the number of divisions subdividing the cell length creating smaller subcells. If the division was 10, then each subcell created would be about 8 m (26 feet) on a side. The maximum allowable number of divisions is 52 which will create subcells with 1.54 m (5 feet) side lengths.

After this data is input, the program will request the name of the plotting file, as discussed in the previous section, and will write this file onto the disk area while returning the user to the option mode.

Option=3

The third option is a request for a three-dimensional plot of the calculated fracture porosity for an individual cell (Figure 29, p. 84). The required input for this option is the latitude, longitude, and cell increment as discussed above. An additional input of the drill hole number is required and will be used to obtain lithology information for all calculations.

DRILL HOLE NUMBER (1-8);

If a carriage return or a number outside of the range is entered, a listing of all available drill holes and their coordinates are displayed.

AVAILABLE CORES ARE;
LONG, LAT
1 - OR12 - (30870,19315)
2 - OR13 - (31397,19289)
3 - OR14 - (32240,19001)
4 - OR15 - (35711,18373)
5 - OR17 - (35922,16976)
6 - OR18 - (35843,17846)
7 - OR19 - (36528,16845)
8 - OR20 - (35553,17582)

The coordinates are of the actual drill hole locations. The latitude is very important in the calculation, and the user should select a core number representing a latitude value very near that of the cell location. The model considers the dip of the strata as well as the surface elevation in determining the appropriate lithology.

The depth of interest for the calculation to be performed is the next question to be answered:

DEPTH (METERS) OF INTEREST;

This depth is the depth below the actual ground surface as determined from a topographic map. An example of this is: if the entered depth was 15, then the calculation would be performed at 15 meters below the ground surface for each individual subcell.

If the drill core provides no lithologic information for any subcells, the data within the file POROS.DAT will contain voids and no results will be plotted.

The user will be requested to input the plot file name, as previously, and the user will be returned to the monitor mode upon plot completion.

Option=4

The tabulation of the calculated data requires the same answers to the questions discussed in option 3 with the exception of the plot file name. The output file will be written to the user's disk area with the extension of LPT and can be printed at the user's convenience.

Multiple Requests

If multiple requests are made, the plot file will contain all of the plots and the .LPT file will contain all of the tables selected. The only restriction existing is that the data stored in file POROS.DAT will contain results of the most current calculations. If these data are required for any alternate use, the file should be renamed after exiting from the program for each request allowing for the preservation of the results.

APPENDIX C

TABLES

TABLES

Table C-1. Listing of commonly used variable names in the FRAFLO program

<u>NAME</u>	<u>DESCRIPTION</u>
NPRIN	printing device
INTTY	input device
IOTTY	output device
IUNIT	file unit number
LONG	longitude
LAT	latitude
INCRE	incremental divisions of cell
KEYDEP	depth of calculation
IROCK	percent lithologic constituents
LNAM	lithology name
SILGAP	surface joint gap width in siltstone
SHAGAP	surface joint gap width in shale
AVGGAP	mean subsurface joint gap width
TMAX	total bed thickness
THK	individual bed thickness
VX	unit direction vector
TFPOR	fracture porosity
TDARCY	intrinsic permeability
TCMDAY	hydraulic conductivity

Table C-2. Descriptions of files used in the FRAFLO program

<u>FILE NAME</u>	<u>FORMAT</u>	<u>DESCRIPTION</u>
STOPO.DAT		Source file of coded surface elevations
	2I2	Latitude code
	2I2	Longitude code
	27I2	Elevation code
CORE.DAT		Source file of coded drill cores
	I3	Subsurface depth
	I8	Percent siltstone, shale, glauconite, and limestone
CONTUR.DAT		Surface elevations and coordinates created in sub: TOPMAK
	I5	Longitude
	I5	Latitude
	I4	Surface elevation
SIALO.DAT		All coordinates and elevations in rectangular area created in sub: BLDMAT
	I5	Longitude
	I5	Latitude
	I4	Surface elevation
SMAT.DAT		Surface elevation for each coordinate created in sub: MATFIX
	(I4)	Surface elevation
CELL.OUT		Calculated subcell coordinates and surface elevations created in sub: MATFIX
	I5	Longitude
	I5	Latitude
	F7.1	Surface elevation

Table C-2. (continued)

<u>FILE NAME</u>	<u>FORMAT</u>	<u>DESCRIPTION</u>
POROS.DAT		All model results created in sub: PORCAL
	I5	Longitude
	I5	Latitude
	A5	Rock name
	F7.2	Depth of calculation
	I2	Drill core used
	F5.4	Mean gap width
	F6.3	Fracture porosity
	F6.3	Intrinsic permeability
	F6.3	Hydraulic conductivity
	F6.2	X-unit vector
	F6.2	Y-unit vector
	F6.2	Z-unit vector
	I2	Percentage of siltstone
	I2	Percentage of shale
	I2	Percentage of limestone

INTERNAL DISTRIBUTION

- | | | | |
|--------|----------------|--------|-----------------------------|
| 1-2. | S. I. Auerbach | 25. | B. P. Spalding |
| 3. | R. E. Blanco | 26. | L. H. Stinton |
| 4. | J. H. Coobs | 27. | E. G. St. Clair |
| 5. | N. H. Cutshall | 28. | S. H. Stow |
| 6. | F. W. Dickson | 29. | J. Switek |
| 7. | C. S. Haase | 30. | T. Tamura |
| 8-12. | D. D. Huff | 31. | D. B. Trauger |
| 13. | J. R. Jones | 32. | J. E. Vath |
| 14. | E. M. King | 33. | N. D. Vaughan |
| 15. | C. A. Little | 34. | D. A. Webster |
| 16-17. | R. S. Lowrie | 35. | G. T. Yeh |
| 18. | R. J. Luxmoore | 36-37. | Central Research Library |
| 19. | M. S. Moran | 38-50. | ESD Library |
| 20. | M. Naney | 51-52. | Laboratory Records Dept. |
| 21. | T. W. Oakes | 53. | Laboratory Records, ORNL-RC |
| 22. | D. R. Rima | 54. | ORNL Y-12 Technical Library |
| 23. | R. A. Robinson | 55. | ORNL Patent Section |
| 24. | O. M. Sealand | | |

EXTERNAL DISTRIBUTION

56. William J. Coppoc, Texaco, Inc., P.O. Box 509, Beacon, NY 12508
57. G. H. Daly, Acting Director, Technology Division, Office of Waste Operations and Technology, Department of Energy, MS B-107, Washington, DC 20545
58. J. L. Dieckhoner, Director, Operations Division, Office of Waste Operations and Technology, Department of Energy, Washington, DC 20545
59. Ralph Franklin, Office of Health and Environmental Research, Department of Energy, Washington, DC 20545
60. E. Fray, EG&G Idaho, P.O. Box 1625, Idaho Falls, ID 83401
61. John Higgins, Geology Department, University of Tennessee, Knoxville, TN 37916
62. Fred B. Keeler, Geology Department, University of Tennessee, Knoxville, TN 37916
- 63-67. M. L. Krupinski, Program Manager, National Low Level Waste Program, EG&G Idaho, P.O. Box 1625, Idaho Falls, ID 83401
68. D. Jacobs, Evaluation Research Corporation, Oak Ridge, TN 37830
69. Elizabeth Jordan, Operations Division, Office of Waste Operations and Technology, Department of Energy, MS B-107, Washington, DC 20545
- 70-75. D. E. Large, Manager, ORO Low-Level Radioactive Waste Management Programs, Department of Energy, Oak Ridge Operations, P.O. Box E, Oak Ridge, TN 37830
76. J. A. Lenhard, Assistant Manager for Energy Research and Development, Department of Energy, Oak Ridge Operations, P.O. Box E, Oak Ridge, TN 37830

77. G. B. Levin, EG&G Idaho, P.O. Box 1625, Idaho Falls, ID 83401
78. Robert A. Lewis, EV-34, GTN, Department of Energy, Washington, DC 20545
79. Helen McCammon, Director, Division of Ecological Research, Office of Health and Environmental Research, Department of Energy, Washington, DC 20545
80. R. Nelson, Program Manager, Radioactive Waste Programs Branch, Nuclear Fuel Cycle Division, Idaho Operations Office, Department of Energy, 550 Second Street, Idaho Falls, ID 83401
81. G. Oertel, Director, Office of Waste Operations and Technology, Department of Energy, MS B-107, Washington, DC 20545
82. William S. Osburn, Jr., Division of Ecological Research, Office of Health and Environmental Research, Department of Energy, Washington, DC 20545
83. A. Perge, Office of the Deputy Assistant Secretary for Nuclear Waste Management, Department of Energy, Washington, DC 20545
84. Paul G. Risser, Department of Botany and Microbiology, University of Oklahoma, Norman, OK 73019
85. George R. Shepherd, Department of Energy, Room 4G-052, MS 4G-085, Forestal Bldg., Washington, DC 20545
- 86-90. James J. Sledz, Conoco, Inc., R&D West, P.O. Box 1267, Ponca City, OK 74601
91. Richard H. Waring, Department of Forest Science, Oregon State University, Corvallis, OR 97331
92. Robert L. Watters, Office of Health and Environmental Research, Department of Energy, Washington, DC 20545
93. J. B. Whitsett, Chief, Radioactive Waste Programs Branch, Nuclear Fuel Cycle Division, Idaho Operations Office, Department of Energy, 550 Second Street, Idaho Falls, ID 83401
94. F. J. Wobber, Department of Energy, Washington, DC 20545
95. Robert W. Wood, Office of Health and Environmental Research, Department of Energy, Washington, DC 20545
- 96-122. Technical Information Center, Department of Energy, Oak Ridge, TN 37830